High-loaded Activated Sludge

Effects of Different Aeration Strategies at Sjölunda WWTP

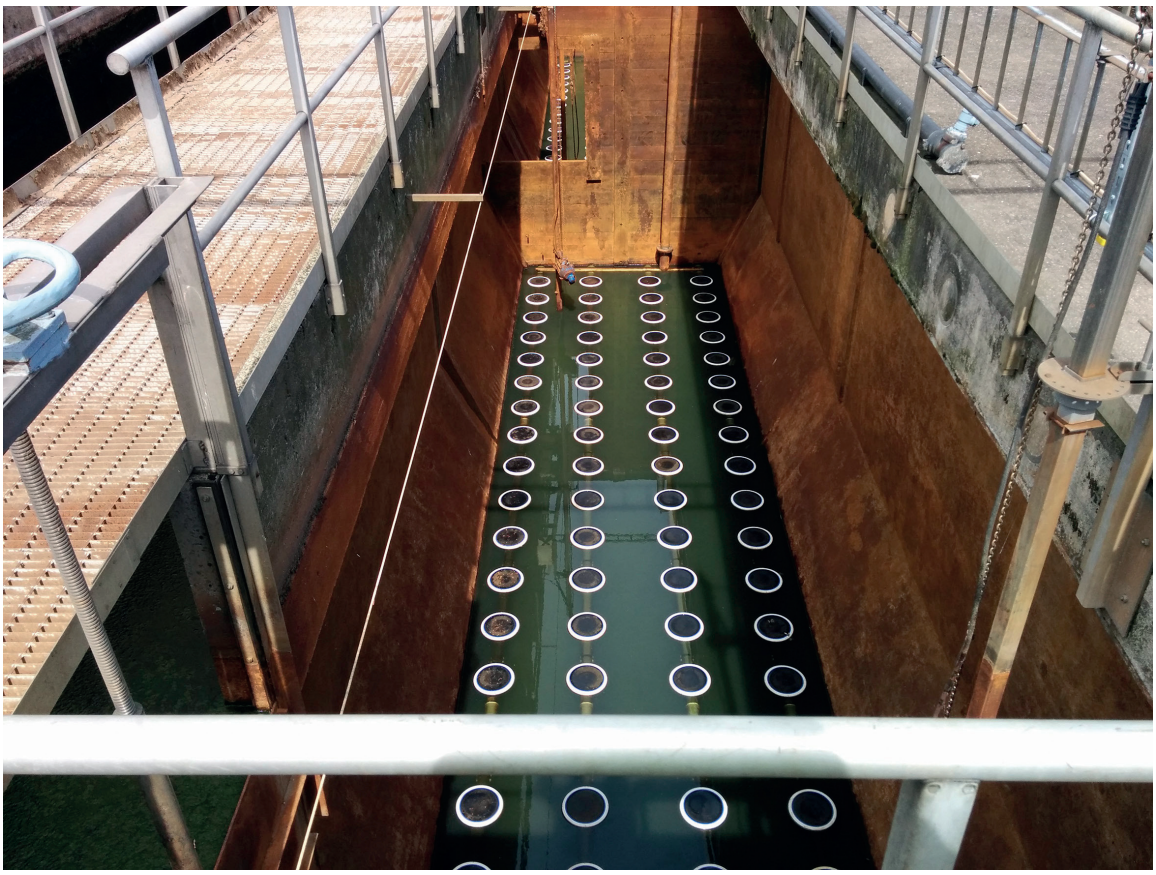

Gabriel Persson

Water and Environmental Engineering
Department of Chemical Engineering
Master Thesis 2015

LUND UNIVERSITY

High-loaded Activated Sludge
Effects of Different Aeration Strategies at Sjölunda WWTP

by

Gabriel Persson

Master Thesis number: 2015-15

Water and Environmental Engineering
Department of Chemical Engineering
Lund University

December 2015

Supervisors: **PhD Åsa Davidsson, LTH**
PhD David Gustavsson, VA SYD
Examiner: **Professor Jes la Cour Jansen, LTH**

Picture on front page: Fine-pore membrane diffusers in an empty activated sludge basin at Sjölunda WWTP. Photo by G. Persson 2015

Postal address	**Visiting address**	**Telephone**
P.O. Box 124	Naturvetarvägen 14	+46 46-222 82 85
SE-221 00 Lund, Sweden		+46 46-222 00 00
Web address		**Telefax**
www.vateknik.lth.se		+46 46-222 45 26

Preface

Writing a master's thesis of this magnitude has been daunting, trying but ultimately a very rewarding experience. Completing this project would not have been possible without the support of a number of people that deserve a special mention in this report:

My family for all their support in me and in my work with the thesis.

My supervisors: Åsa Davidsson at LTH, for all her feedback and help with our BMP tests, and David Gustavsson at VA SYD, whose inexhaustible passion for wastewater treatment inspired me to try my very best, and whose knowledge and invaluable feedback helped push this thesis in the right direction.

My examiner, Jes la Cour Jansen for his assistance with improving the thesis.

Gertrud Persson at the Department of Chemical Engineering for all her help with lab activities and for making me feel very welcome in the lab environment.

The staff at VA SYD, especially Max Granqvist, Ylva Eriksson, Nelson Llano Alvarez and everyone working in the lab at Sjölunda.

Thanks also to DHI, who provided me with the license for MIKE WEST.

Finally, I would like to thank Per Nobel, who worked on a closely related master's thesis project at VA SYD simultaneously, and who has contributed with so much knowledge, enthusiasm and skill. Without all his help and encouragement I would not have been able to complete this thesis.

Abstract

The activated sludge process has existed for over a century and despite its age the development of new theories, methods and technologies is ongoing. Despite huge technological breakthroughs in the last decades the activated sludge process is still a very energy demanding process however, and it is possible to make significant energy savings by optimizing the aeration strategy of an activated sludge plant. Sjölunda WWTP, one of the largest wastewater treatment plants in Sweden, have gradually lowered the oxygen concentrations in its high-loaded activated sludge process to try to find an optimal aeration solution through full-scale tests.

The treatment plant is facing challenges in the form of increasing load and a need to expand or change the current nitrogen removal process. A pilot study is investigating the possibility of implementing total autotrophic nitrogen removal, i.e. the nitritation-anammox process, as an alternative for the next nitrogen removal upgrade. The nitritation-anammox process is sensitive however, and required a low organic matter to nitrogen ratio to function optimally, a ratio that is difficult to accomplish with the aeration strategy in use at the plant today.

An ASM2d model was created in the wastewater modelling software MIKE WEST with the aim to investigate if it was possible to find an optimized aeration strategy that could increase the treatment efficiency of the activated sludge process and reduce the COD/N ratio without causing significant increases in energy demand. As the treatment plant is producing biogas it was also of interest to investigate whether the methane production potential of the activated sludge would benefit from low oxygen concentrations in the process.

It was discovered that the settling model most commonly in use in activated sludge modelling today was not able to sufficiently estimate what happens with the treatment efficiency of at different oxygen concentrations in the activated sludge process and focus was therefore spent on full-scale tests of different aeration strategies. The full-scale tests showed that it was not possible to see a clear trend that the oxygen concentration were affecting the methane potential of the sludge, but it was possible to lower the energy demand of the process while maintaining the same treatment efficiency by evening out the oxygen concentrations between the aerated basins.

Keywords: High-loaded activated sludge, activated sludge modelling, methane potential, aeration strategies, ASM2d

Sammanfattning

Aktivtslamprocessen har funnits i hundra år, och trots dess ålder går utvecklingen av nya teorier, metoder och tekniker framåt. Trots stora teknologiska landvinningar under de senaste årtiondena är aktivtslamprocessen fortfarande en mycket energikrävande process, och det går att göra stora energivinster genom att optimera en aktivslamanläggnings syrestyrningsstrategi. Sjölunda avloppsreningsverk, ett av Sveriges största avloppsreningsverk, har under den senaste tioårsperioden gradvis minskat på syrenivåerna i verkets högbelastade aktivtslamprocess för att försöka hitta optimala syrestrategier genom fullskaleförsök.

Reningsverket står inför utmaningar kring ökande belastningar och behov av en förändrad kvävereningsprocess. Pilotförsök genomförs med nitritation-anammox-processen manammox – som en tänkbar lösning för framtiden. Manammoxprocessen är dock känslig, och kräver ett lågt C/N-förhållande för att fungera optimalt, vilket är svårt att uppnå med den syrestrategi Sjölundaverket använder idag.

En ASM2d modell sattes upp i simuleringsprogrammet WEST med syfte att undersöka om det gick att hitta en optimal syrestrategi för att förbättra aktivtslamprocessens reningsgrad och det renade vattnets C/N-förhållande utan att orsaka kraftigt förhöjd energiåtgång. Då reningsverket producerar biogas var det även intressant att undersöka om slammets metanpotential var högre vid låga syrehalter.

Den vanligaste sedimentationsmodellen i dagens aktivtslammodellering upptäcktes vara otillräcklig för att kunna visa vad som händer med reningsgraden vid olika syrenivåer i aktivtslambassängerna och fokus lades därför på att visa skillnader mellan olika strategier i fullskaleförsök. Fullskaleförsöken visade att det inte gick att se en tydlig skillnad på metangaspotential hos slam från aktiv slamlinjer med olika luftningsstrategier, men att det är möjligt att sänka energiförbrukningen med bibehållen reningsgrad genom att utjämna syrenivåerna i de syresatta bassängerna.

Abbreviations

BOD	Biochemical oxygen demand. Measurement for degradable organic matter
COD	Chemical oxygen demand. Measurement for organic matter
D1	A treatment block at Sjölunda WWTP consisting of primary settler basins.
DO	Dissolved oxygen. Measurement for oxygen concentration in water
F/M	Food to microorganism ratio. The ratio describes the balance between the daily organic load and the biomass in the activated sludge basins.
G1	A treatment block at Sjölunda WWTP consisting of the two activated sludge lines G1:1 and G1:2
G2	A treatment block at Sjölunda WWTP consisting of the two activated sludge lines G2:1 and G2:2. Line G2:1 has a solids retention time controller which the other lines lack.
HLAS	High-loaded activated sludge.
PE	Person equivalents. Measurement for pollution load in wastewater treatment.
SRT	Solids retention time.
SS	Suspended solids
TKN	Total Kjeldahl nitrogen
TN	Total nitrogen
TOC	Total organic carbon. Measurement for organic matter
TP	Total phosphorus
TS	Total solids
VFA	Volatile fatty acids
VS	Volatile solids
VSS	Volatile suspended solids
WWTP	Wastewater treatment plant

Table Of Contents

1 Introduction

Discoveries from the late 19th century and onward led to the first activated sludge treatment facility being constructed in 1914, thereby making the activated sludge process one of the oldest wastewater treatment processes still in use today (Alleman and Prakasam, 1983). The process is still the dominating technology for biological wastewater treatment.

The activated sludge process was first introduced in wastewater treatment as a primarily aesthetic solution which reduced the smell and clarified the treated water by removing contaminants (organic matter) (Alleman and Prakasam, 1983).

A simple activated sludge plant consists of an aerated basin and a sedimentation basin. The aeration is necessary to facilitate the growth of the microorganisms that form the biomass (activated sludge) that consume organic matter in the wastewater. Activated sludge that settle in the sedimentation basin is pumped back into the aerated basin, which gives the sludge a longer retention time (SRT) in the system than the hydraulic retention time (HRT) for the water. The bacteria in the biomass form flocks, which degrade organic matter and adsorb particles that are too light to settle on their own, and the flocks then settle in the sedimentation basin. To control the accumulation of biomass in the basins a portion of the return sludge flow, called the waste sludge flow, is led out of the process to sludge treatment (Carlsson and Hallin, 2003).

With the introduction of new technologies and demands for nutrient removal, nitrogen removal, where the biomass contain both heterotrophic denitrifiers and autotrophic nitrifying bacteria, was included in many activated sludge processes in the 1990s. Due to the slow growth rate of the autotrophs the solids retention time was increased, which increased the oxygen demand and reduced the sludge production of the activated sludge process (Gustavsson *et al.,* 2012). Nitrogen removal furthermore required a combination of aerated and non-aerated zones, since denitrifiers need anaerobic conditions (Carlsson and Hallin, 2003).

New nitrogen removal processes and an increasing focus on biogas production, nutrient recovery and energy efficiency has led to a re-evaluation of the usefulness of the old solution – activated sludge processes without nitrogen removal (Gustavsson *et al.,* 2012) where the load of organic matter in the influent can be higher than in conventional activated sludge plants with enhanced nitrogen removal. In these treatment steps, called high-rated activated sludge (HLAS) plants, the SRT is kept low while the F/M ratio is high, which prevents nitrification and requires extra treatment steps for nitrogen removal.

The Sjölunda wastewater treatment plant (WWTP) has a HLAS unit with preceding primary settlers. Each HLAS line is divided into five basins – two anaerobic and three aerated basins, where the two anaerobic basins have roughly the same combined volume as each aerated basin. Unlike many other activated sludge plants the HLAS at Sjölunda is only used for COD removal – enhanced nitrogen removal occurs mostly in subsequent trickling filters and moving-bed biofilm reactors.

The treatment plant is expected to undergo a number of changes over the next ten years as a response to a need to expand the treatment capacity of the plant due to increased load and demands for higher degree of nitrogen removal. The treatment plant is evaluating the introduction of a total autotrophic nitrogen removal treatment step, called Anammox in the mainstream or Manammox, as a partial solution. The nitritation-anammox process benefits

from a low COD/N ratio (Gustavsson *et al.,* 2013), which can be achieved with a HLAS process. It is therefore possible that there would be an increased interest from other wastewater treatment plants in the HLAS setup used at Sjölunda if the Manammox pilot project yields promising results.

A reduction of the aeration rate will decrease the aeration energy demand, and thus the operational costs of the activated sludge unit. In addition, the resulting decrease in airflow is expected to reduce the endogenous respiration rate since part of the endogenous respiration is oxygen dependent (Vanrolleghem, 2002). This is in turn expected to increase the biogas production potential of the sludge. However, low dissolved oxygen concentrations have been found to have a negative impact on settling properties (Martins *et al.,* 2004) and COD removal rates (Fang *et al.,* 2011). Low oxygen concentrations could also cause excessive growth of filamentous bacteria (Martins *et al.,* 2004), which could cause issues with foaming (Pal *et al.,* 2014). It is therefore important to look at a broad picture when considering the aeration strategy of the HLAS.

Sjölunda WWTP has recently moved away from automated aeration control in some of the HLAS lines and has begun to use manual set-points. This new aeration strategy needs to be evaluated and compared to other possible strategies.

Aim

The purpose of the thesis project was to evaluate different aeration strategies in relation to the current aeration strategy in the high-loaded activated sludge process at Sjölunda WWTP and to find an optimized strategy in terms of treatment quality (COD/N ratio), energy consumption and biogas production.

A secondary aim was to evaluate if using a model is a suitable approach for finding optimized aeration strategies in a HLAS system.

2 The activated sludge process at Sjölunda WWTP

2.1 The treatment process at Sjölunda WWTP

The Sjölunda WWTP is the larger of two wastewater treatment plants located in Malmö, Sweden. Sjölunda WWTP treats wastewater from Malmö and several surrounding municipalities, and discharges the treated water into the Öresund strait. The wastewater treatment plant has been in operation since 1963 and has seen several large expansions of its treatment capabilities, including a pre-precipitation step for phosphorus removal constructed in 1974, post-treatment for enhanced COD and phosphorus removal in a dissolved air flotation plant in 1979 and enhanced nitrogen removal functions in 1999.

Wastewater flows of on average 1350 l/s are led through an inlet pumping station, with the possibility to redirect flow to an overflow plant under wet weather conditions. The wastewater continues through screening and grit removal steps, designed to remove large particles, and a ferrous-based precipitant is added in the aerated grit removal basin in order to cause precipitation of phosphorus. Primary clarification, where larger particles settle is followed by the activated sludge process.

The activated sludge process, which includes a high-loaded activated sludge plant and secondary clarifiers is the first biological treatment step at Sjölunda, and the process is designed to remove suspended solids, organic matter and a part of the phosphorus through assimilation. That the process is high-loaded means that the solids retention time (SRT) is low and the F/M ratio is high. Anoxic zones in the beginning of the activated sludge process allows for removal of nitrite and nitrate (i.e. heterotrophic denitrification), but unlike the much more common low-loaded activated sludge process the treatment step at Sjölunda is not designed for nitrification, and the process thus only represent a minor part of the nitrogen removal steps at the wastewater treatment plant.

Nitrogen removal takes place in the two subsequent biological treatment steps: nitrifying trickling filters, where ammonium is reduced to nitrate under aerobic conditions, and post-denitrification with moving carrier material, where the nitrate produced in the previous step is transformed into nitrogen gas. Biological flocs that have formed in the wastewater during the biological treatment steps are removed from the water in the dissolved air flotation plant, which is the final treatment step of the water line.

The activated sludge that is removed in the waste sludge flow is combined with sludge flows from several of the other treatment steps, thickened and led into anaerobic digesters, where a part of the organic matter in the sludge is degraded by microorganisms to form biogas. The remaining sludge is dewatered and utilized as fertilizer on farmland. Water from the sludge thickening and water removal processes are pumped back to the beginning of the wastewater treatment process (VA SYD, 2011).

The total load was 300 000 – 390 000 person equivalents in 2013 (VA SYD, 2014).

2.2 Historical COD/N ratio

Sjölunda WWTP has been investigating the possibility of introducing an Anammox treatment step in the mainstream after the activated sludge treatment as a means to increase the treatment plant's nitrogen removal capabilities. For the Anammox process to function optimally the

COD/N ratio in the inflow (the effluent of the secondary clarifiers) should be low (Gustavsson *et al.,* 2012). Ballinger et al. (2002) showed that nitrification rates drop at COD/N ratios above 2 since ammonia-oxidizing bacteria has difficulties competing with other bacteria in systems with high concentrations of organic matter.

In recent years Sjölunda WWTP has had difficulties maintaining a low COD/N ratio in the effluent from the activated sludge process, but historical data showed that the treatment process had been able to keep ratios of on average 2.5 during the period of 2002-2005, with ratios dropping to approximately 2 during the second half of 2005 (see Figure 1). At the end of 2005 Sjölunda WWTP stopped measuring COD in favor of BOD tests, and since the COD measurements did not recommence until 2013 the COD/N-ratio cannot be determined during this time period.

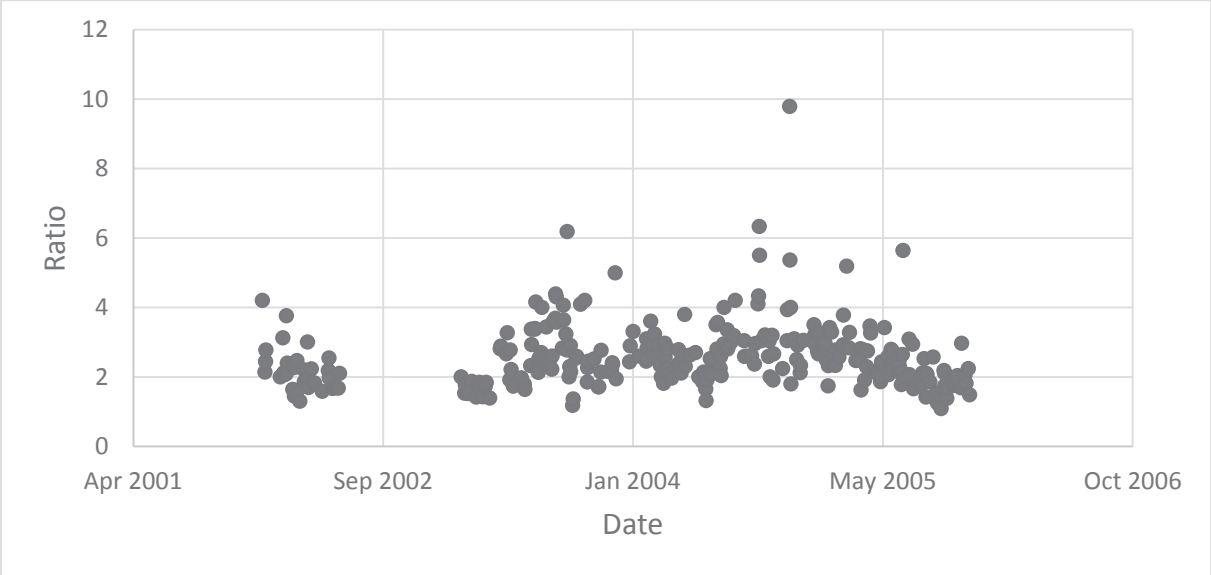

Figure 1 Historical COD/N ratio in the effluent from the activated sludge process at Sjölunda WWTP.

3 Earlier research and theoretical background

3.1 Previous studies on activated sludge at Sjölunda

Several other studies on the properties of the activated sludge process at Sjölunda WWTP has been performed since 2007.

Rydh & Åkesson (2007) studied the energy conservation at Sjölunda and at another wastewater treatment plant in Malmö. The report estimated that the activated sludge process at Sjölunda made up 30% of the total electrical energy consumption and that 70% of this energy was caused by the aeration system. At the time of the study all activated sludge processes had dissolved oxygen set-points of 2 mg/L, and parts of the aeration system have been changed since 2007, which have decreased the energy consumption of the aeration at the plant.

Martinello (2013) investigated the possibilities to optimize the energy efficiency of the high-loaded activated sludge plant and anaerobic digestion. A model of the treatment process was created using the simulation environment BSM1 and an experimental campaign was carried out to characterize the wastewater and sludge. The report recommended that the SRT should be reduced to 20 hours as a means to increase biogas production.

Optimization of the activated sludge process required if subsequent biological treatment steps were to be changed was studied in *Dynamic evaluation of a high loaded activated sludge plant as pretreatment for deammonification in the mainstream* (Polizzi, 2013). Polizzi also used BSM1 to model the treatment process and found that using a sludge age of 1.2 days and aerating all five zones in the activated sludge process with a set-point of 1.5 mg DO/L provided the best solution for a subsequent Manammox treatment step.

Polizzi and Martinello largely used data from the same experiments, carried out in 2013, in their separate master's theses.

Klingstedt (2015) studied the effects of an expected increased load on Sjölunda WWTP due to population growth in Malmö. An ASM2d model was set up in MIKE WEST in order to simulate the effects of the increased load. Klingstedt's model included an iron-based pre-precipitation and pre-settling step, two primary clarifiers, five activated sludge basins and one secondary clarifier for three blocks (G1-G3). The report estimated that it would only be possible to continue operating the plant for an additional nine years while still meeting effluent quality demands, before it would be necessary to enlarge the treatment processes.

Nobel (2015) also constructed an ASM2d model in MIKE WEST, but did so with the aim to study the SRT and find optimization strategies with regards to treatment quality, energy consumption, biogas production and foaming issues. The model was designed to be as similar as possible to the one used as the basis for this report, so that it would be possible to use the model to simulate effects of both aeration and SRT optimization. The characterization data used as the basis of the initial calibration of the model, and the majority of the sedimentation data is shared between Nobel's report and this thesis.

3.2 Aeration strategies

Significant technological breakthroughs have been made in the activated sludge process in the last decades, especially in the aeration field. The development of sensor technology in the 1970s

made automated control of aeration based on dissolved oxygen measurements possible (Olsson, 2012). The number of publications concerning activated sludge modelling has been steadily growing since the 1980s. In 1995 approximately 100 activated sludge modelling publications were released. By 2010 the number had grown to over 300 publications per year (Rieger *et al.,* 2013). The energy demand associated with aeration ensures that many of these publications are focused on aeration strategies.

Due to the relative scarcity of large high-loaded activated sludge plants most publications on optimizations of aeration strategies include nitrogen removal, i.e. nitrification and denitrification, and it might therefore be difficult to apply the knowledge directly to a high-loaded activated sludge process.

3.2.1 Aeration control systems

Åmand *et al.* (2013) have written a comprehensive review on aeration control. While DO set-point configuration is the focus of this project there are other strategies that can be just as beneficial to improving the efficiency of the aeration, as detailed in the review. Åmand *et al*. (2013) touch on the importance of trustworthy sensor equipment and maintenance of diffusers but the focus is on different control strategies. Many of these strategies are mainly focused on energy conservation, and generally the optimizations are found to reduce energy usage by 10-40%.

Thunberg (2006) performed a study to optimize the aeration strategy of Käppala WWTP. The treatment plant controlled aeration in the activated sludge process through DO sensors in the first and in the last aerated zones. By controlling aeration with DO sensors in each aerated zone individually airflow could be reduced by 16%.

Fernández *et al.* (2011) described an alternative control solution to PI/D regulators: multiple on/off controllers. On/off controllers are often used to control aeration in smaller wastewater treatment plants which lack the sensor equipment necessary for more advanced control strategies. By using and optimizing the DO set-points for multiple on/off controllers the stability and treatment efficiency of the process could be increased.

While Fernández *et al.* (2011) described a simpler control system than the PI-regulators used to control aeration at Sjölunda WWTP there are several control systems that are significantly more advanced. One such example is the control strategy presented by Kandare and Nevado Reviriego (2011): adaptive predictive control of DO concentrations. Adaptive predictive control systems are designed to predict changes in process variables and to alter the controller set-points to prevent these variations. The presented strategy included control of both DO and the air-pressure. By controlling the air-pressure energy consumption could be reduced by 25% at the studied WWTP.

3.2.2 Measures to improve the oxygen transfer rate

A review by Pittoors *et al*. (2014) noted that aeration and oxygen mass transfer is affected by a large amount of different geometric, physico-chemical and dynamic factors. The influence of these factors furthermore depend on wastewater composition and the type of aerator and the oxygen transfer coefficient (k_La) models therefore have to be calibrated and tested for each individual WWTP if the models are to be effective.

Henkel *et al.* (2011) described the α-factor as the most important variable when optimizing a submerged aeration system in an activated sludge plant. The review showed that the α-factor

decreases with increasing MLSS concentrations. Germain *et al.* (2007) made a similar discovery when studying the effect on k_La and on the α-factor by different biomass concentrations in a membrane bioreactor. Henkel *et al.* (2011) also showed that decreasing the SRT decreases the α-factor and that the α-factor is lowest at the influent and reaches its highest value at the effluent if the system resembles a plug-flow reactor. This would indicate that aeration is most efficient in the last aerated basin.

A series of experiments presented in Schierholz *et al.* (2006) showed that fine-bubble membrane aeration systems had a k_La that was six times higher than equivalent coarse-bubble aeration systems. The experiments also showed that the mass transfer coefficient increases with increasing airflow rates and with increased water depth.

While most wastewater treatment plants use fine-pore membranes in current aeration systems, which have significantly decreased the required airflow compared to older coarse-bubble membranes the oxygen transfer efficiency of the fine-pore membranes can be severely reduced in old or ill-maintained aeration systems. Rosso and Stenstrom (2006) concluded that the oxygen transfer efficiency decrease is greatest in the first two years after a new system is installed and that the degradation leads to an increase in power consumption and a decrease in process efficiency. Liu *et al.* (2011) showed that this effect is more significant the greater the airflow rate. In a separate study by Gori *et al.* (2014) the oxygen transfer efficiency was nearly halved over a two year period in a plant where no membrane cleaning was performed. This efficiency drop led to a 40% increase in energy consumption for the entire WWTP.

Rosso and Stenstrom (2006) showed that the oxygen transfer efficiency can be largely restored by cleaning the membranes and that routine cleaning operations therefore can be recommended.

3.2.3 Consequences of low oxygen concentrations

Wang *et al.* (2007) studied optimization at very low oxygen concentrations, comparable to the concentrations that have been used in zone 3 in the activated sludge process at Sjölunda block G1. A flock model was introduced to make it possible to simulate the effect of denitrification in aerated basins, which could occur in the flocks as oxygen is depleted and anoxic cores are formed.

Fang *et al.* (2011) saw that effluent COD would be relatively unaffected by aeration rate until the rate dropped below a threshold value, at which point the removal rate of COD would decrease quickly.

Too low dissolved oxygen concentrations could also lead to higher N_2O emissions in systems with nitrification, according to several studies (Kampschreur *et al.,* 2009) and can cause problems with bulking sludge (excessive growth of filamentous bacteria) in the activated sludge basins (Martins *et al.,* 2004).

3.3 The Activated Sludge Model ASM2d

3.3.1 ASM1, ASM2 and ASM2d

The breakthroughs in computer technology in the 1970s and the 1980s made it possible to consider developing modelling software for wastewater treatment processes, and in the early 1980s the International Water Association Pollution Research and Control, IWAPRC, (today IWA) set up the Task group of mathematical modelling for design and operation of biological

wastewater treatment with the purpose to create a model for activated sludge (Henze *et al.,* 2000).

The first ASM model, ASM1, was introduced by the IWAPRC task group in 1987. In its first iteration the ASM model was able to make use of a large number of kinetic equations to simulate nitrification-denitrification processes, but ASM1 could not model biological phosphorus removal.

The limitations of the first model was partially addressed in the ASM2 model, first published in 1995, which added more components to the model, including more biological processes and internal cell storage structure for the biomass. ASM2d further extended the model by adding processes to simulate growth of denitrifying phosphorus accumulating organisms and chemical precipitation of phosphorus (Henze *et al.,* 2000).

An extension to the original ASM2d model, called ASM2dMod, was introduced by Gernaey and Jørgensen (2004). The extended model makes the decay process rates electron acceptor dependent. DHI further extended this model in ASM2dModTemp, which introduced correction factors to calculate the temperature-dependent kinetic parameters under non-standard temperatures (DHI, 2014).

Earlier studies of the activated sludge plant at Sjölunda made by Martinello (2013) and Polizzi (2013) have used the ASM1 model whereas Klingstedt (2015) used the ASM2dModTemp model.

3.3.2 Mass fractions in ASM2d

The ASM models uses mass fractionation to make it possible to use the models even if only a limited set of compound measurements are available from the real process. ASM2d includes 21 different components which are sorted based on whether they are soluble, denoted S, or particulate, denoted X (see Table 1).

COD was selected as an input and model variable for organic matter over BOD or TOC since it could be used to set up mass balances and since it could be used to link the electron equivalents between biomass, organic matter and utilized oxygen (Henze *et al.,* 2000).

Table 1 Model components in ASM2d.

Component	Unit	Description
S_A	g COD/m^3	Fermentation products, considered to be acetate
S_{ALK}	mol(HCO_3^-)/m^3	Alkalinity of wastewater
S_{COD}	g COD/m^3	Soluble COD
S_F	g COD/m^3	Fermentable, readily-biodegradable organic substances
S_I	g COD/m^3	Inert soluble organic matter
S_{N2}	g N/m^3	Dinitrogen, product of denitrification
S_{NH4}	g N/m^3	Ammonium and ammonia nitrogen
S_{NO3}	g N/m^3	Nitrite and nitrate nitrogen
S_{O2}	g O_2/m^3	Dissolved oxygen.
S_{PO4}	g P/m^3	Inorganic soluble phosphorus, orto-phosphates
S_S	g COD/m^3	Readily biodegradable substrate (replaced with S_A and S_F)
X_{AUT}	g COD/m^3	Nitrifying (autotrophic) organisms
X_{COD}	g COD/m^3	Particulate COD
X_H	g COD/m^3	Heterotrophic organisms
X_I	g COD/m^3	Inert particulate organic material
X_{MeOH}	g TSS/m^3	Metal-hydroxides
X_{MeP}	g TSS/m^3	Metal-phosphate
X_{PAO}	g COD/m^3	Phosphate-accumulating organisms, PAOs
X_{PHA}	g COD/m^3	Cell internal storage product of PAOs
X_{PP}	g P/m^3	Poly-phosphate
X_S	g COD/m^3	Slowly biodegradable substrates
X_{TSS}	g TSS/m^3	Total suspended solids

COD has the most complex fractionation in the ASM models, with ten different compound fractions in the ASM2d model. COD fractions sorted by biodegradability can be found in Figure 2, but it is also common to sort the fractions according to solubility. When sorted by biodegradability COD can be divided into three categories: biodegradable COD, non-

biodegradable COD and active biomass. In the model, active biomass uses biodegradable COD to form new biomass, whereas non-biodegradable COD is inaccessible to the active biomass and will therefore pass through the activated sludge process without taking part in any chemical reactions.

The soluble biodegradable fraction S_S was split into the two components fermentation products S_A (acetate) and fermentable, readily biodegradable organic substrates S_F in ASM2. Soluble biodegradable COD reacts significantly faster than particulate biodegradable X_S in the model.

Non-biodegradable COD is divided into two fractions: soluble and particulate inert organic material (S_I and X_I). The soluble fraction S_I is the minimum COD concentration in the effluent, since the fraction does not settle.

The active biomass include heterotrophs X_H, autotrophs X_{AUT} and phosphate-accumulating organisms X_{PAO}. The PAO storage products X_{PP} is not a COD fraction, it is instead considered to be a phosphorus fraction in the model, but it is closely tied to the concentration of PAOs in the system. The cell internal storage product X_{PHA} is similarly a COD fraction which only occur in connection to PAOs, but is not a fraction of the PAO mass.

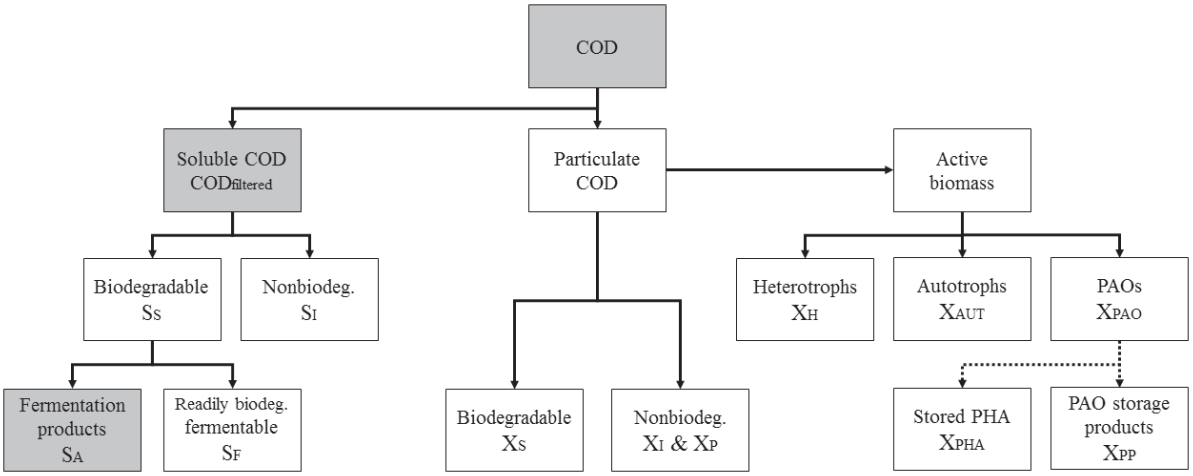

Figure 2 COD fractions in the ASM2d model sorted by biodegradability. Stored PHA and PAO storage products are closely tied to the PAO fraction, but are not COD fractions. Measured COD fractions are shown as grey boxes. Adapted figure from Nobel (2015). Used with permission.

The model total nitrogen is divided into ammonium, organic nitrogen and nitrate plus nitrite nitrogen (see Figure 3). The first two concentrations can be combined to form Total Kjeldahl Nitrogen. Organic nitrogen is not its own fraction in the model, but is instead calculated as the sum of nitrogen content in the COD fractions.

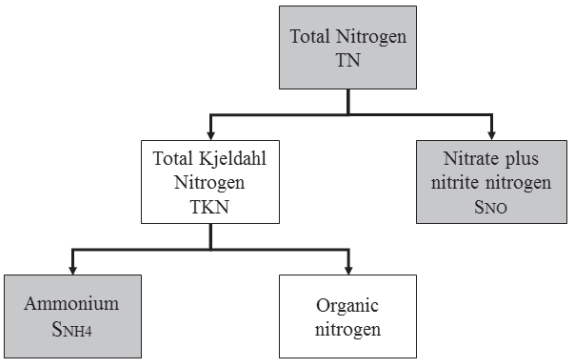

Figure 3 Nitrogen fractions in the ASM2d model. Measured nitrogen fractions are shown as grey boxes.

Total phosphorus is divided into inorganic soluble phosphorus, organic phosphorus and polyphosphate (see Figure 4) in the model. Like organic nitrogen organic phosphorus is not its own fraction in ASM2d, but is calculated as the sum of phosphorus fractions of the different COD components.

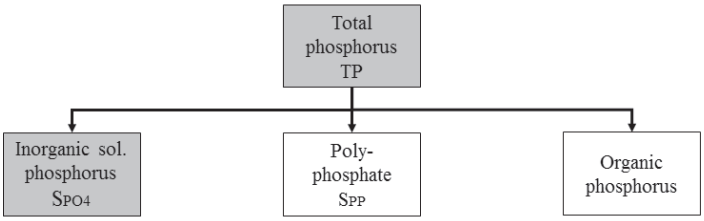

Figure 4 Phosphorus fractions in the ASM2d model. Measured phosphorus fractions are shown as grey boxes.

3.4 Aeration sub-model: The Irvine Carbon Footprint model

The Irvine Carbon Footprint model is based on a theory by Boyle *et al*. (1989) which is combined with a method for correlating the standardized oxygen transfer efficiency in process water (αSOTE) to SRT and the air flux (DHI, 2014).

The oxygen transfer coefficient k_La can be calculated as a function of the normal airflow rate from equation 3.1:

(Equation 3.1) $$k_L a = \frac{\rho * Q_{Air} * Y_i * OTE}{(\beta * C_S^* - C_0) * V}$$

ρ	density of air (kg/m^3)
Q_{Air}	normal airflow rate (Nm^3/h)
Y_i	inlet mole fraction of oxygen (-)
OTE	oxygen transfer efficiency (%)
β	correction factor for oxygen saturation concentration (-)

C_S^* standard oxygen saturation concentration (g O_2/m^3)

C_0 dissolved oxygen concentration in the aerated tank (g O_2/m^3)

V volume of the aerated tank (m^3)

The standard oxygen saturation concentration is dependent on the hydrostatic pressure of the water column and differences from standard pressure at the test site according to equation 3.2 (Baillod *et al.,* 1986):

(Equation 3.2) $$C_S^* = C_{sT} * \frac{\gamma * H * f + P_{site} - p_{site}}{P_{atm} - P_{std}}$$

C_{sT} oxygen saturation in clean water at 1 atm (g O_2/m^3)

γ specific weight of sludge (kN/m^3)

H tank depth (m)

f fraction of tank depth (measured from the surface) in which pressure corresponds to average saturation concentration (-)

P_{site} atmospheric pressure at test site (Pa)

ρ_{site} saturated water vapor pressure at test site (Pa)

P_{atm} standard atmospheric pressure ($1.013*10^5$ Pa)

P_{std} standard water vapor pressure (2300 Pa)

The oxygen saturation coefficient is temperature dependent according to equation 3.3:

(Equation 3.3) $$C_{sT} = 14.65 - 0.41 * T + 0.0049T^2 + 0.0000778T^3$$

where T is the temperature of the liquid in °C.

Rosso *et al*. (2005) proposed a method for linking the standardized oxygen transfer efficiency in process water to SRT and airflow, using equations 3.4-3.6:

(Equation 3.4) $$\alpha SOTE = A * log\chi - B$$

α alpha factor, correction factor for process water/clean water efficiency (-)

A model parameter (-)

B model parameter (-)

X plant characteristic number (T^2)

(Equation 3.5) $$\chi = \frac{SRT}{Q_n}$$

Q_n normalized air flow (s^{-1})

(Equation 3.6) $$Q_n = \frac{Q_{Air}}{A_{sp} N_d * Z}$$

A_{sp} specific area of diffuser (m^2)

N_d total number of diffusers (-)

Z diffuser submergence (m)

The Irvine Carbon Footprint model also allows for calibration of the energy requirements of the aeration system through equations to calculate the power consumption of the blowers. These calculations are not included in the report since they were not used in the MIKE WEST model.

3.5 Sedimentation sub-model: Takács settling model

Takács *et al*. (1991) described four types of settling characteristics that can be observed in a secondary clarifier: discrete and flocculent particle settling, hindered settling and compression settling. Discrete particle settling is explained as the settling of solids as individual particles that are not effected by other particles, for example the removal of sand. Flocculent particle settling is the flocculation of solid particles, primarily found in the upper layers of the secondary clarifier. Hindered settling is a settling process where particles settle as a unit since the settling of individual particles is hindered by inter-particle forces. Finally, compression settling is the compression of the particle mass caused by the weight of particles.

The Takács settling model defines four ranges of sludge concentration where these settling characteristics are of different importance and are thus primarily governed by different parts of the model equations 3.7 and 3.8:

(Equation 3.7) $$ZSV = v_0 e^{-r_h(X - X_{min})} - v_0 e^{-r_p(X - X_{min})}$$

(Equation 3.8) $$0 \leq ZSV \leq v_0'$$

ZSV zone settling velocity (m/d)

v_0 Vesilind maximum theoretical settling velocity (m/d)

v_0' maximum practical settling velocity (m/d)

r_h settling parameter, hindered settling (L/mg)

r_p settling parameter, low concentration (L/mg)

X sludge concentration in the zone (mg/L)

X_{min} minimum attainable suspended solids concentration in effluent (mg/L)

According to the model, no settling occurs in zone I, where the concentration of suspended solids is below X_{min}. In zone II, which ranged from X_{min} to X_l, settling primarily occurs in the form of slow individual particle settling and the settling velocity is mainly influenced by r_p. Zone III, between X_l and X_u has a concentration-independent settling velocity, the maximum practical settling velocity v_0' since floc particles in this range reach their maximum size. The final range (zone IV), concentrations greater than X_u, is mainly influenced by the hindered

settling parameter r_h. In this range the settling velocity will gradually decrease as the suspended solids concentration increases (see Figure 5).

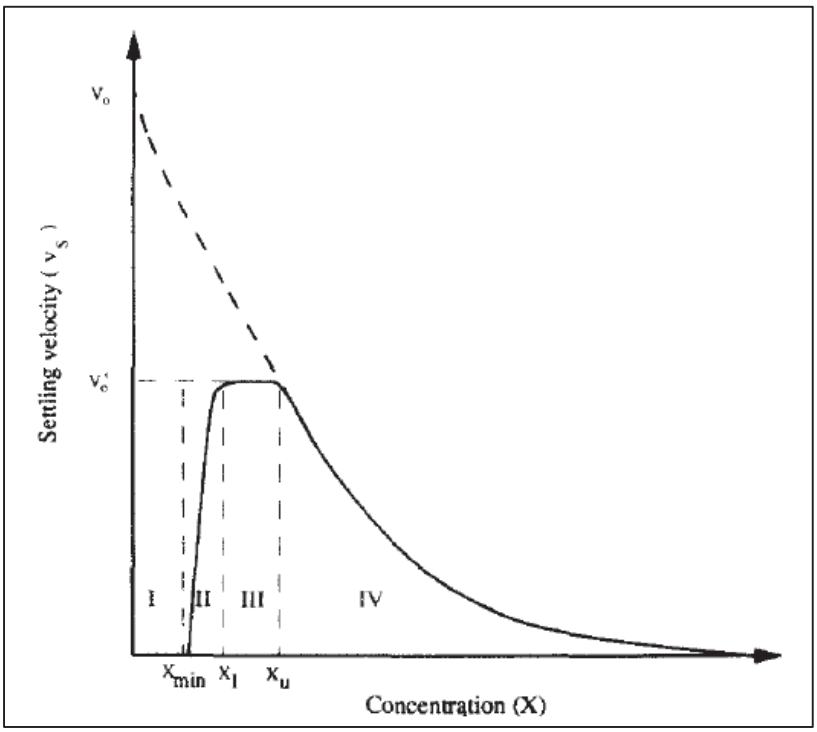

Figure 5 Settling velocity, represented by the solid line, of activated sludge at different concentrations according to the Takács settling model. The four ranges with different settling properties in the Takács settling model are defined as: I. No settling. II. Slow individual particle settling. III. Maximum settling velocity. IV. Hindered settling. The hindered settling velocity is based on the Vesilind settling model, shown in the figure as the thick dotted line v_0. Figure from Takács et al. (1991). Used with permission from Elsevier.

4 Materials and methods

4.1 Outline of the project

4.1.1 The GMP Unified Protocol

In 2013 an IWA task group on good modelling practices proposed the Good Modeling Practice (GMP) Unified Protocol as a framework for modelling activated sludge processes. Five general steps are presented in the protocol (Rieger *et al.,* 2013):

1. Project definition
2. Data collection and reconciliation
3. Plant model set-up
4. Calibration and validation
5. Simulation and result interpretation

The GMP Unified Protocol was used with some modifications to the order of steps being made to manage the time constraints of the project. The modified approach used in this project can be summarized into the following steps:

1. Project definition
2. Data collection and reconciliation
3. Plant model set-up
4. Calibration
5. Initial simulation
6. Full-scale tests and further data collection
7. Validation and re-calibration
8. Final simulation and result interpretation

4.1.2 Implementation of the GMP Unified Protocol in project

Step 1: Project definition

The project definition was discussion in section 1 Introduction.

Step 2: Data collection and reconciliation

The process of characterizing the incoming wastewater was based on the data collection methods used by Martinello (2013) and Polizzi (2013) during their similar modelling projects at Sjölunda WWTP. Historical and current sensor data were collected from the wastewater treatment plant's database. Two high resolution (2 hour samples) characterization campaigns were performed in February 2015 and in May 2015 to provide data for calibration and validation of the model. A low resolution 24-hour flow-proportional sampling campaign was performed in between the characterizations in order to evaluate full-scale tests of aeration strategies.
Based on recommendations from Lysberg and Neth (2012) and Henze *et al.* (2000) supplementary oxygen uptake rate tests were carried out to characterize COD fractions. In addition, experiments to determine settling properties were carried out in connection to, and after the conclusion of the sampling campaigns.

Step 3: Plant model set-up

A model of the activated sludge process at Sjölunda WWTP was created in the wastewater modeling software MIKE WEST using plant data from the data collection phase. The model included five activated sludge basins and a secondary clarifier, representing one activated sludge line. Three sub-models were included to simulate the chemical and biological processes in the activated sludge, aeration and settling. Fractionation models were used to estimate different compound fractions and concentrations in the influent and effluent.

Step 4: Calibration

The model was calibrated using data from the activated sludge line G2:1, and was recalibrated to better match the aeration system used in line G1:1. The calibration made use of effluent and waste sludge data from the first characterization campaign to match model values with real measurements. Target values from Rieger *et al.* (2013) were used as a guideline to determine when the model was well calibrated.

Step 5: Initial simulation

Initial scenario simulations on different aeration strategies were run in the calibrated MIKE WEST model as a means to find an aeration strategy that showed promise and could be tested in full-scale. Strategies were evaluated based on a number of different factors, and a large part of the simulation phase was to determine which factors would be most useful to study.

Step 6: Full-scale tests and further data collection

Full-scale tests of three different aeration strategies were performed as part of the 24-hour flow-proportional sampling and second characterization campaigns, to provide data necessary for the validation of the MIKE WEST model. The aeration strategy in use at Sjölunda, with low dissolved oxygen concentrations were compared to an older, high DO aeration strategy. A third strategy, based on optimization results from the initial simulation was then tested.

Step 7: Validation and re-calibration

Data from the second characterization campaign was used to validate the model for two different aeration strategies. The model was shown to perform poorly during the validation process and there was too little time left in the project to properly re-calibrate the model. The problems with the model were instead identified, and suggestions for how the recalibration could be performed were presented.

Step 8: Final simulation and result interpretation

Since the model could not be validated it could not be used for a final simulation of optimized strategies. Instead, the results from the full-scale tests were evaluated, and optimization strategies were suggested.

4.2 Data collection

4.2.1 Availability of plant data

There are a number of sensors in each activated sludge line which feed measurement data to the wastewater treatment plant's database. Flow sensors are found in the inflow channels to

each block ($G1_{in}$ and $G2_{in}$), in the return sludge flow channels (G1:1, G1:2, G2:1) and on the overflow weirs of the waste sludge (G1:1, G1:2, G2:1). SS sensors are found in zone 5 of each activated sludge line. Since line G2:1 has an SRT controller, additional sensors measures SS in the waste sludge and in the effluent from the line.

DO and air flow sensors are found in, or connected to, every aerated zone (zones 3-5 in each activated sludge line). The SS and DO sensors are placed close to the outflow from each zone, and the zones are assumed to be perfectly mixed.

Sensor measurements are stored at a time interval of 1/minute in the database, and in the model five minute averages for all sensor measurements were used.

Temperature gauges, which measure both water and air temperature can be found in a subsequent biological treatment step, and the temperatures were assumed to be similar enough to the actual temperatures in the activated sludge process that the gauge measurements could be used in the calibration of the model.

In addition to sensor measurements Sjölunda WWTP has its own laboratory, which conducts analyzes on a large number of different compound concentrations at an average interval of one to three times per week. The need to gather high resolution data to properly calibrate the model led to a series of experiments being planned and carried out as part of the project (see Table 2).

Table 2 Sources of the different parameters and variables used in the model.

Parameters/variables	Source	Note
Concentrations: COD, COD filtered, TN, TP, PO_4^{3-}-P, Acetate, Propionate, NH_4^+-N, $NO_{2,3}^-$-N, SS_{in}, SS_{eff}, SS_{zone5} , SS_{waste} Alkalinity (HCO_3^-)	Characterizations in February, May 24-hour flow-proportional sampling campaign in April-May	
Flow rates: Inflow, return sludge flow, waste sludge flow, airflow zones 3-5 **Concentrations:** $SS_{zone\ 5}$, SS_{waste}*, DO**	Sensor measurements	*Only used in the initial calibration of the model. **Found in the aerated zones 3-5
Physical properties: T_{air}, T_{ww}		
COD fractions: X_H, S_S	OUR experiments (Wentzel)	
COD fractions: S_A, S_F	OUR experiments (Ekama)	
Settling parameters: SVI, r_H	Settling column tests	
Settling parameters: v0, v00, r_P	Zone Settling Velocity tests	
COD fractions: X_S, X_I, S_I, S_F	Model calibration	
Concentrations: X_{MeOH}, X_{AUT}		
Other parameters: f_{ns} A, B, T_I, K_P		

4.2.2 Accuracy of plant data

Inflow sensor evaluation

Wastewater is intended to be evenly split between blocks G1 and G2, and before the start of the project laser measurements were used to determine that the splitter was within 0.5 cm of its intended location.

The sensors measure the water depth in the inflow channels, and the channels are assumed to have the same cross-sectional areas. However, the flow channels between D1 and blocks G1 and G2 are several decades old, and years of wear could have affected the channels to different

degrees. Fouling could also have influenced the measurements, as solid waste could have stuck to the sides of the channel and altered its shape, thereby causing the flow sensor to overvalue the flow rate.

The presence of a systematic measurement difference between the inflow sensors on blocks G1 and G2 was investigated by comparing daily average flow rates.

The flow sensors were shown to give the same measurements at approximately Q = 400 l/s. At lower flow rates the sensor on $G2_{in}$ would systematically show a higher flow rate than the sensor at $G1_{in}$ during the same days, at higher flow rates the opposite effect could be seen (see Figure 6). A linear function (see equation 3.1) with a very high accuracy ($R^2 = 0.9995$) could be set up to calculate Q_{G2in} from Q_{G1in}:

(Equation 4.1) $$Q_{G2in} = 0.9405 Q_{G1in} + 26.318$$

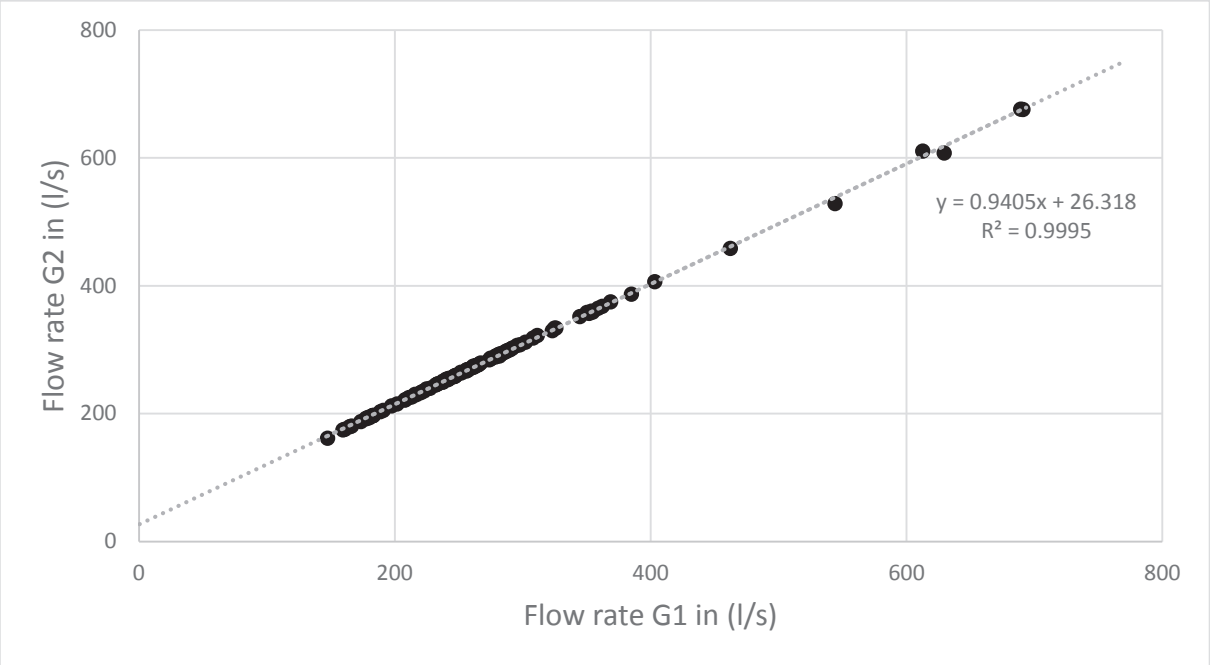

Figure 6 Illustration of a systematic measurement difference between inflow sensors on block G1 and block G2.

Mass balance calculations

Mass balances in a system with defined boundaries can be used as an investigative tool to find errors in measurement equipment or experimental data.

$$Input + Production = Output + Accumulation$$

If the system is studied under steady-state conditions then the accumulation term = 0 (Warfvinge, 2011).

Mass balances for SS, TN and TP were set up for two different system boundaries, bringing the total number of studied mass balances to six per characterization event and activated sludge line. The two system boundaries used was the secondary clarifier (see Equation 4.2 and Figure

7) as well as the entire system (activated sludge basins + secondary clarifier) (see Equation 4.3). This defined the mass balances in terms of measurement data for SS as:

(Equation 4.2) $$(Q_{in} + Q_r - Q_{was}) * SS_{zone5} = Q_r * SS_{was} + (Q_{in} - Q_{was})SS_{effluent}$$

(Equation 4.3) $$Q_{in} * SS_{in} + Production = Q_{was} * SS_{was} + (Q_{in} - Q_{was})SS_{effluent}$$

Equation 4.2 assumed that the return sludge flow rate Q_r was measured before the removal of the waste sludge Q_{was}. Flow rate sensors were placed before the waste sludge weir in some of the activated sludge lines at Sjölunda WWTP, and the equation had to be adapted for lines where the flow rate sensors were placed after the waste sludge had already been removed.

Equivalent mass balances were set up for TN and TP. Production was assumed to only occur in the activated sludge zones, and not in the secondary clarifier. Furthermore, while some production of SS and TN was expected to occur in the activated sludge process, TP concentrations should be unaffected by production.

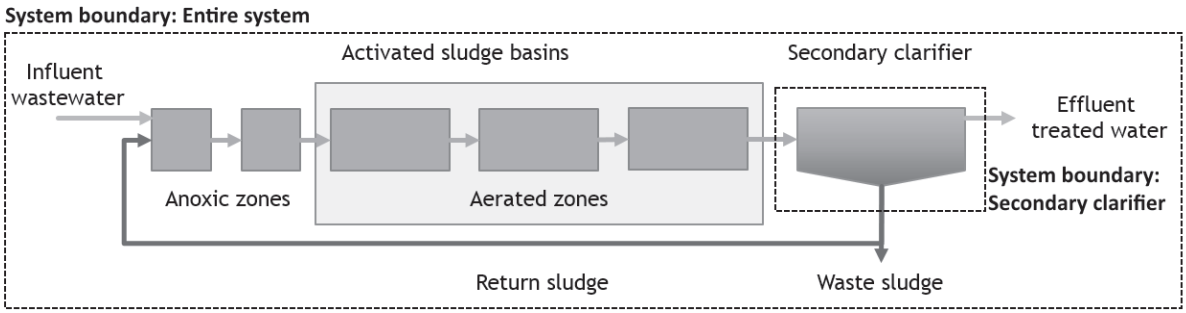

Figure 7 Conceptual model of an activated sludge line at Sjölunda WWTP. System boundaries for the entire system and for the secondary clarifier mass balance equations are shown as dotted lines.

4.2.3 Activated sludge plant characteristics

The activated sludge process at Sjölunda WWTP consists of 9 lines divided into four blocks: G1-G4. Of the blocks, G1-G3 each has two lines with approximately the same dimensions, whereas the three lines in block G4 have a volume that is about as large as the total volume of blocks G1-G3.

The report focuses on the activated sludge blocks G1 and G2, and their connected secondary clarifiers. Wastewater that enters the two blocks come from the same source, the primary clarifier block D1. Each activated sludge line in blocks G1 and G2 consist of five activated sludge basins designated zone 1-5 with volumes of 183, 196, 417, 422 and 385 m^3 respectively. Each line has two secondary clarifiers with surface areas of 233 m^2. The depth of both the activated sludge basins and the secondary clarifier is 3.8 m.

Waste sludge from the clarifiers are recirculated into zone 1 of their connected activated sludge line by six pumps per line (three pumps per clarifier). The pumps work in tandem, and the number of pumps that are active are automatically controlled based on the inflow rate. A part of the return sludge flow, called the waste sludge flow, is removed from the process through an overflow. Line G2:1 has the option to control this waste sludge flow based on the SRT of the

line, while the waste sludge flow in all other lines are controlled by manual selection of flow set-points. The latter solution creates a steady waste sludge flow, but can lead to large variations of the SRT of the process.

The activated sludge process is designed to be able to handle flow rates of up to 4400 l/s (VA SYD, 2014).

4.2.4 The aeration system in the activated sludge plant

Fine pore membrane disc diffusers are installed in all five zones of the activated sludge lines, but it is only practically possible to aerate zones 3-5 without reconstructing the aeration system. Block G1 use ABS Nopon PIK300V diffusers with a surface area of 0.060 m^2 (Sulzer, 2012) while G2 use Xylem Sanitaire Silver Series II diffusers with a surface area of 0.041 m^2 (Xylem, 2011). The number of diffusers and the operational limitation of the airflow in each zone is presented in Table 3:

Table 3 The aeration system in activated sludge blocks G1 and G2: Number of diffusers and airflow capacity.

G1:1		**Airflow (Nm^3/d)**	
Zone	Diffusers	Min	Max
1+2	164	5904	31488
3	168	6048	32256
4	164	5904	31488
5	164	5904	31488

G1:2		**Airflow (Nm^3/d)**	
Zone	Diffusers	Min	Max
1+2	164	5904	31488
3	168	6048	32256
4	172	6192	33024
5	152	5472	29184

G2:1 & G2:2		**Airflow (Nm^3/d)**	
Zone	Diffusers	Min	Max
1+2	224	2688	21504
3	612	7344	58752
4	460	5520	44160
5	320	3840	30720

The distribution of diffusers per zone differs between the activated sludge lines. For lines G1:1 and G1:2 the diffusers are distributed relatively evenly between the zones, with distribution discrepancies mainly being caused by the zones being slightly different in size. For lines G2:1 and G2:2 a distribution strategy in which zone 3 has more diffusers whereas zones 1+2 and zone 5 has a less than average number of diffusers. This distribution strategy is based on practical experience from the treatment plant, where it has been found that airflow demands are higher in the first aerated zone than in the following zones.

The membranes are run at full capacity, which exceed the maximum capacity used under normal operating conditions, for 15 minutes each Tuesday, as part of the maintenance cycle.

During this period each membrane operates at an airflow of 10 Nm^3/h per diffuser disc for membranes in G1 (Gustavsson, 2009) and at 7 Nm^3/h for membranes in G2 (Xylem, 2011).

4.2.5 Characterization campaigns

Two high-resolution characterization campaigns were carried out as part of the project to allow for calibration and validation of the MIKE WEST model.

During the high-resolution campaigns Efcon wastewater vacuum samplers (EN 16479, EN ISO 5667, NEN 6600-1) were placed to gather wastewater from the water channels leading into the activated sludge process and out from the secondary clarifiers of the studied lines. The samplers were configured to collect 70-80 mL of wastewater every 6 minutes, and to rotate between bottles at a 1 hour interval. The collected water was mixed to give a water sample resolution of 2 hours per sample.

The first characterization was performed on activated sludge line G2:1 on February 11-12th 2015, 24 water samples (one every 2 hours) were gathered and analyzed for G2:1 in (D1) and G2:1 effluent respectively. In addition, sixteen sludge samples were collected: eight from aerated zone 5 and eight from the waste sludge. The sludge samples were gathered at 08.00, 10.00, 12.00 and 14.00 each day.

The second characterization was performed on activated sludge lines G1:1 and G1:2 on May 11th 2015. Twelve water samples (one every 2 hours) were gathered and analyzed for G1:1 in (D1) and for both G1:1 and G1:2 effluents. A total of sixteen sludge samples, four zone 5 and four waste sludge samples for each line, were collected at 08.00, 10.00, 12.00 and 14.00.

Water samples from the characterizations were analyzed for SS, COD, COD $filtered_{1.6\mu m}$, TN, NH_4^+-N, NO_2^--N, NO_3^--N, TP, PO_4^{3-}-P and alkalinity (HCO_3^-). Additional tests for COD $filtered_{0.1\mu m}$ and $Iron_{(II/III)}$ were performed on two to three samples per series and characterization event. The standard methods used in the measurements are presented in Table 4:

Table 4 Equipment and standard methods used in the analyzes of different compounds.

Variable	Equipment and standard method
SS	SS 028113 (SIS 1981)
COD	Hach-Lange LCK414, standard method ISO 6060-1989
NH_4^+-N	Hach-Lange LCK303, standard method ISO 7150-1
NO_2^--N	Hach-Lange LCK341, standard method EN ISO 26777
NO_3^--N	Hach-Lange LCK339, standard method ISO 7890-1-2-1986
$Iron_{(II/III)}$	Hach-Lange LCK320, standard method DIN 38405-D17

Samples were filtrated using 1.6 µm glass microfiber discs from MGA Munktell Filter AB, Falun, Sweden (art 410124). Supplementary tests were performed for SS and COD using 0.1 µm cellulose nitrate membrane filters from Whatman International Ltd, Maidstone, England (cat 7181-004) and GE Healthcare UK Limited, Buckinghamshire, UK (cat 10402014).

Nitrogen analyzes using Hach-Lange LCK cuvettes were read in a Hach-Lange DR2800 spectrophotometer while COD and Iron was read using a Hach-Lange DR 5000 spectrophotometer. The COD cuvettes were heated in a Hach-Lange LT 200 block heater.

Sludge samples from zone 5 and the waste sludge were analyzed for SS, COD, TN and TP. In addition, SVI tests were performed on the activated sludge samples from zone 5.

Samples of TN, TP, PO_4^{3-}-P and alkalinity were performed by the accredited laboratory at Sjölunda WWTP. Samples of the filtrate were conserved and sent to the Department of Chemical Engineering at LTH for VFA analysis. The samples were analyzed for acetate and propionate.

In addition to the measurements that were performed to be used in the model volatile suspended solids (VSS), biological oxygen demand (BOD_7), BOD_7 filtrated, total organic carbon (TOC), TOC filtrated and TP filtrated were measured during the first characterization. During the second characterization TOC and TOC filtrated were measured. While these measurements are not used in the report the data could be used in future studies that are based on the results of this project.

4.2.6 24-hour flow-proportional sampling campaign

A 24-hour flow-proportional sampling campaign was performed in between the two characterization campaigns as a means to evaluate the effect of process changes on the treatment efficiency of the activated sludge plant. The sampling campaign was low-resolution, using daily water samples taken 1-3 times per week.

The water samplers were set to collect water based on the wastewater inflow rate from block G1. 20 mL samples were collected for every 100 m^3 wastewater by two samplers placed on the effluents of the sedimentation basins from G1:1 and G1:2, which gave an average sampling rate of 6-10 times/hour depending on flow conditions. Dates to perform the 24-hour flow-proportional campaign were selected to correspond with the Sjölunda laboratory sampling schedule on the activated sludge lines, to ensure that as many measurements as possible were carried out on both the influent and the effluents.

Approximately half of the campaign dates only included SS measurements. The other half included analyses for SS, $SS_{0.1\mu m}$, COD, COD $filtrated_{1.6\mu m}$, COD $filtrated_{0.1\mu m}$, NH_4^+-N, NO_2^--N, and NO_3^--N for the influent and the two effluents of G1:1 and G1:2. SS measurements were also performed on the activated sludge in zone 5 and the waste sludge for both lines during the large measurement events. All measurements were carried out according to the methods described in section 4.2.5.

4.2.7 Sedimentation tests to determine settling properties

Three types of sedimentation tests based on similar methods were used to estimate the settling properties in the secondary clarifier: Zone Settling Velocity, Sludge Volume Index and f_{ns}.

Zone Settling Velocity tests

A practical method for determining the zone settling velocity was presented in Catunda and Handel (1992). Sludge was placed in a graduated cylinder with a slowly moving stirrer. Shortly after the start of the experiment a separation between a sludge blanket at the bottom of the cylinder and a clear supernatant at the top of the cylinder could be observed. Initially, the velocity with which the sludge blanket level decreased was low, but after a few minutes it would

increase significantly before dropping again as the sludge blanket level approached the bottom of the cylinder. The settling rate during the rapid settling phase was determined to be linear, and the rate could then be calculated as the tangent of the height of the sludge blanket plotted against time.

Two adaptations were made in the experiments at Sjölunda. No stirrer was used, since the plant lacked the necessary equipment. Furthermore, since it was often not possible to observe a linear decrease of the sludge blanket level over time in the high velocity phase the zone settling velocity of a particular sludge concentration was instead determined to be the maximum settling velocity between two measurement points. It is possible that these two changes led to an overestimation of the settling velocities of the sludge.

In order to estimate the Vesilind theoretical and practical maximum velocities using limited equipment activated sludge from zone 5 was diluted to create a number of different sludge concentrations. The dilutions were allowed to settle in standardized 1 L graduated cylinders and the sludge blanket level was measured every minute for between 15 and 30 minutes (see Figure 8). The maximum settling velocity, which would typically occur within the first 10 minutes of the experiment, was determined for each dilution, and values were plotted against the sludge concentration. The maximum settling velocities were estimated to be analogous to the zone settling velocities used in the Takács settling model.

Figure 8 Graduated cylinders used for the settling tests. A dark sludge blanket is visible at the bottom of the cylinders, while a clear supernatant has formed at the top.

At low sludge concentrations the sludge blanket level could not be clearly observed during the period in which the maximum settling velocity should have occurred. It was therefore not possible to determine r_P by using the experimental setup, and this settling parameter was instead estimated through calibration of the MIKE WEST model. Catunda and Handel (1992) explained that zone settling does not typically occur in TSS concentrations below approximately 500-1000 mg/L, where solids rather tend to settle individually.

Sludge Volume Index (SVI) tests

A large number of SVI tests were carried out at Sjölunda WWTP in February and May 2015 in order to investigate if the SVI changed throughout the day and to determine if any differences could be noticed between the lines under different operating conditions.

The sludge volume index (SVI) is the volume in mL taken up by 1 g activated sludge after 30 minutes of settling (Dick and Vesilind, 1969). The standard test for determining SVI is to place 1 L of activated sludge in a graduated cylinder and allow the sludge to settle for 30 minutes. The sludge volume is measured at the tip of the sludge blanket and is divided by the concentration of suspended solids:

(Equation 4.4) $$SVI = \frac{SV(30\text{min})\left(\frac{\text{ml}}{\text{L}}\right)*1000}{SS\ (\frac{mg}{L})}$$

Dick and Vesilind (1969) show that the SVI can vary greatly between different plants with similar sludge concentrations, and that factors such as sludge concentration, cylinder diameter and depth influence the SVI. It can therefore be misleading to use SVI as a tool to determine settling properties of activated sludge. Nevertheless, the ease with which an SVI test is performed has led to SVI, changes in SVI over time might indicate that the properties of the sludge has changed and that further analysis of the settling properties are necessary.

Daigger and Roper (1985) introduced a method for partial estimation of the settling velocity from SVI using the Vesilind settling velocity model:

(Equation 4.5) $$V_i = V_0 e^{-kC_i}$$

k is found to be highly dependent on SVI over a wide range of sludge samples. However, since Daigger and Roper only studies sludge concentrations over 2000 mg/L – a range in which the settling velocity is primarily governed by the first exponential term in equation 3.6 – k can be seen as analogous to r_h. This gives an expression for the dependency between r_h and SVI:

(Equation 4.6) $$r_h = \frac{0.148+0.00210*SVI}{1000}$$

Fraction of non-settleable solids

A simple method for estimating the fraction of non-settleable solids was devised and performed during the second characterization campaign. The experimental setup was similar to the SVI and ZSV tests.

Activated sludge from zone 5 in the activated sludge lines were allowed to settle in a 1L graduated cylinder for 20-24 hours. Afterwards, the sludge blanket level was typically very low, and a large amount of clear supernatant had formed above the sludge blanket. Some of the supernatant was carefully sampled from the cylinder, so as to remove liquid from the topmost portion of the cylinder, and an SS analysis was then performed on the sample. The fraction of

non-settleable solids was calculated as the quotient of the SS concentration in the supernatant divided by the SS concentration in the sludge prior to the start of the experiment.

It was theorized that this test would give an indication on the minimum obtainable SS concentration in the settler, since the settling time was significantly longer than the hydraulic retention time of the secondary clarifiers, which was on average 3.6 hours in the secondary clarifiers on block G1 and G2.

4.2.8 Oxygen Uptake Rate (OUR) tests to determine COD fractions and kinetic parameters

Three types of OUR tests were performed as part of the characterization of wastewater: a method to determine the fraction of heterotrophic bacteria using only influent wastewater (Wentzel *et al*., 1995), a method using activated sludge and acetate to estimate kinetic parameters (Hagman and la Cour Jansen, 2007) and method similar to Hagman and la Cour Jansen, but using wastewater instead of acetate as the carbon source (Ekama *et al*., 1986). All tests were performed multiple times with sludge and wastewater that were sampled from different lines at different times of the day, to increase the chances of finding variations. A total of 16 OUR tests were performed as part of the characterization: six Wentzel tests, three Hagman and Jansen acetate tests and seven adapted Ekama wastewater tests.

The same experimental setup, based on Hagman and la Cour Jansen (2007) was used in all experiments. 450 mL of the solution that was to be tested was added to a 500 mL cylinder that was put in a 20°C water bath. A magnetic stirrer was added and set to turn at 350 rpm to ensure that the solution was mixed. Next, a HACH HQ40d oximeter and an air pump was inserted into the solution, and a constant stream of air was turned on. The solution would initially have a low oxygen rate, but under constant aeration the dissolved oxygen concentration would eventually reach 7-8 mg/L. After some time, the length being dependent on the type of experiment performed, the oxygen level would stabilize. At this point 1.35 mL of 12 mg/L allylthiourea (ATU) was added to inhibit nitrification, while 4.5 mL 0.236 g/L $(NH_4)_2SO_4$ and 5.5 mL 0.044 g/L KH_2PO_4 were added to ensure that there would be no heterotrophic growth hampering due to nutrient limitations. The substances were allowed to mix into the solution, and the air pump was then connected to a 5+5 minute timer, which caused air to flow for 5 minutes, and the flow to stop for the next 5 minutes.

When the airflow stopped, the dissolved oxygen concentration in the batch reactor would start to decline, and after five minutes, when the air was turned back on, the oxygen concentration would begin to increase. The maximum decline rate, expressed in mg O_2/(L*h), of each 10 minute cycle was plotted. Running the experiments for several hours created patterns that could be used to calculate COD fractions of the wastewater.

The acetate tests were intended to enable the estimation of the kinetic parameters b_H (decay rate coefficient), μ_{maxH} (maximum specific growth rate) and K_s (half-saturation coefficient) (Henze *et al*., 2000) but it proved difficult to properly aerate the activated sludge before the addition of acetate which prevented determination of the parameters. The default model parameter values were instead used.

Wentzel OUR

The solution used in the Wentzel *et al.* (1995) experiments was 450 mL of the wastewater entering the activated sludge process. Since the analysis was primarily intended to be used to find the fraction of COD in the influent wastewater that was heterotrophic biomass, which had a much smaller concentration than the active biomass in activated sludge, the experiments took significantly longer time than the other OUR tests. The solution was put under constant aeration until it reached a steady-state dissolved oxygen concentration, a step that took 10-15 minutes. At this point nutrients and ATU were added according to the general OUR set-up, and the 5 minute cycles of aeration and no aeration were started after the substances had mixed with the solution. It was found that it could take eight hours for the biomass in the sample to consume all readily biodegradable organic matter and the experiment would therefore be run for up to 14 hours to ensure that it this event had occurred.

Wentzel *et al*. (1995) devised a method for calculating the heterotrophic biomass X_H in wastewater using an OUR test. The growth of the biomass can be calculated according to equation 4.7:

(Equation 4.7) $$\frac{dX_{H,in}}{dt} = \left(\mu_{H,in} + K_{MP,in} - b_{H,in}\right) * X_{H,in}$$

X_H heterotrophic biomass in influent (mg COD/L)

μ_H heterotroph maximum specific growth rate on readily biodegradable substrate (d^{-1})

K_{MP} heterotroph maximum specific growth rate on slowly biodegradable substrate (d^{-1})

b_H decay rate of heterotrophic biomass (d^{-1})

When equation 4.7 is integrated it becomes equation 4.8:

(Equation 4.8) $$X_{H,in}(t) = X_{H,in}(0) * e^{\mu_{H,in} + K_{MP,in} - b_{H,in}}$$

At time t the OUR can be determined as a function of X_H and $\mu_H + K_{MP}$ according to equation 4.9:

(Equation 4.9) $$OUR(t) = \frac{1 - Y_{H,in}}{Y_{H,in}}\left(\mu_{H,in} + K_{MP,in}\right) * X_{H,in}(t)$$

Y_H heterotrophic yield (mg COD/mg COD)

Substituting X_H in equation 4.9 for equation 4.8 and taking natural logarithms gives equation 4.10:

(Equation 4.10)

$$\ln OUR(t) = ln\left[\frac{1 - Y_{H,in}}{Y_{H,in}}\left(\mu_{H,in} + K_{MP,in}\right) * X_{H,in}(t)\right] + \left(\mu_{H,in} + K_{MP,in} - b_{H,in}\right)t$$

Equation 4.10 is a linear function, and it is therefore possible to determine the y-intercept point and the slope according to equation 4.11:

(Equation 4.11)
$$y - intercept = ln\left[\frac{1-Y_{H,in}}{Y_{H,in}}\left(\mu_{H,in} + K_{MP,in}\right) * X_{H,in}(t)\right]$$
$$slope = \left(\mu_{H,in} + K_{MP,in} - b_{H,in}\right)$$

Rearranging the equation gives equation 4.12:

(Equation 4.12)
$$X_{H,in}(0) = \frac{e^{y-intercept}}{\frac{1-Y_{H,in}}{Y_{H,in}}\left(\mu_{H,in}+K_{MP,in}\right)} = \frac{e^{y-intercept}}{\frac{1-Y_{H,in}}{Y_{H,in}}\left(slope+b_{H,in}\right)}$$

Wentzel *et al.* (1995) estimated that $Y_{H,in}$ = 0.666 mg COD/mg COD and that b_H = 0.62/d, which makes it possible to calculate X_H by plotting the logarithmic function of OUR (mg O_2/(L*h) and determining the slope and the y-intercept point. If the particulate COD (X_{COD}) in the wastewater is known the fraction fX_H can be calculated as X_H/X_{COD}.

Ekama wastewater OUR

Ekama wastewater OUR experiments used the activated sludge to provide the heterotrophic biomass and wastewater from the inlet of the activated sludge process as food for the biomass (Ekama *et al.,* 1986). The activated sludge was taken from zone 5 in the activated sludge blocks G1 and G2. A 450 mL sample of sludge was put under constant aeration for 30-45 minutes, to attempt to ensure that any biodegradable substrates in the activated sludge would be consumed so that it would not influence the results of the experiment. Nutrients and ATU were added to the sludge and the aeration was switched to 5+5 minute on/off cycles. After one and a half to two hours 50 mL of the activated sludge solution would be mixed with 400 mL of the wastewater, and the oxygen uptake rate of this new solution would then be measured. The experiments ran for four to six hours and were found to not reach a steady state OUR in this time.

The first series of experiments used wastewater which had been heated up to 20°C, but which had not been aerated prior to mixing with the activated sludge. Since a small portion of activated sludge, with a dissolved oxygen rate of approximately 8 mg/L, was mixed with a large portion of wastewater with a very low oxygen concentration the oxygen concentration in the solution would rapidly decrease to under 2 mg/L between two measurements as a result of the mixing. This rapid drop was picked up by the oximeter as the oxygen uptake rate of that cycle, and caused disturbances when trying to calculate the COD fractions S_A and S_F. Later experiments attempted to reduce the effect by aerating the wastewater for a few minutes immediately prior to mixing the solutions, but it was found that a significant disturbance still occurred.

When wastewater is mixed into the sludge the OUR will initially be high, as the heterotrophic biomass consumes the readily biodegradable organic matter. When this COD fraction is depleted, the OUR drops rapidly before reaching a plateau. The area above the plateau in an OUR/t diagram, which is the OUR associated with S_S, can be utilized to calculate the readily biodegradable COD.

In the Ekama *et al*. (1986) wastewater OUR experiment the readily biodegradable COD (S_S, or $S_A + S_F$) can be determined through equation 4.13:

(Equation 4.13) $S_S = \frac{1}{1-Y_H} * OUR_{S_S} * t_d * \frac{V_{mL}+V_{ww}}{V_{ww}}$ $(mg\frac{COD}{L})$

Y_H yield coefficient for heterotrophs = 0.67 mg COD/mg COD

OUR_{Ss} oxygen uptake rate associated with oxidation of S_S (mg O_2/L)

t_d time it takes for S_S to deplete after the wastewater is mixed into the sludge (h)

V_{mL} volume of activated sludge (L)

V_{ww} volume of wastewater (L)

4.3 Plant model set-up

4.3.1 Model structure

Two activated sludge lines (G1:1 and G1:2) were modelled in MIKE WEST 2014. Each sludge line included five activated sludge basins (of which two are anoxic and three are aerated), one secondary clarifier, recirculation of activated sludge and outlets for treated water and waste sludge (see Figure 9). Each aerated basin was connected to its own PI-regulators which controlled the airflow into individual aerator controllers. The aerator controllers were included in order to relate the airflow to the oxygen transfer coefficient k_La and thereby allowing calibration of the airflow necessary to estimate power consumption of different aeration scenarios.

The two lines used a common wastewater inlet, mirroring the real situation where the source of both lines is the primary settling line D1 and a splitter was used to distribute the flow between the lines. Flow regulators using real measurements for the return sludge flow and the waste sludge flow was used to control these flows in the model.

As opposed to the real situation, where there were two secondary settling basins per activated sludge line, a single settling basin per line was used in the model. The basins had the same dimensions and since the flow splitter was set up to split the flow evenly a simplified setup, with only one basin that was twice the size of each of the real basins, could be used in the model.

For the model to function properly it was necessary to run steady-state simulations in which the average properties of all components in the model are found. For some components it took several days to reach steady-state values, and since only one to two days of measurement values were available manipulated input files were created. In the new input files the measurements from the characterizations were repeated 15-30 times in order to generate input files that were one month long.

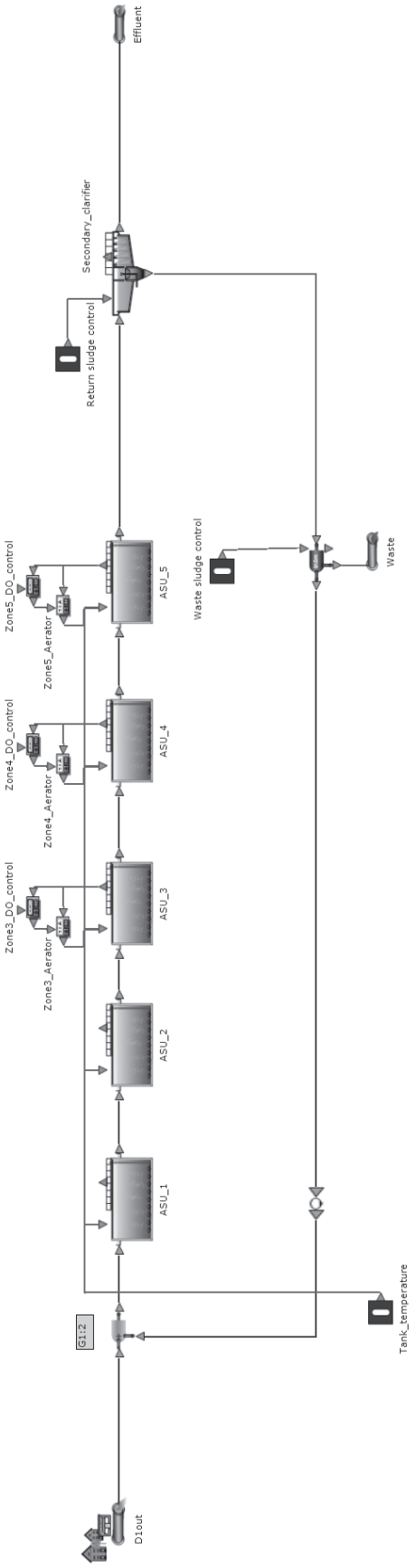

Figure 9 Layout of the activated sludge process modelled in WEST.

4.3.2 Use of sub-models

The WEST model made use of three different sub-models that have been presented in the Literature section of the report: ASM2dModTemp, the Irvine Carbon Footprint model and the Takács settling model with SVI.

ASM2dModTemp (see section 3.3) was used as the over-arching model controlling the process reactions in the activated sludge basins and forming the basis of the fractionation models.

Aerators using the Irvine Carbon Footprint model (see section 3.4) was used to enhance the accuracy of the aeration model, and to allow estimations of the power consumption of different aeration strategies.

The secondary clarifier used the Takács settling model, with an extension for determining the hindered settling parameter r_H from SVI (see section 3.5).

4.3.3 Fractionation model

The input fractionation model that was used in the MIKE WEST model was based on the ASM2d model, but it was possible to make changes to decrease the model's reliance on fractions due to the high number of different compounds that were available from the characterization campaigns (see Figure 10): 11 input variables were transformed into 20 model variables.

The fractionation model used a combination of direct input with or without correction factors, fractionation and fixed value variables. Alkalinity, phosphate, acetate and ammonium nitrogen could be transformed directly from measurement values into model variables without using correction factors, though the acetate used in the input file was the calculated combination of the acetate and propionate concentrations in the measurements from the VFA analyses. S_{NO} was similarly generated by combining the input variable concentrations of nitrate and nitrite-nitrogen. The COD fractions S_F, S_I, X_S and X_I, which could not be directly calculated from measurements, were estimated through model calibration while the fraction for X_H could be estimated from Wentzel OUR tests.

Correction factors were introduced to transform SS into the model variable X_{TSS}, inflow rate into the H2O and COD filtrated 1.6 µm into S_{COD}. Variables with a fixed concentration were used for X_{AUT} and X_{MeOH} based on model calibration. The remaining input variables were kept at their default values (0.01 mg/L) since no additional information was available that could hint towards the concentrations of those compounds.

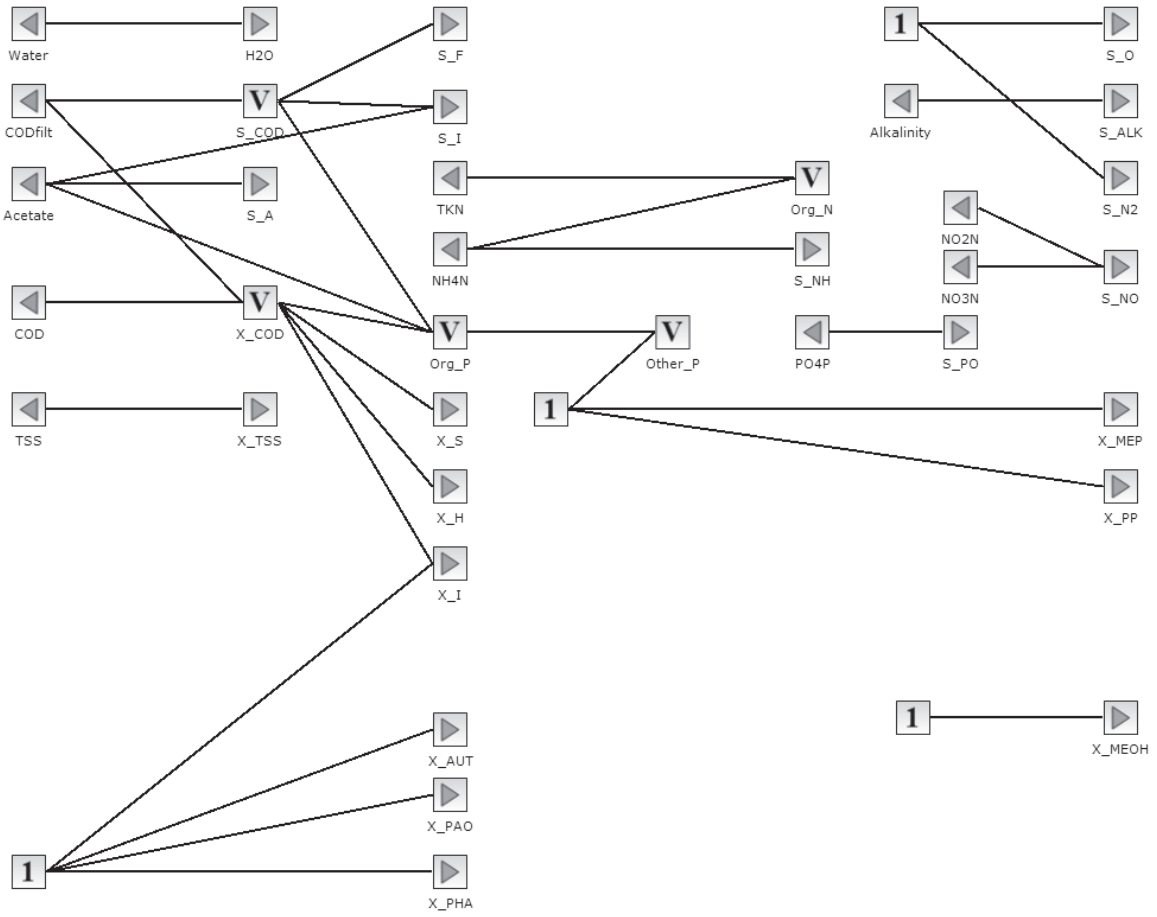

Figure 10 Influent fractionation model in ASM2d, adapted for eleven input variables represented by leftward-pointing arrows.

An output fractionation model was used for the effluent and waste sludge to create model parameters which could be compared to the substances measured in the characterization and grab-sample campaigns (see Figure 11). Since correction factors had been used to transform SS and COD filtrated into model parameters equivalent correction factors were introduced to change S_{COD} and X_{TSS} in the effluent and waste sludge back into COD filtrated and SS. COD, TP, TKN and TN were calculated based on the ASM2d fraction models (see section 3.3.2). Other parameters, such as S_{NH} were found to be directly translatable into their measurement counterparts without requiring correction factors.

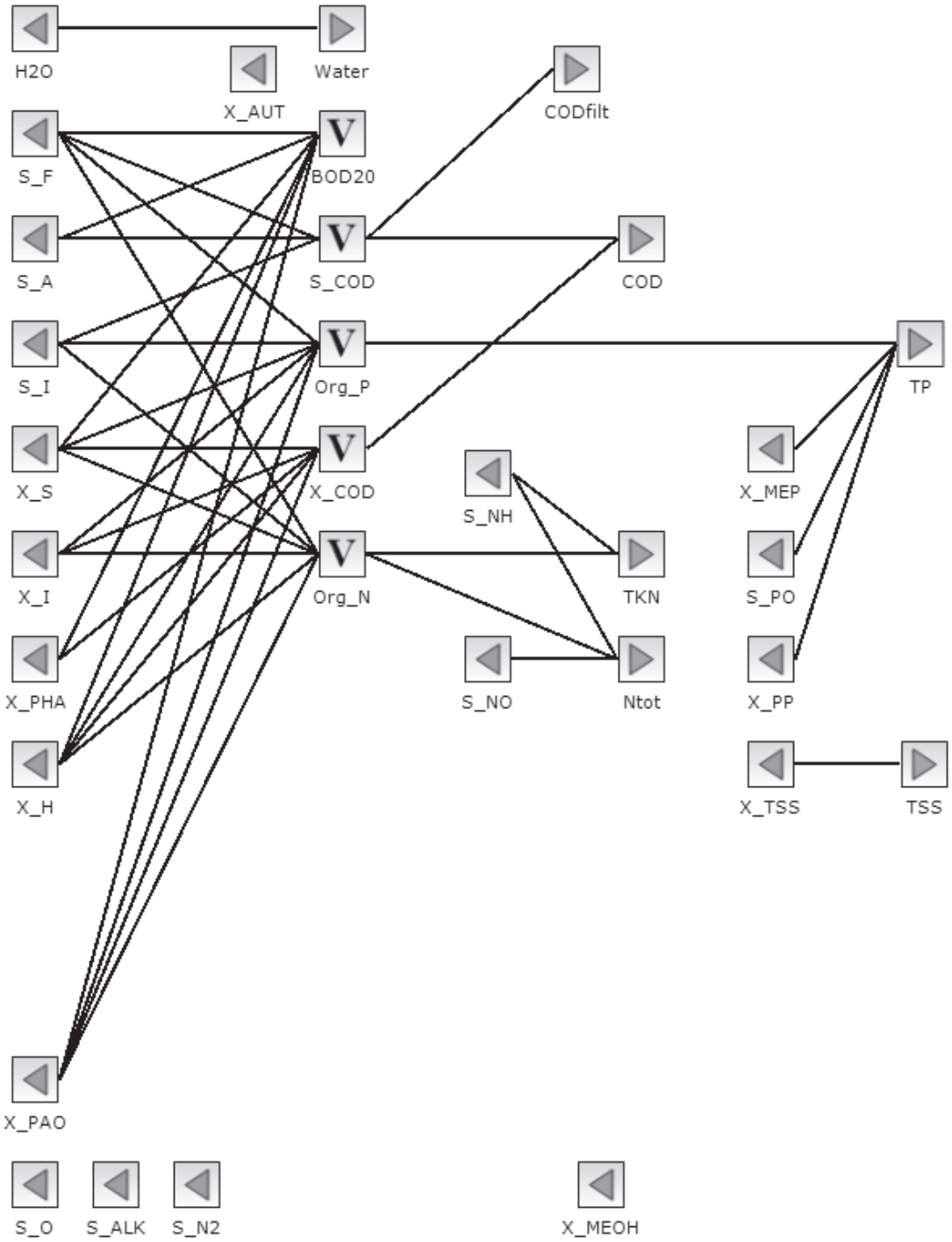

Figure 11 ASM2d fractionation model of the effluent adapted for six effluent variables represented by rightward-pointing arrows.

4.4 Calibration of the plant model

Rieger *et al*. (2013) set three targets that should be met for a well calibrated model developed for aeration control optimization: the airflow rate should be within 10% of the measured values,

the dissolved oxygen profile should be within 0.5 mg/L and the NH_4^+-N concentration in the effluent. Since nitrogen removal was not a desired function of the high-loaded activated sludge process the last target was considered to be non-applicable. Instead, a good match between effluent COD in the model and in the measurements was used as a focus for the calibration.

Additional goals were recommended for calculating sludge production, which were included in the evaluation of the aeration strategies' effects on biogas production. Rieger *et al.* (2013) suggested that acceptable error ranges for monthly steady-state data was 10% for MLSS, 5% mass load for the waste activated sludge, a difference of 5 mg TSS/L in the effluent and an SRT difference of 15%. A 5% error in the MLVSS/MLSS ratio was also recommended, but since the ASM2d model does not include a function to estimate VSS this calibration target was not considered.

In the calibration process changing parameters which could be investigated through experiments was prioritized, while changing kinetic parameters in the ASM2d model was for the most part avoided, since it would have required very extensive experiments to achieve more reliable parameter values than the default model values. The calibration therefore focused on the fractionation models used in the input and output segments of the model, on the sedimentation properties of the secondary clarifier and on fine-tuning the aerators and PI-controllers of the aeration control system. Attempts to estimate kinetic parameters tied to growth of the biomass in the activated sludge process had to be abandoned after it was found that the OUR tests, designed to give experimental data that would allow for such estimations, were inconclusive.

4.5 Full-scale and model scenarios

MIKE WEST includes a scenario analysis tool which makes it possible to simulate the effects of changing sets of model parameters on any number of model variables. The dissolved oxygen set-points of zones 3-5 were used as input parameters, and several hundred sets of parameters were analyzed.

The first characterization was performed on activated sludge line G2:1 which in February 2015 had the same dissolved oxygen set points as line G1:1 – 0.3, 0.8 and 2.0 mg DO/L for the aerated zones 3-5 respectively. Due to lack of high resolution data from G1:1 the data from G2:1 was used to set up and calibrate the model, and the model was then recalibrated to account for differences between lines G2:1 and G1:1.

After the first characterization a full-scale test of changing the aeration strategy to 2.0 – 2.0 – 2.0 mg DO/L in the aerated zones 3-5 was performed on line G1:1. This was an old aeration strategy which had been used at Sjölunda before 2006. A second full-scale test of 0.6 – 0.6 – 1.0 mg DO/L was performed on line G1:2 based on one of the optimized parameter sets found in the model scenario analysis. It was expected that it took at least 7 days for a change in the aeration strategies to have fully taken effect, which limited the number of aeration strategies that could be tested in full-scale.

The model scenarios were evaluated based on treatment efficiency and energy demand whereas the aeration strategies that were tested in full-scale were evaluated based on the four criteria specified in the project aims: treatment efficiency, energy demand, COD/N ratio and biogas production.

4.6 Biomethane potential tests

Two series of biomethane potential (BMP) experiments were performed on waste sludge from Sjölunda WWTP based on an adaptation of the methodology presented in Hansen *et al.* (2004) in order to evaluate if the methane potential is affected by different aeration strategies.

Inoculum from mesophilic full-scale anaerobic sludge digesters at Sjölunda WWTP was collected and placed in an incubator operating at 37°C 3-4 days prior to the start of the experiments. Waste sludge was collected approximately 24 hours prior to the start of the experiment, placed in a refrigerator and was allowed to settle. Since the SS concentration in the waste sludge was relatively low and it was beneficial to the accuracy of the experiment to have an as high mass of volatile solids as possible the supernatant was then carefully removed, so that the sludge was thickened.

A mixture of inoculum and substrate was poured into 2.2 L glass bottles, which were then sealed with rubber septum caps that allowed for removal of gas samples with a syringe without opening the bottles. Three flasks were prepared for each substrate: waste sludge (from one or more activated sludge lines), a reference substance (cellulose), which was used to compare the experiment to other BMP tests, and blanks which only included the inoculum and water. The amount of inoculum and waste sludge or cellulose used in each batch was calculated based on two criteria:

1. The ratio of the mass of volatile solids in the inoculum and the mass of volatile solids in the sludge/cellulose should be 60/40
2. The mass of the volatile solids should be the same in all flasks

Up to 700 mL of each solution was added to the flasks. For the first experiment 380 mL inoculum and 280-320 mL waste sludge, depending on the VS ratio of the sludge, was added to each flask. An amount of 3.4 g cellulose reference, a mixture of 50 % Avicel (Fluka, Sigma-Aldrich, Vallensbaek Strand, Danmark) and 50% cellulose powder (Bie & Berntsen, Rødovre, Denmark), was added to the reference bottles. This gave a total VS mass of approximately 8.4 g in the sludge and cellulose flasks, of which 3.4 g was sludge/cellulose VS and 5 g was inoculum VS. The flasks with blank only had inoculum VS and thus had a total VS mass of 5 g. The same proportions were used for the second experiment, but the VS content in the inoculum was found to only be approximately 4.6 g per flask, which gave a total VS of 8 g per flask. Water was used to fill up the missing volume in flasks where the total volume of the inoculum and sludge/cellulose was less than 700 mL. The flasks were kept in a 37°C incubator for the duration of the experiments.

The methane volume in the flasks was determined by repeated measurements using a Varian 3800 gas chromatograph. 0.2 mL of gas was extracted from the flasks using a pressure tight syringe and added to the gas chromatograph, which returned an area of methane. Triplicate measurements were performed on each flask, and an average area was determined. Values that were not within 2% of the average measurements of the flask were not included in the calculations.

The areas X_m from the gas chromatography measurements were standardized by relating the room temperatures T_m and pressures P_m at the time of the measurement to standard temperature $T_{standard}$ (273.15 K) and standard pressure $P_{standard}$ (1013.25 hPa):

(Equation 4.14) $$X_{STP} = X_m * \frac{T_{standard} * P_m}{T_m * P_{standard}}$$

The volume of methane gas in each flask V could then be calculated by relating the standardized area to the area of a sample consisting of 100% methane gas X_{100} and the headspace, the total gas volume in the flasks, V_h:

(Equation 4.15) $$V = V_h * \frac{X_{STP}}{X_{100}}$$

The methane potential of the waste sludge was evaluated by relating the net accumulated methane volume in the flasks to the mass of the volatile solids in the sludge added at the start of the experiment, according to equation 3.16:

(Equation 4.16)

$$Net\ production\ (NmL\ CH_4/g\ VS) = \frac{\left(V_{acc,flask} - average(V_{acc,inoculum})\right)}{m(VS_{sludge,flask})}$$

The flasks had to be emptied several times during the course of the experiment due to the buildup of pressure, and measurements were then made before and after the emptying in order to determine the volume of methane that had been removed. A needle was used to let out gas, so as to keep oxygen from entering the flasks.

Hansen *et al.* (2004) recommended that the experiments were to run for 35-50 days, but it was established during the first series of experiments that most of the volatile solids from the sludge and cellulose was expended within two weeks of the start of the experiment. The continued methane production after this stage appeared to be almost only a result of the methane production from remaining volatile solids in the inoculum and thus did not change the net production of methane gas. It was therefore concluded that the experiments only needed to be run for between 20 and 30 days.

The concentrations of volatile solids, total solids TS, COD (standard method ISO 6060-1989) and ammonium NH_4^+-N (Hach-Lange LCK303, standard method ISO 7150-1) were determined for each sludge and the inoculum at the start of the experiments. At the end of the experiments TS, VS and COD analyses were carried out on each flask, and NH_4^+-N analyses were performed on one flask per triplicate.

5 Results and discussion

5.1 First characterization campaign

After corrections had been made to the flow measurements (see Section 5.5.1) to account for the systematic error from the flow sensor the measured average flow during the campaign was 120 l/s, 15% lower than the yearly average flow (see Table 5). Data from the flow sensor on $G1_{in}$ was used to calculate the average flow for the period of May 2014 – May 2015, since both line G2:1 and line G2:2 had been turned off during parts of the period, and since the flow sensor on $G1_{in}$ was deemed to be more accurate.

Table 5 Flow rates and temperatures compared to yearly average at Sjölunda WWTP.

	February 10-11	**May 2014 – May 2015**
Inflow per line (L/s)	120	141
Air temperature (°C)	4	11.7
Water temperature (°C)	14	16.8

The SS concentration in the influent was the same in the characterization as in the yearly average, but the daily load was 15% lower due to the difference in flow rates, while the COD concentration was higher in the characterization but the daily load almost the same as in the yearly data (see Table 6). TN and TP loads were both relatively similar to the yearly averages, both being within 10% of the measured average daily load.

Table 6 Influent concentrations and load compared to yearly average (May 2014 to May 2015) at Sjölunda WWTP. The average propionate concentration was below the accuracy threshold of 20 mg COD/L for the analysis method used to determine the concentration.

	Concentrations (mg/L)		**Load (kg/d)**		
	February 10-11	May 2014 – May 2015	February 10-11	May 2014 – May 2015	Diff (%)
SS	138	138	1430	1680	-15%
COD	360	300	3730	3650	2%
COD filtered 1.6 µm	150	95	1560	1160	34%
TN	45	42	470	510	-8%
NH_4^+-N	24.8	25.3	257	308	-17%
NO_2^--N	0.62	1.31	6.4	16.0	-60%
NO_3^--N	0.63	0.51	6.5	6.2	5%
TP	5.0	4.0	52	49	6%
TP filtered 1.6 µm	1.5	0.8	16	10	60%
PO_4^{3-}-P	1.2		12		
Acetate (mg COD /L)	26.7		277		
Propionate (mg COD /L)	*6.7*		69		

Larger differences could be observed in the filtered measurements: COD filtered had a 34% higher load and TP filtrated a 60% higher load in the characterization campaign. Meanwhile,

the nitrite load was 60% lower than in the yearly measurement series, which was to be expected due to the closure of the reject water return flow to block D1.

The total concentration of volatile acids in the inflow was calculated as the combined concentrations of acetate and propionate in g COD/m^3, Propionate measurements which were significantly below the accuracy threshold of the VFA analysis method were included in the calculations. This might have caused the calculated S_A concentrations to become inaccurate, but since the propionate concentrations were 10-20% of the acetate concentration it was considered likely that the error would be larger if propionate had not been included in S_A.

Comparison between the outflow concentrations in G2:1 during the characterization campaign and the yearly average in the effluent concentrations from block G1-G3 shows that the SS concentration in the effluent was higher than normal during the characterization – 26 mg/L versus a normal value of 17 mg/L (see Table 7). The difference was also visible in the treatment efficiency, which was 81% in the characterization, significantly lower than the yearly average of 88%. This could be explained by yearly variations however, since the cold weather during the characterization could have reduced the activity of the biomass.

*Table 7 Effluent concentrations and treatment efficiency of the first characterization campaign compared to the average yearly average at Sjölunda WWTP. * The yearly average for nitrate is negative because there typically is some nitrification, in which nitrate is formed, in the aerated basins.*

	Concentrations (mg/L)		**Treatment efficiency**	
	February 10-11	May 2014 – May 2015	February 10-11	May 2014 – May 2015
SS	26.2	17.1	81%	88%
COD	73	59	80%	80%
COD filtered 1.6 µm	46	40	69%	58%
TN	29	29	36%	31%
NH_4^+-N	21.0	22.5	15%	11%
NO_2^--N	0.012	0.195	98%	85%
NO_3^--N	0.31	1.85	51%	-263%*
TP	1.1	0.9	78%	78%
TP filtered 1.6 µm	0.35	0.36	77%	55%
PO_4^{3-}-P	0.33		73%	

The treatment efficiency of COD was the same as the yearly average, 80%, in the activated sludge process during the characterization, but the effluent concentration was higher due to the influent concentration being higher than normal.

The activated sludge process at Sjölunda is not primarily intended to reduce the nitrogen concentrations, but reductions of all measured nitrogen fractions could be observed. TN was reduced by a third of the influent concentration, and ammonium NH_4^+-N by 15%, both rates being higher than the yearly average treatment efficiency. This gave an average COD/N ratio of 2.5, higher than the desired ratio of 2.0. High nitrite or nitrate concentrations in the effluent could indicate activity by autotrophic bacteria, but both parameter concentrations were low in the February measurements.

The phosphorus concentrations in the effluent and the treatment efficiency was found to be close to the yearly average in the measurement campaign. 78% of TP, and 73% of the phosphate was removed in the activated sludge and secondary clarifier treatment steps.

Initial mass balance calculations with data from the first characterization campaign showed large imbalances. The entire activated sludge process had an influx of SS that was 16% smaller than the out flux, Total phosphorus had a difference of 27% more phosphorus entering the system than leaving it, and for nitrogen the system difference was 15%. TP also had large differences in the secondary clarifier mass balance, 24%.

After adding correction factors to the inflow rate and the TSS concentration in the inflow the system difference for suspended solids was reduced to 1%, TN's mass imbalance was reduced to 11% and TP's difference to 18%. In the secondary clarifier, the mass imbalance for TP was reduced to 15% and for TN to 0%.

5.2 Settling properties

5.2.1 Sludge volume index

A total of sixteen SVI tests were carried out during the characterization campaigns, the first eight on G2:1 in February 2015 and an additional eight SVI tests during the characterization on May 11th 2015: four for each G1 line. The sludge volume index was determined to be on average 123 mL/g in the February measurements, with variations between 110 and 140 mL/g being observed. Non-standardized graduated 1L cylinders, which had a dimension of 6.1 cm as opposed to the standard diameter of 7.7 cm, were used in the February SVI tests, which might have influenced the test results. During the second characterization campaign in May cylinders with the standard diameter of 7.7 cm were used.

SVI tests in the second characterization campaign gave an average SVI of 98.5 mL/g for G1:1, with variations between 94 and 104 mL/g. For G1:2 the SVI was measured to be 92.8 mL/g on average, with variations between 87 and 102 mL/g. While there were large differences in the SS concentrations in zone 5 of the two lines at the time of the second characterization (see Section 5.8) the differences in SVI were comparatively small between G1:1 and G1:2.

5.2.2 Zone settling velocity tests

Zone settling velocity tests were performed six times during the course of characterizing settling properties in the secondary clarifier: two tests on line G2:1 at different times of the day on March 24th 2015, and four tests, one on each of the lines G1:1, G1:2, G2:1 and G2:2, on April 22nd 2015. Three tests did not give sufficient data to calculate the theoretical and practical maximum settling velocities according to the Takács model. One of the tests on March 24th did not reach a noticeable practical maximum settling velocity, while the SS of the undiluted sludge of both line G2:1 and line G2:2 was so low in the April experiments that it was not possible to estimate the theoretical maximum settling velocity.

The practical maximum velocity v_0' was observed in the range 1000-1500 mg SS/L. At ranges below 1000 mg SS/L a sludge blanket level was not observable until several minutes into the experiment, at which point most particles had already settled. It was therefore assumed that phase 2 in the Takács settling model, where particles primarily settle individually and not through zone settling, had occurred. The three successful zone settling velocity tests gave practical maximum velocities in the range between 100 and 120 m/d.

The velocity correction factor for slowly settling, small particles (the second term in equation 3.7, see page 12) was not considered when estimating the theoretical maximum settling velocity v_0 during the first experiments. This caused a significant overestimation of the theoretical maximum velocity, which was calculated to be 840 m/d. During calibration the parameter was reduced to 600 m/d for better fitting in the effluent and waste sludge.

In the second series of experiments a trial and error approach was used to estimate the unknown settling parameters v_0 and r_p. Fixed values for r_h, which was calculated from the SVI and v_0' were used and a zone settling velocity curve was fitted to the experimental measurement values by changing v_0 and r_p. It was found that a good fit for both G1:1 and G1:2 could be found by keeping r_p set to its default parameter value of 0.00286 and setting v_0 to 170 m/h (see Figure 12 and Figure 13).

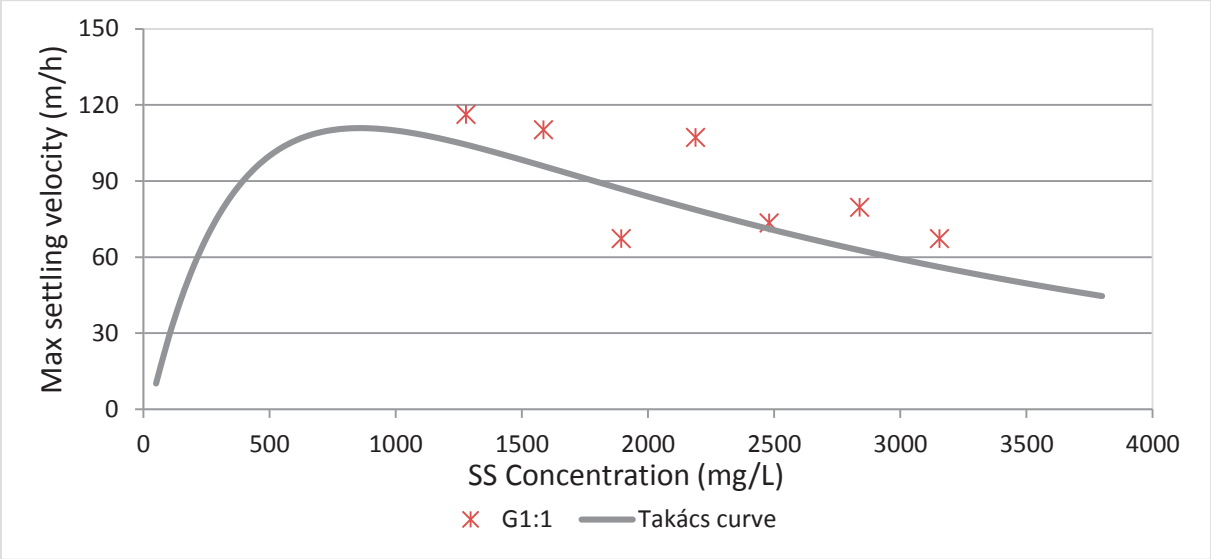

Figure 12 Takács zone settling velocity curve and settling velocity measurements for line G1:1 on May 11th 2015.

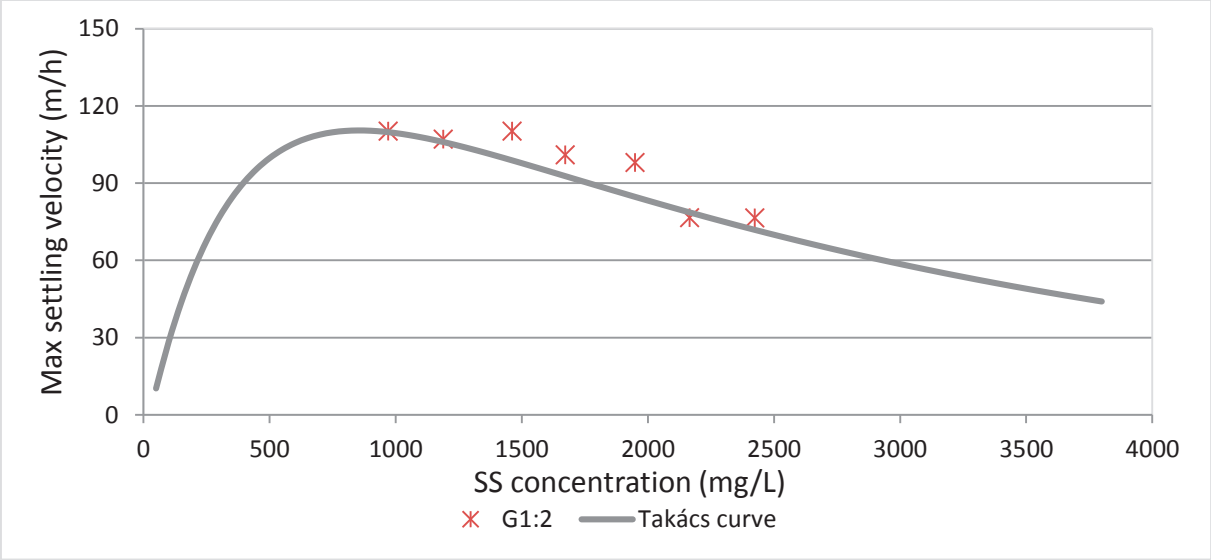

Figure 13 Takács zone settling velocity curve and settling velocity measurements for line G1:2 on May 11th 2015.

5.2.3 Fraction of non-settleable solids

Tests to determine the fraction of non-settleable solids in the secondary clarifier were only performed on sludge from zone 5 during the second characterization campaign. Samples from two different times of the day, 10.00 and 14.00, were taken from lines G1:1 and G1:2. After the sludge had settled overnight the $SS_{supernatant}$ to SS_{zone5} ratio was calculated to be on average 0.011 in G1:1 and 0.016 in G1:2.

5.3 Oxygen Uptake Rate tests

Several oxygen uptake rate tests using Ekama, Dold and Marais method (Ekama *et al.*, 1986) were performed, but only a few tests gave reasonable results. In particular, one test performed during the first characterization campaign looked promising (see Figure 14). Three different plateaus could be seen as the OUR dropped after addition of wastewater, and these were thought to represent the directly biodegradable COD (S_A), the easily biodegradable COD (S_F) and the slowly biodegradable COD (X_S). The area down to the first plateau represented 30 mg COD/L, and this value corresponded well with results from the VFA analysis, which had determined S_A to an average of 32 mg COD/L. The second area was 22 mg COD/L, but this value was too low to represent S_F since it would have made the inert soluble fraction too big.

Combining the second area with the third area, to 50 mg COD/L, and considering the entire area to be S_F gave a better fraction value. However, the low number of successful OUR tests and the lack of research that supported the theory that both the second and the third area belonged to S_F led to the decision to use calibration and assumptions on the size of S_I to find a likely fraction coefficient for S_F instead of using OUR results.

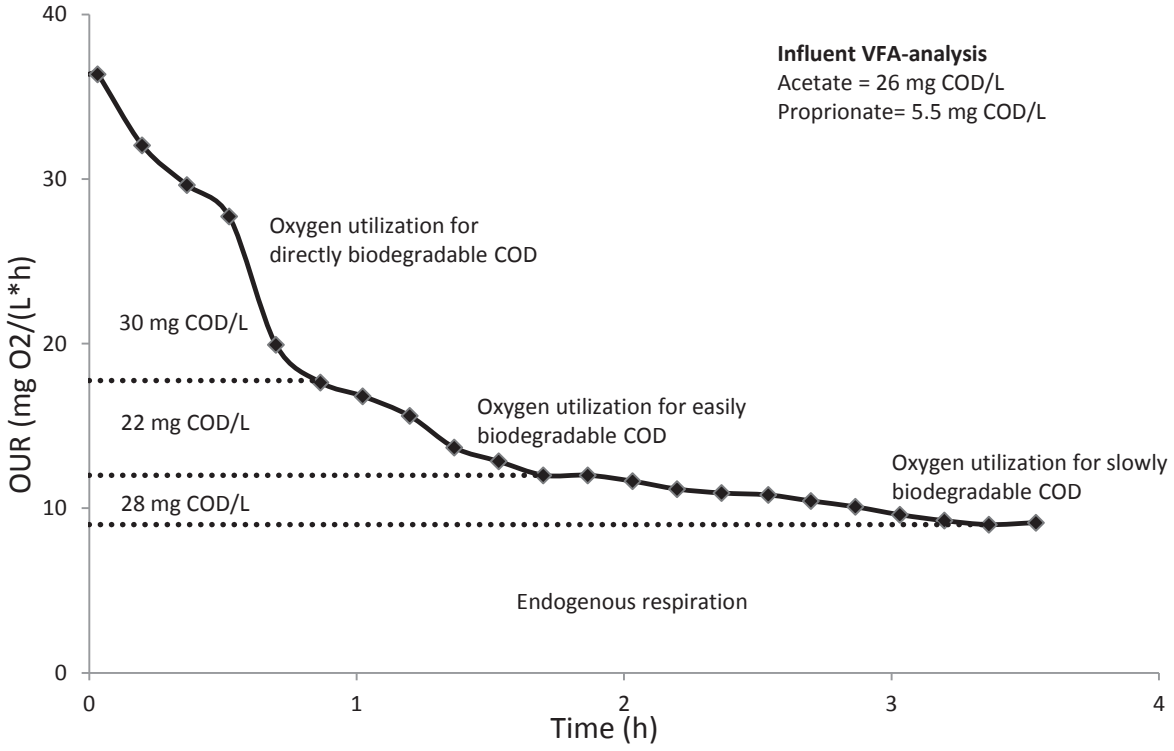

Figure 14 Wastewater batch OUR experiment according to the Ekama, Dold and Marais method (Ekama et al.*, 1986). Figure from Nobel (2015). Used with permission.*

A supplementary Wentzel OUR experiment was performed in February 2015 to determine if the default model fraction for X_H appeared to be accurate. The experiment was run for eight hours, which proved to be just enough time to be able to use experimental data to determine X_H, but not enough time to find S_S (see Figure 15).

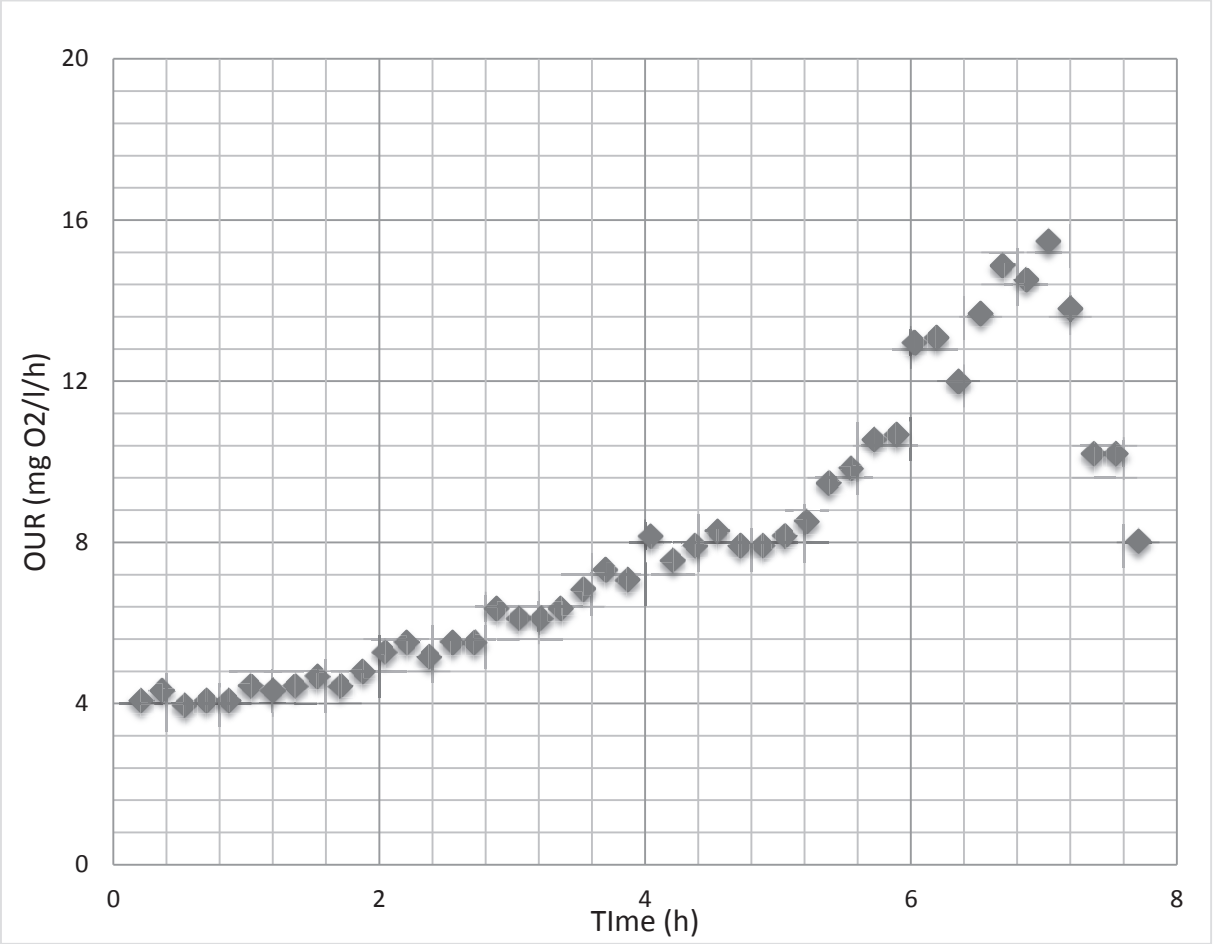

Figure 15 Oxygen Uptake Rate diagram of Wentzel experiment on wastewater.

Y-intercept was found to be 1.2 and the slope 0.205 in the logarithmic OUR over time graph (see Figure 16). Using equations 4.7 to 4.12 it was possible to determine the concentration of heterotrophic biomass in the wastewater to be 28.8 mg COD/L, which corresponded to an X_H fraction of 0.16.

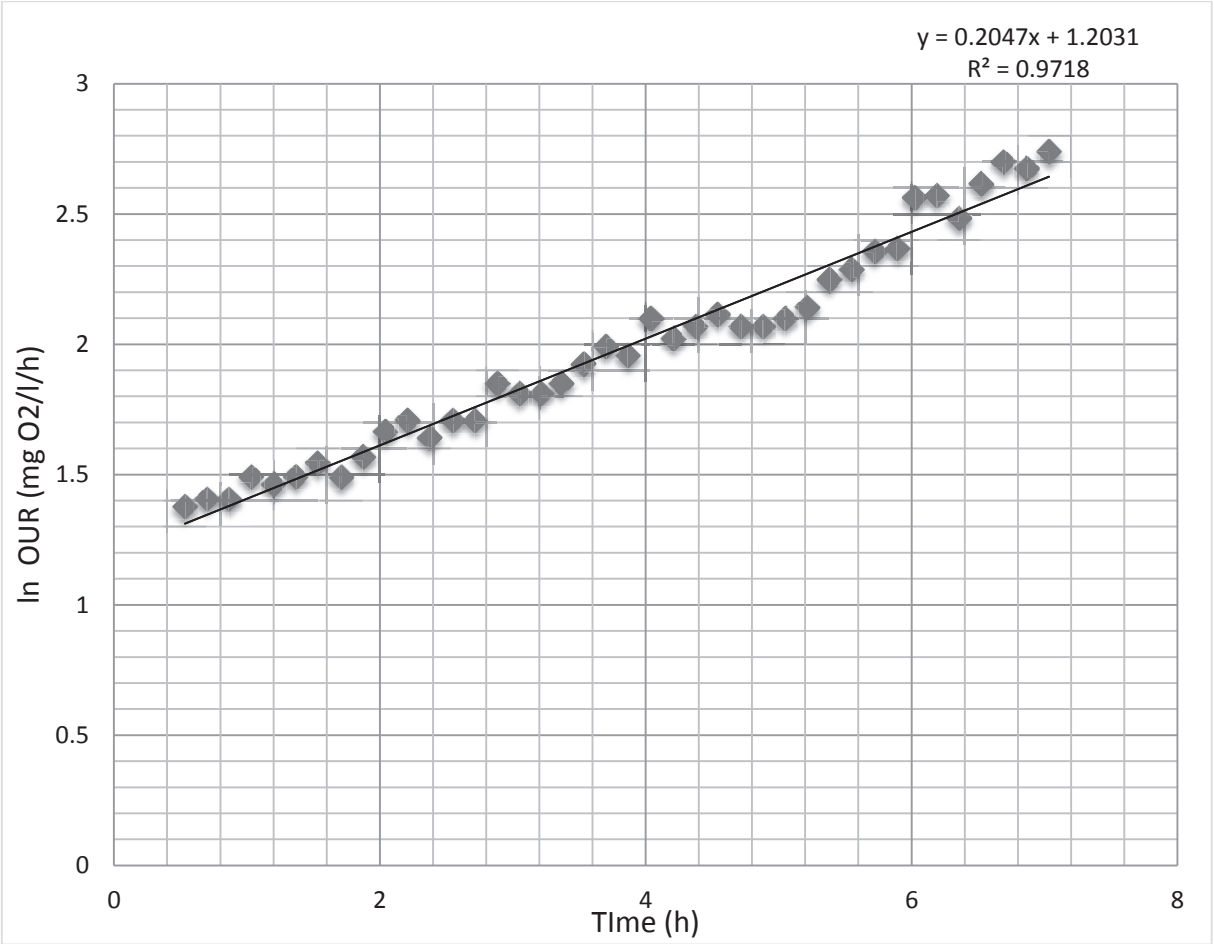

Figure 16 Oxygen Uptake Rate diagram of Wentzel experiment (heterotrophic growth phase) on wastewater, logarithmic scale.

A second series of Wentzel experiments were carried out in connection to the second characterization on May 11th 2015 (see Figure 17). One of the two experiments gave clear results, and from the experiment it was possible to calculate an X_H of 28.6 mg COD/L and a fraction of 0.173. In the second experiment the biomass activity was very low, which was likely due to the sample having been stored without aeration for several hours. The result was therefore not considered to be representative. The average value of the February experiment and the successful OUR experiment in May was determined as 0.17, which was also the default model parameter for X_H, and the value was used in both the calibration and in the validation attempt of the model.

An attempt was also made to use the experiment to determine the readily biodegradable COD S_S graphically, and from that and from measurements of S_A attempt to estimate S_I and S_F. The integral area that represented S_S in Figure 17b was graphically determined as 75 mg COD/L, which would give an S_I value of 66.2 mg COD/L. Since the value for S_I was almost twice as large as the COD filtered$_{0.1\mu m}$ measurements in the effluent the calculations were deemed to give unreasonable values.

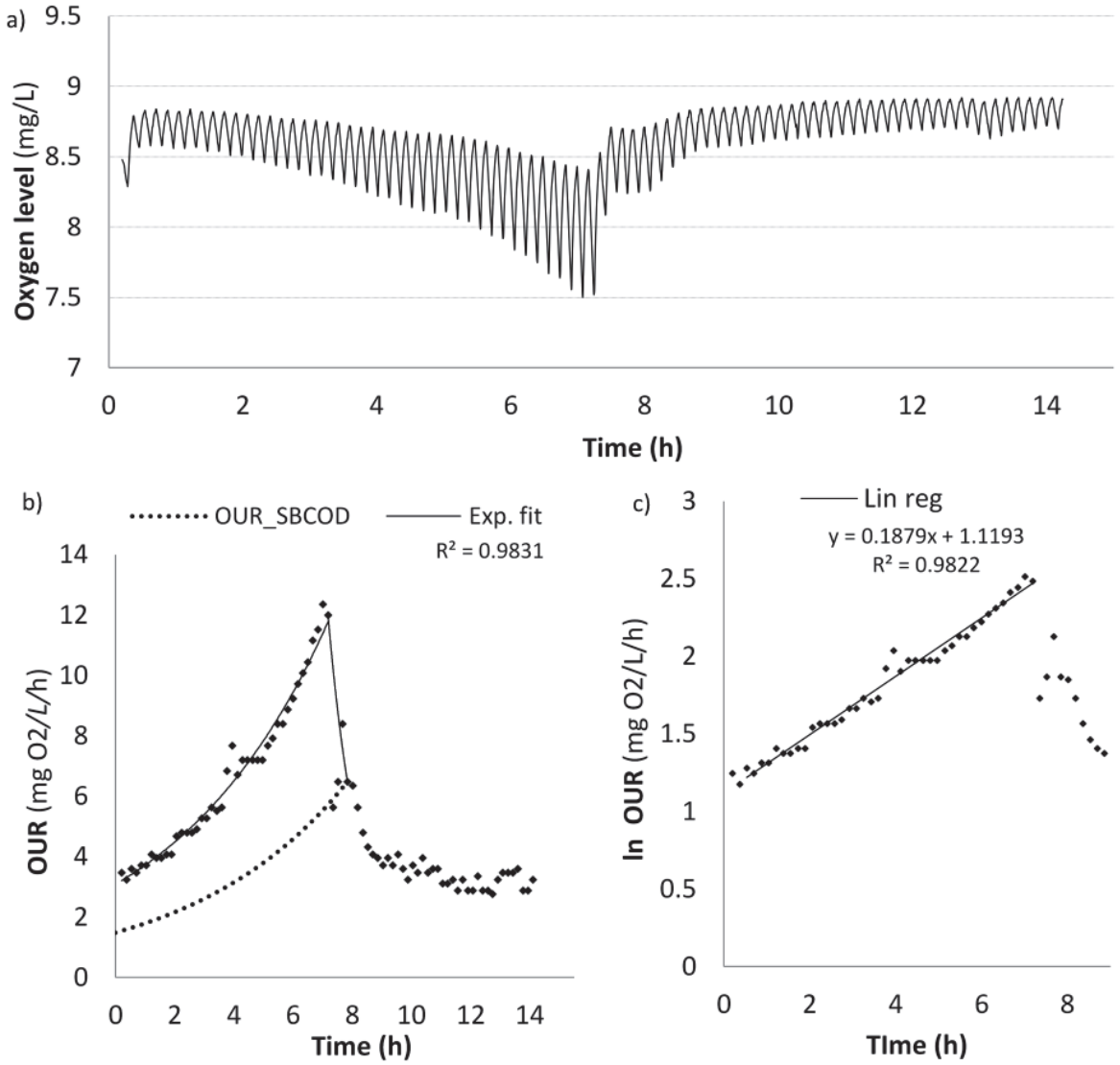

Figure 17 Wentzel experiment from the second characterization on May 11th 2015. A) Oxygen level over time in the solution. B) Oxygen Uptake Rate during the Wentzel experiment on wastewater. C) Oxygen Uptake Rate during the Wentzel experiment (growth phase), logarithmic scale. Figure from Nobel, 2015. Used with permission.

5.4 Biomethane potential tests

Two series of biomethane potential tests were performed as part of the project. For the first series of experiments triplicate batches for waste sludge from lines G1:2 and G2:1, a cellulose reference as well as flasks with only inoculum (blanks); 12 flasks in total were used. One flask with waste sludge from G1:2 and one flask with cellulose were discovered to have leaked gas during the experiment and the two flasks were not included in the calculations of the average methane potential.

The total methane production of the flasks with waste sludge from line G1:2, which at the time of the experiments were using a 0.3 – 0.8 – 1.7 mg DO/L aeration strategy and which had an SRT of 1.2 days, was found to be in the range of 1700 – 1800 mL CH_4 (see Figure 18).

Noticeable deviations between flasks with the same substrate began to occur after approximately two weeks.

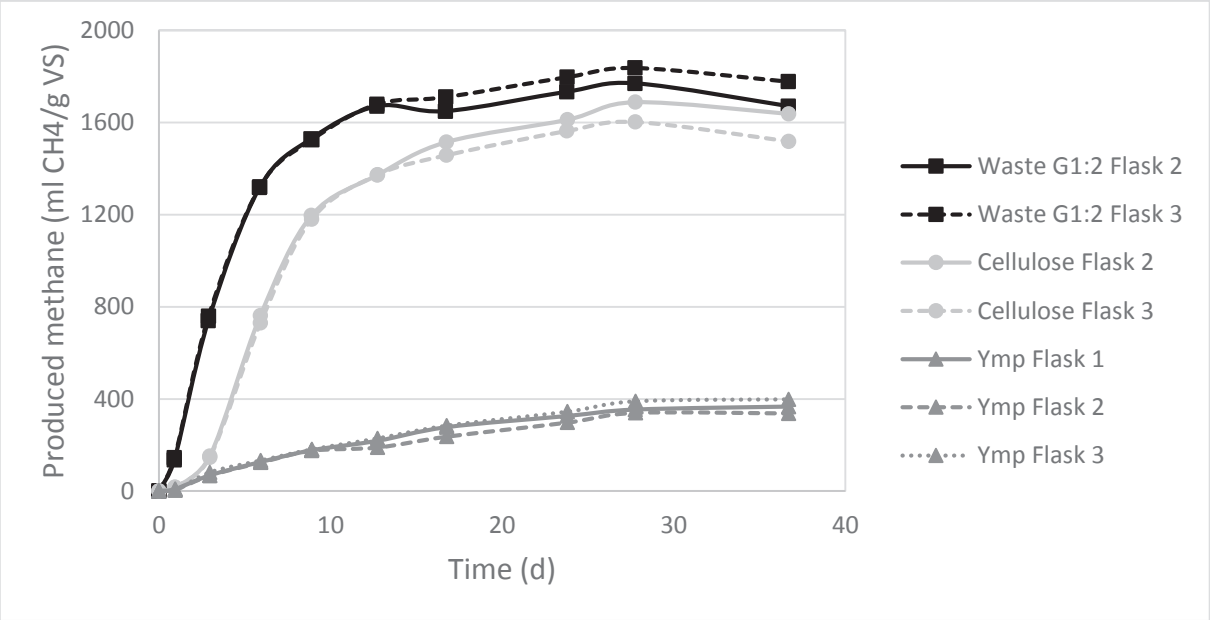

Figure 18 Total methane production in the flasks of the first methane potential series.

When the influence of inoculum had been removed, and the production was tied to the amount of volatile solids in the waste sludge or cellulose reference the net production of methane could be calculated (see Figure 19). The net production in the waste sludge flasks was found to be on average 420 mL CH_4/g VS whereas the cellulose produced 380 mL CH_4/g VS.

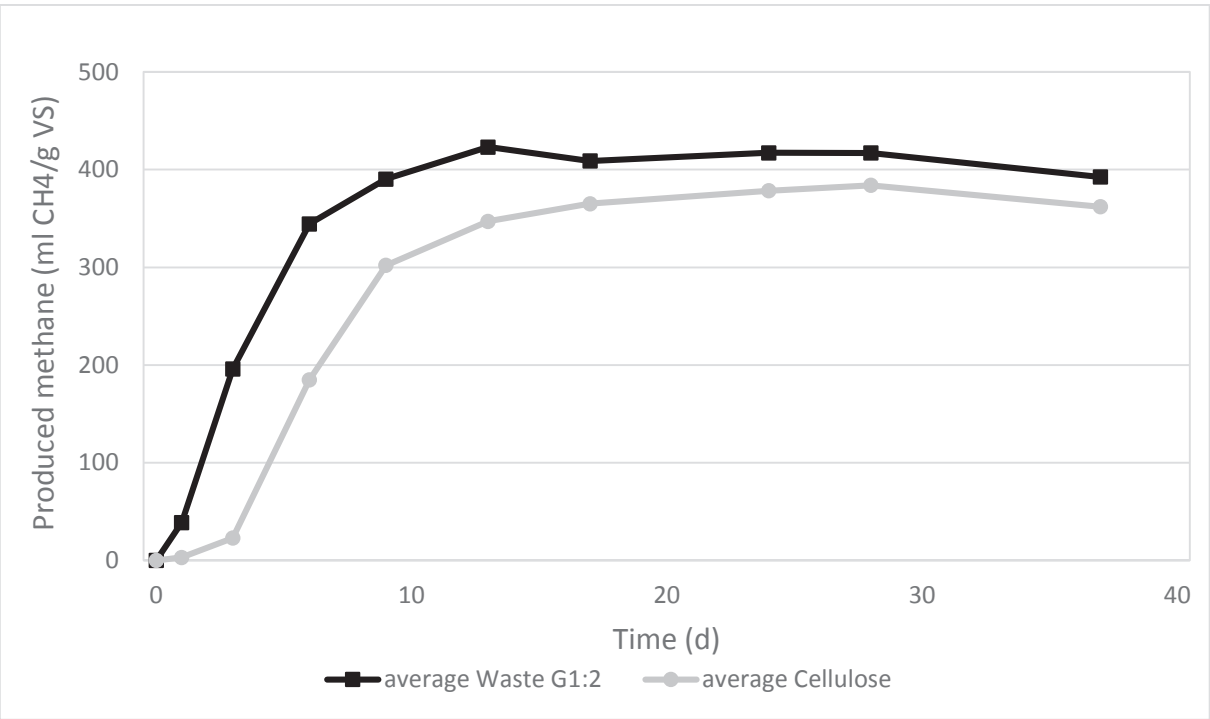

Figure 19 Average net produced methane per g volatile solids from waste sludge from G1:2 and from the cellulose reference in the first BMP experiment.

The second series of experiments used waste sludge from lines G1:1, G1:2, G2:1 and G2:2, a cellulose reference and flasks with only inoculum. Three flasks were prepared for each type of carbon source, bringing the total number of flasks to 18. The same experimental setup was used for both series of experiments. Line G1:1 used a set-point configuration of 2.0 – 2.0 – 2.0 mg DO/L (high aeration) whereas line G1:2 used a configuration of 0.3 – 0.8 – 1.7 mg DO/L (low aeration). The SRT of the two lines was similar – approximately 1.0 days for G1:1 and 1.1 days for G1:2. At the conclusion of the experiment, after 23 days, the flasks from both waste sludge series (G1:1 and G1:2) had reached very similar levels of net produced methane, approximately 430 mL CH_4/g VS (see Figure 20). The cellulose had an average net production of methane of 350 mL CH_4/g VS.

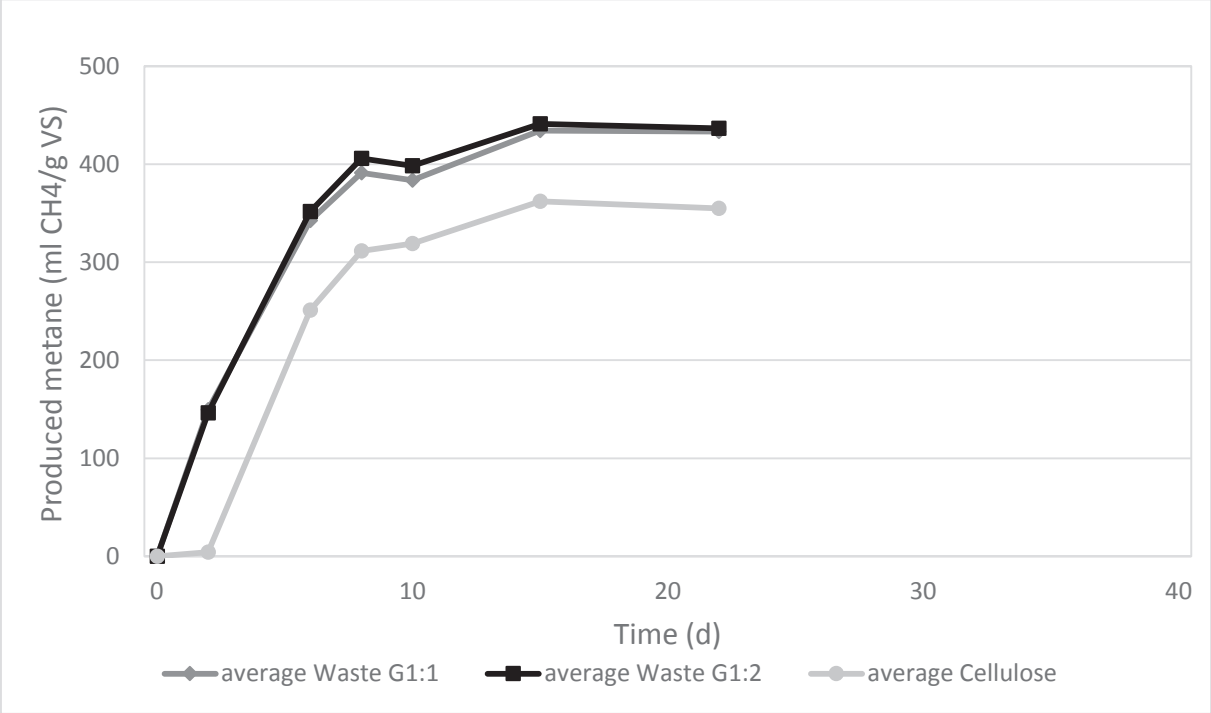

Figure 20 Average net produced methane per g volatile solids in the waste sludge from G1:1 and G1:2 as well as the cellulose reference from the second series of experiments.

The second series of experiments included relatively sizeable deviations from the average production, especially for flasks that used waste sludge from G1:2 (see Figure 21). While it cannot be ruled out that deviations occurred due to leakage or some other hindrance the deviations were significantly smaller than for the two flasks in the first series of experiments that almost certainly leaked.

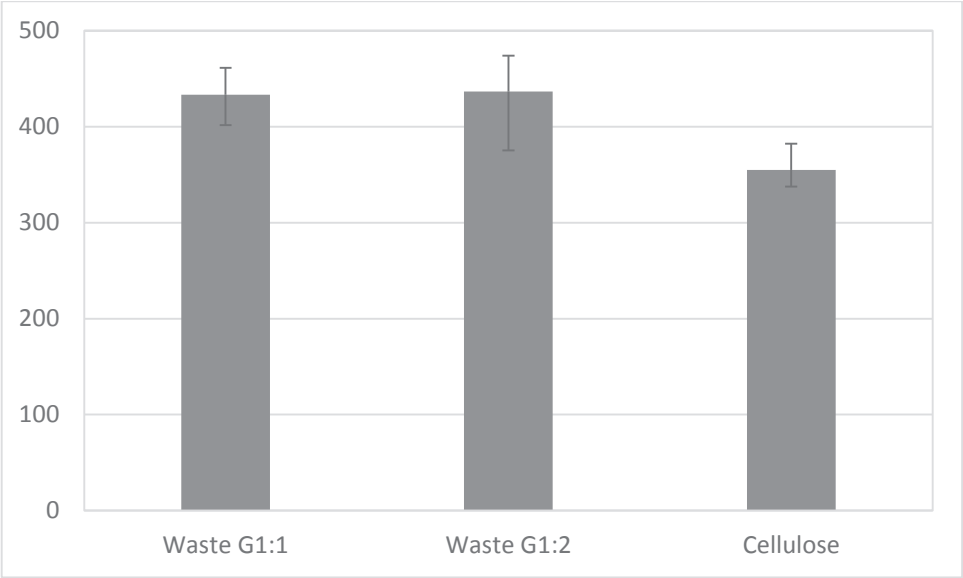

Figure 21 Average values and deviations of single flask net produced methane per g volatile solids from the average production in the second series of experiments. Flasks with waste sludge from G1:2 had the largest deviations, with total methane production between 370 and 470 mg CH_4/g VS.

Based on the results from the second series of experiments no significant difference could be found in the biomethane potential of the activated sludge from lines G1:1 and G1:2. Since these two samples represented two outlier set-point configurations for aeration, G1:1 having very high aeration while G1:2 had low aeration, it is unlikely that an aeration strategy can be found that noticeably optimizes the biomethane production.

5.5 Model calibration

The initial calibration of the MIKE WEST model was split into six parts – the calibration of flow rates, the calibration of the aeration system (airflow and dissolved oxygen concentration) as well as the calibration of the pollutant concentrations in the influent wastewater, in the aerated zone 5, in the waste sludge and in the effluent for G2:1. The model was then recalibrated to fit physical conditions in line G1:1.

5.5.1 Flow rates

Line G2:2 was shut down due to maintenance during the characterization campaign on February 11th-12th 2015, which meant that it could be assumed that the flow gauge on the inlet to the G2 block measured the flow into only line G2:1, and not into both lines.

Since the mass balance calculations for G2:1 showed that the flow gauge likely gave values that were 15-20% too high the flow gauge on $G1_{in}$ was assumed to give the actual flow rate. The relationship between the flow gauges on lines G1 in and G2 which was found in Figure 6 could be used to estimate the actual flow rate of $G2_{in}$. The flow measured by the flow gauge was on average 141 L/s, which translated into 120 L/s, or 85% of the measured flow rate. The fractionation model was altered to reduce the flow rate to 85% of the measurements in the input file.

The inflow pattern was very similar for both the days of the measurements – the flow rate started to decrease around midnight and reached a minimum at around 04.00. At 06.00 the flow rate

started to increase up to a peak flow just before noon. Another peak could be observed in the evening at around 20.00. It was dry weather during the measurements, so there was no contribution to the flow rate from storm water. For the majority of the campaign four recirculation pumps were in use, but during the low flow periods in the mornings two pumps were in operation (see Figure 22).

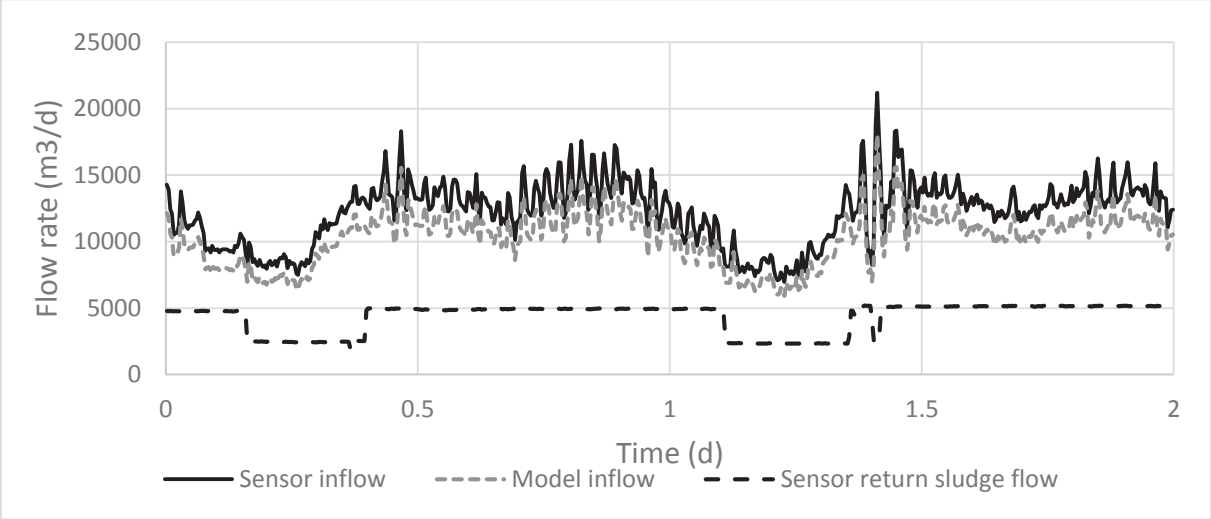

Figure 22 Inflow and return sludge flow rates for the first characterization on G2:1. The model inflow rate was set to be 85% of the inflow rate measured by the flow sensor.

SRT control was turned off during the measurement campaign, and the average sludge age was instead regulated by fixing the overflow chute to let through an overflow around 170 l/s. Some variations occurred anyway, but the waste sludge flow was kept between 155 and 190 l/s (see Figure 23) during the two days.

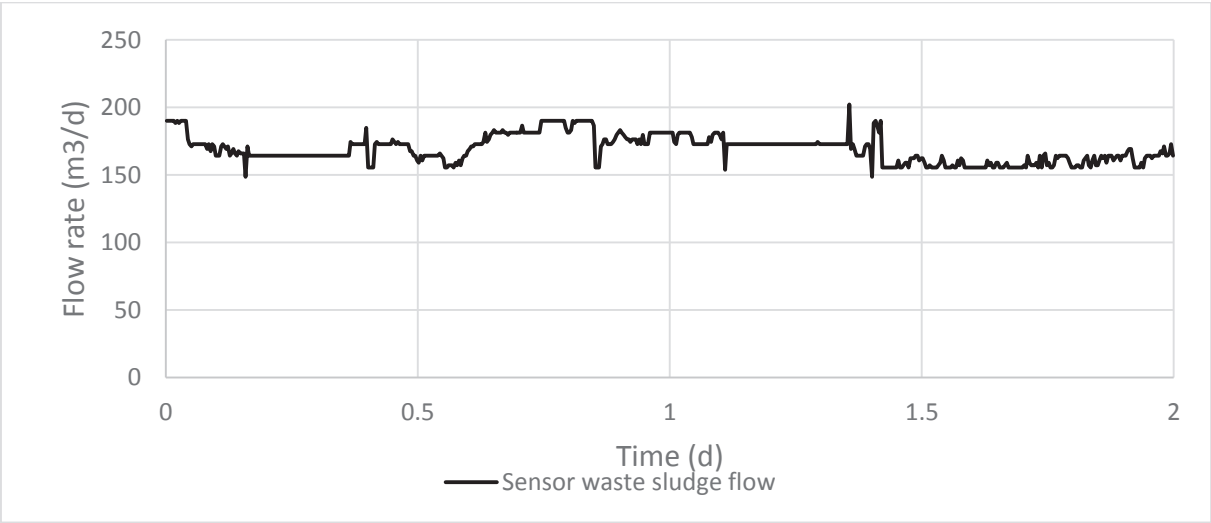

Figure 23 Waste sludge flow for the first characterization on G2:1. The flow rate was relatively stable during the two days of measurements, due to the flow being regulated by an overflow chute.

5.5.2 Influent wastewater calibration

Henze et al. (2000) suggested that the normal analytical methods for determining the concentration of SS in the wastewater undervalued the real total suspended solids content. A fraction of slowly biodegradable substrate, X_S, which is included in the model value for total suspended solids, X_{TSS}, passes through 1.6 µm filters and are not caught in the analysis. Since this fraction will adsorb onto activated sludge in the model both the TSS and the X_{COD}/S_{COD} ratio needed to be modified. Henze et al. (2000) estimated that a measured value of 140 g TSS/m^3 needed to be increased to 180 g TSS/m^3 (29 %) in the model.

The X_S fraction that passed through 1.6 µm filters was assumed to be primarily colloidal, and extra COD analyses were performed as part of the characterization campaign using 0.1 µm filters. These analyses showed that the soluble COD decreased by 10-22% when using 0.1 µm instead of 1.6 µm filters. Calibration of the model and mass balances for suspended solids gave a good fit when X_{TSS} in the influent was set to be 23% higher than the measured SS values (see Figure 24). For COD it was assumed that, on average, 20% of the soluble COD measured samples filtered with 1.6 µm filters were particulate, and a conversion factor between COD filtered and S_{COD} of 0.8 was therefore included in the fractionation model (see Figure 25). Since the same analysis methods were used to determine SS and COD filtered in samples from influent, effluent and waste sludge corresponding correction factors were introduced on outdata from MIKE WEST. The same model TSS to SS correction factor (81%) was used for both the effluent and the waste sludge, and it is possible that the correction should have been smaller for the waste sludge since the correction factors for SS were introduced to catch colloidal particles. These particles can be expected to settle more slowly than larger particles, and the colloidal SS would therefore likely be smaller fraction of total SS in the waste sludge than in the effluent.

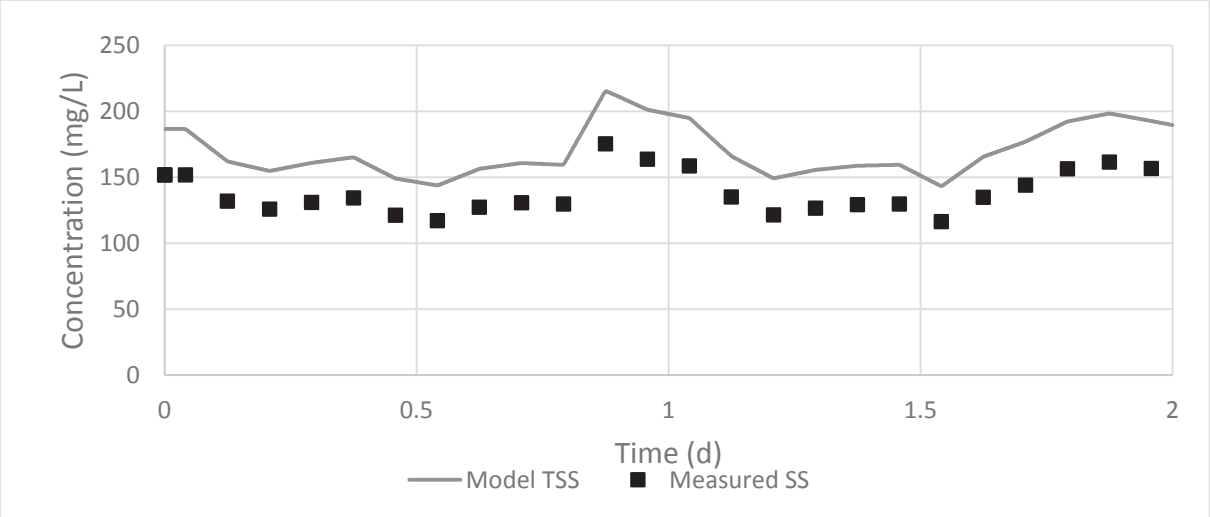

Figure 24 Measured suspended solids and model TSS concentrations in the inflow during the first characterization campaign on G2:1. The model TSS concentration was set to be 23% higher than the measured SS concentration in the inflow, to compensate for colloid particles passing through the filters used in the measurements.

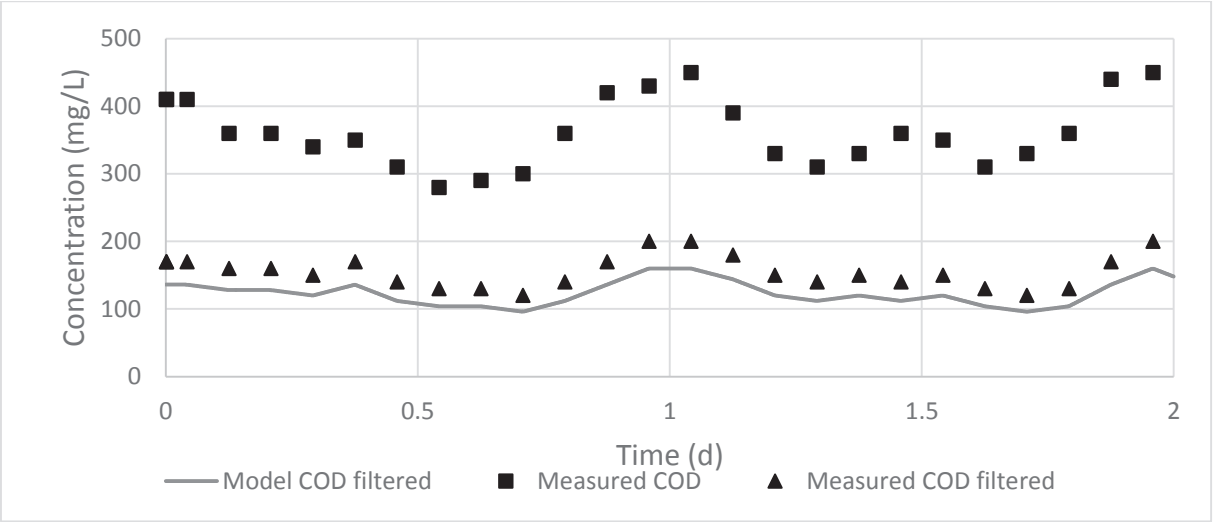

Figure 25 COD, COD filtered and model soluble COD concentrations for the influent in the first characterization on G2:1. The model COD filtered concentration was set to be 80% of the measured COD filtrated concentration, to compensate for colloid particles passing through the filters used in the measurements.

The model COD fractions were determined through a combination of experiments and calibration. The total COD, soluble COD and S_A were available as measurements, and the particular COD could be calculated as the difference between total and soluble COD. The inert soluble COD, S_I, was estimated to be equivalent to 90% of the soluble COD concentration in the effluent from the secondary settler, which translated to 30% of the soluble COD in the influent. This was a slight modification of an assumption that was made by Martinello (2013), who estimated that 90% of the soluble COD in the effluent from the wastewater treatment plant was equivalent to S_I. The modification was made due to the assumption that some soluble COD, which might be inert in the activated sludge process and therefore belong to the model parameter S_I could be degradable in subsequent treatment steps. Having determined S_A and S_I the S_F fraction became 0.43 of the soluble COD, or 15% of the total COD (see Figure 26).

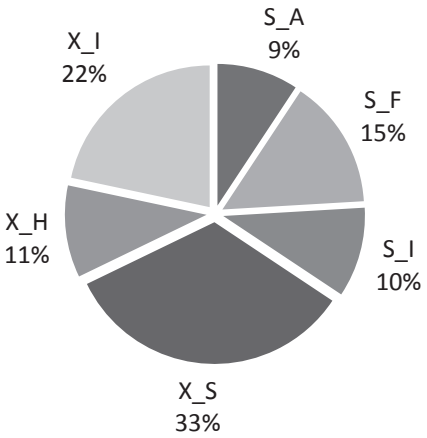

Figure 26 Average COD fractions for the first characterization. S_A is an input variable (acetate + propionate) while the other five fractions are derived from the different types of COD measurements. Figure from Nobel (2015). Used with permission.

OUR experiments carried out two weeks after the characterization campaign had, as shown in section 5.3, given an X_H fraction of 0.16 of the particular COD. This was considered to be close enough to the default model fraction of 0.17 that the latter value could be used. The remaining unknown fractions, X_S and X_I were estimated through model calibration.

TKN was calculated from the TN and $NO_{2,3}^-$ measurements. The ammonium concentration in the inflow generally followed changes in the TKN levels (see Figure 27). Since there were measurement data for all nitrogen factions used in the input file no further calibration was necessary.

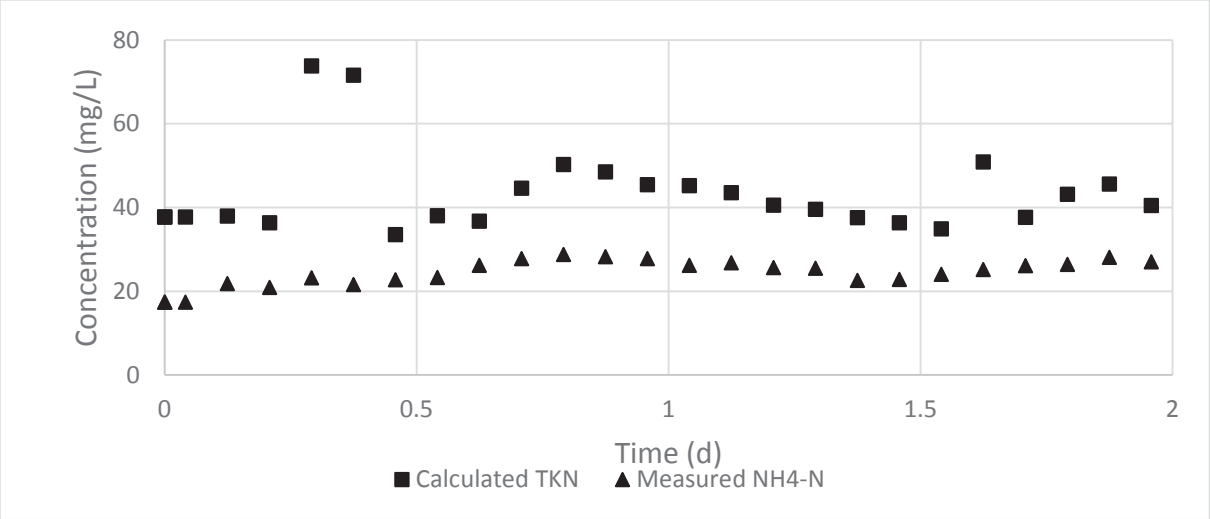

Figure 27 TKN (calculated variable) and ammonium concentrations in the influent in the first characterization campaign on G2:1. The ammonium concentration was approximately half of the TKN concentration throughout the two days of measurements, with the exception of two outlier values for TKN during the morning of day 1.

The recirculation stream from the sludge thickening process was supposed to be led to primary clarifiers not connected to blocks G1-G3 and the nitrite concentration in the inlet was therefore expected to be very low, but peaks values of up to 2 mg/L were observed (see Figure 28). Recirculation streams would normally occur at a 6 hour interval, which was consistent with the spread of peaks in nitrite concentration. Further investigation of the sluice gate that regulated the distribution of the recirculation stream did not give a clear answer to the cause of the problem, but it seemed likely that a portion of the stream could get through into G1-G3.

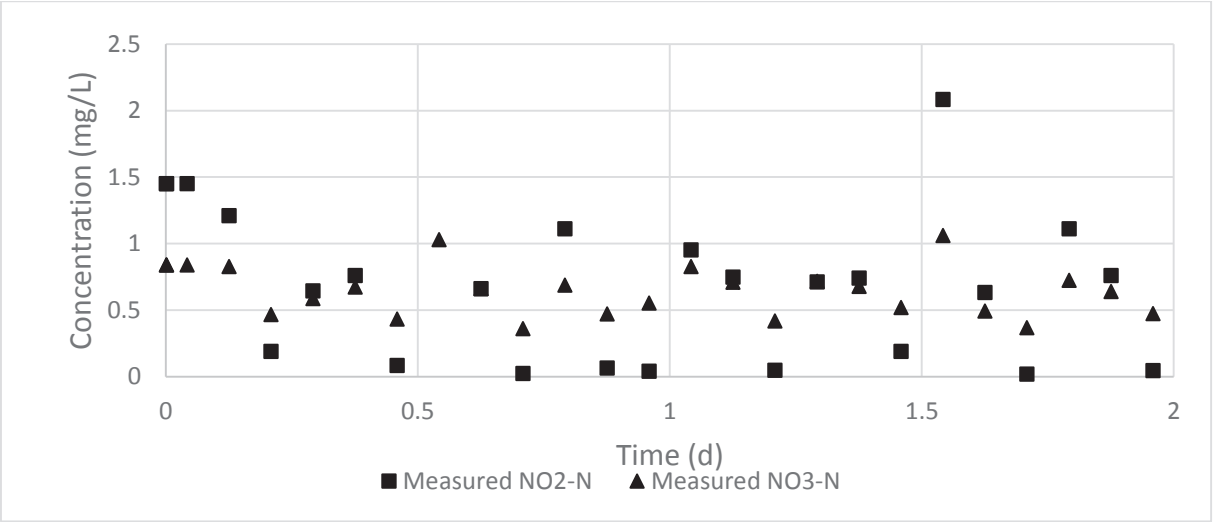

Figure 28 Nitrite and nitrate concentrations in the influent in the first characterization campaign on G2:1. The nitrite concentrations followed a six hour cycle, where very low concentrations were followed by peak values in the subsequent measurements.

TP and phosphate concentrations followed each other closely, which indicated that the organic phosphorus concentration in the wastewater was relatively constant (see Figure 29). Peak values for phosphate during the evening hours of the first day were disregarded since total phosphorus tests performed on the same filtered samples gave lower values than the phosphate tests.

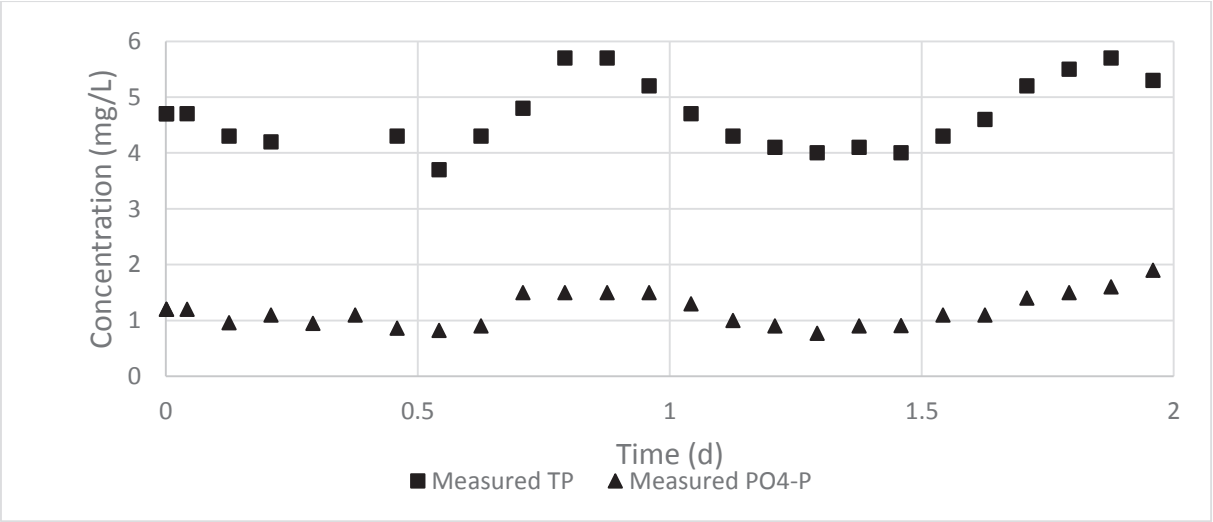

Figure 29 TP and phosphate concentrations in the influent for the first characterization on G2:1. A clear daily cycle, with maximums in the evenings and minimums in the morning could be observed for both TP and phosphate. Two outlier values from the first day of measurements were considered inaccurate and were removed from the graph.

5.5.3 Aeration system calibration

Detailed implementation of the PI-regulators in use at Sjölunda went beyond the scope of the project, and the factor of proportionality (K_P) and integral time (T_i) parameters were therefore calibrated to generate an as good fit as possible between the model and measured airflows and dissolved oxygen concentrations in the zones rather instead of being set to the real values. The model was found to achieve a good match between model and measured variables at a K_P of 70

and a T_I of 0.0001 days (8.6 seconds) for zones 3 and 4. Zone 5 got good results for a K_P of 100 and a T_I of 0.001 days (86 seconds).

The calibration of the aerators focused on changing model parameters from the aeration model, and a limited number of physical parameters. There were no temperature gauges in the activated sludge process, but gauges on a subsequent treatment step showed average temperatures of 4°C in the air and 14°C in the water, and the air density was set to 1272 mg/L to take this into account. SRT was set to a fixed value of 1.87 days, which was the calculated average SRT during the two calibration days. It was possible to achieve good calibration results by only altering the two model parameters A and B (see Table 8 and Figure 30-35).

Table 8 Aerator sub-model parameters A and B for the three aerated zones of G2:1.

	A	**B**
Zone 3	6.6	2.6
Zone 4	5	4.5
Zone 5	7	6.2

Unfortunately routine maintenance of the aeration system was carried out during the first day of the characterization, and 15 minute aeration peaks followed by peaks in dissolved oxygen content in the aerated zones took place in all three zones. The model did not, and was not intended to, pick up this peak.

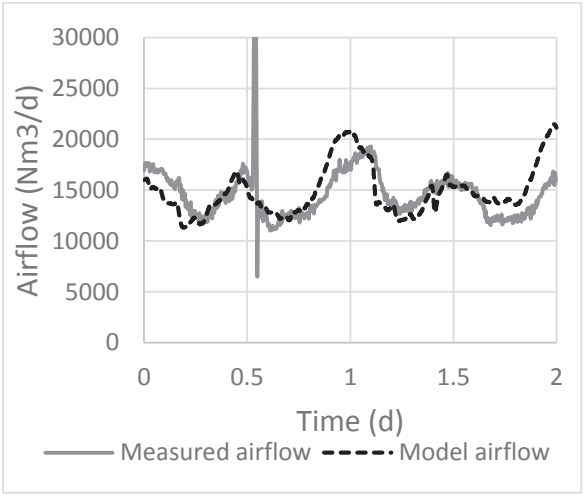

Figure 30 Model and measured airflow of zone 3 in G2:1 during the first characterization. The airflow minimums and maximums occurred at the same in both the model and in the measurements, but the model overestimated some peak values.

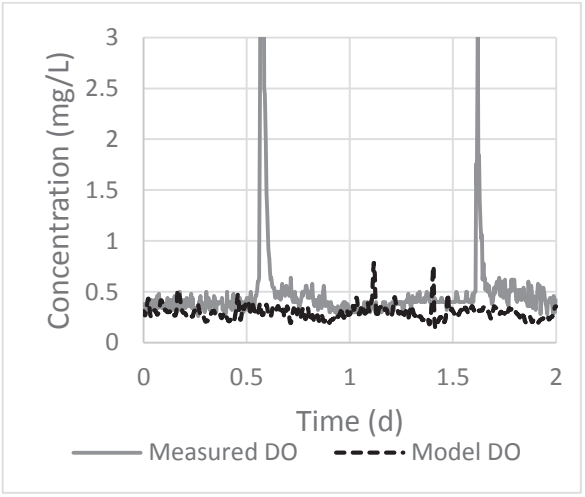

Figure 31 Model and measured dissolved oxygen concentrations in zone 3 of G2:1 during the first characterization. The model concentrations followed the measurements during the first day, but a difference between the model and the measurements could be observed towards the end of the second day.

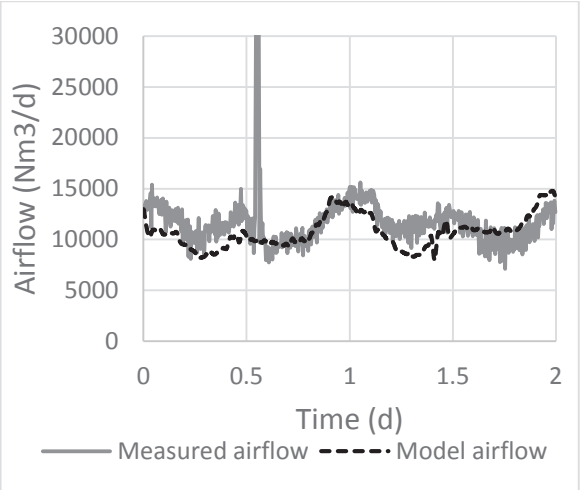

Figure 32 Model and measured airflow of zone 4 in G2:1 during the first characterization. As for zone 3, the model was able to mirror the general airflow cycles throughout the days but was not able to match the magnitude of some of the measurement peaks.

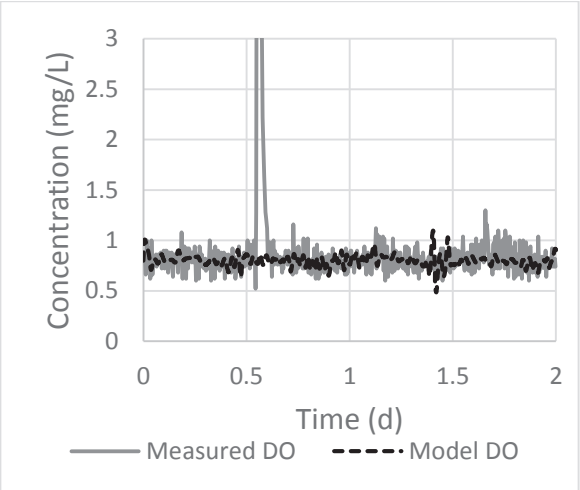

Figure 33 Model and measured dissolved oxygen concentrations in zone 4 of G2:1 during the first characterization. The model concentration was relatively stable throughout the two days whereas the measurements had high fluctuations, but on average matched the shape of the model values.

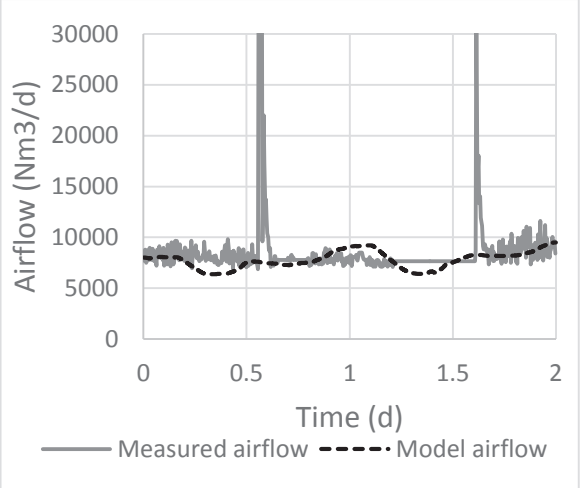

Figure 34 Model and measured airflow in zone 5 of G2:1 during the first characterization. The measured airflow was stable, with only small fluctuations during most of the two days, whereas the model had distinct minimum and maximums.

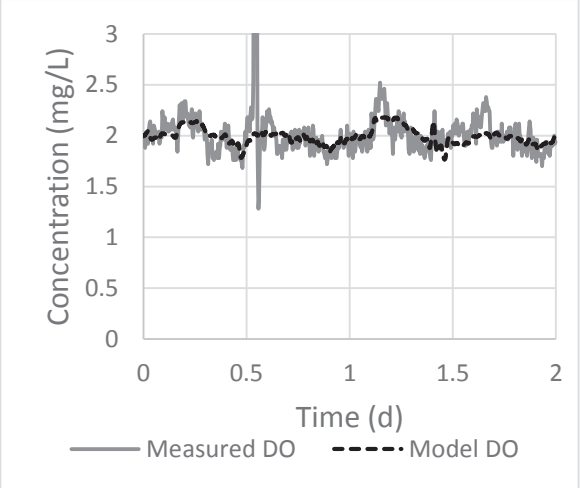

Figure 35 Model and measured dissolved oxygen concentrations in zone 5 of G2:1 during the first characterization. The model oxygen concentration followed most of the larger fluctuations in the measurements.

5.5.4 Zone 5 and waste sludge calibration

The ASM2d model calculates COD, TN and TP in the activated sludge zones and in the waste sludge from fixed TSS ratios, which give similar shapes to all the model concentrations over

the two days. This concept was mostly supported by the measurements for the four different components. Peak values generally occurred in the 08.00 measurements, followed by declining values until 12.00, when the concentrations stabilized. This behavior was observed in both the activated sludge from zone 5 (see Figure 36-38) and in the waste sludge (see Figure 40-42), though for the waste sludge it was only seen during the second day.

Calibration focused on achieving matches between the average concentrations of the measurements and the model values and this aim was achieved with only minor tweaks once changes to achieve mass balances had been performed. The concentration of TN in zone 5 was 10-20% lower in the model than in the measurements, but since a well calibrated nitrogen concentration in the sludge was not central to the aims of the project the initial calibration of the activated sludge process was considered to be sufficiently accurate.

Since there were SS sensors in both zone 5 and in the waste sludge it was possible to compare measured and model results to the sensor values (see Figure 36 and Figure 40). A good match was found between the sensor values and the model values for waste sludge SS, after a correction factor of 0.81 was introduced to the model variable X_{TSS}.

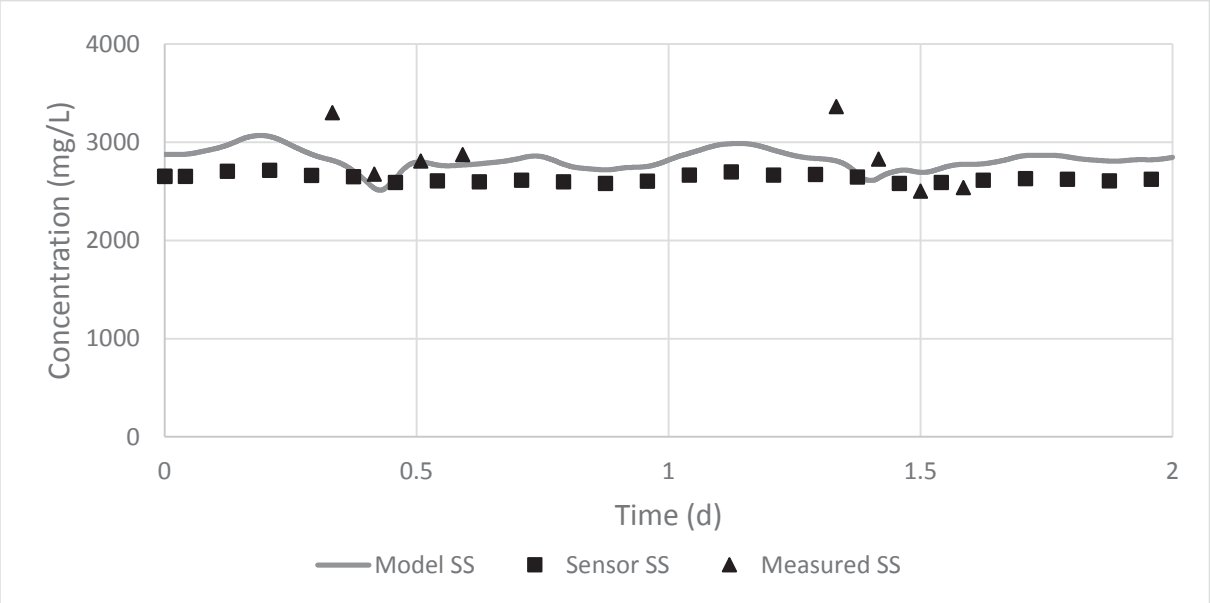

Figure 36 Measured, sensor and model SS concentrations in zone 5 of G2:1 during the first characterization. The sensor SS values were very stable for the two days, and the model mirrored the sensor concentrations. Most of the measurements during the two days were similar to model and sensor values, but samples taken at 08.00 on both days showed higher SS concentrations.

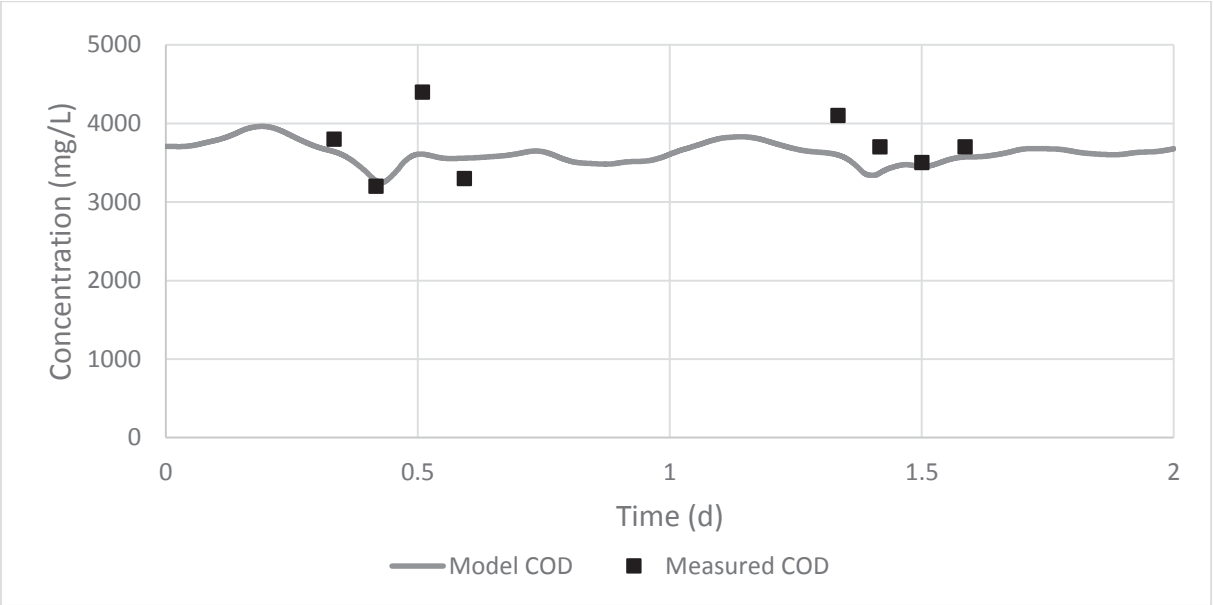

Figure 37 Measured and model COD concentrations in zone 5 of G2:1 during the first characterization. The model COD concentration was relatively stable while COD measurements from the first day fluctuated up to 4500 mg COD/L.

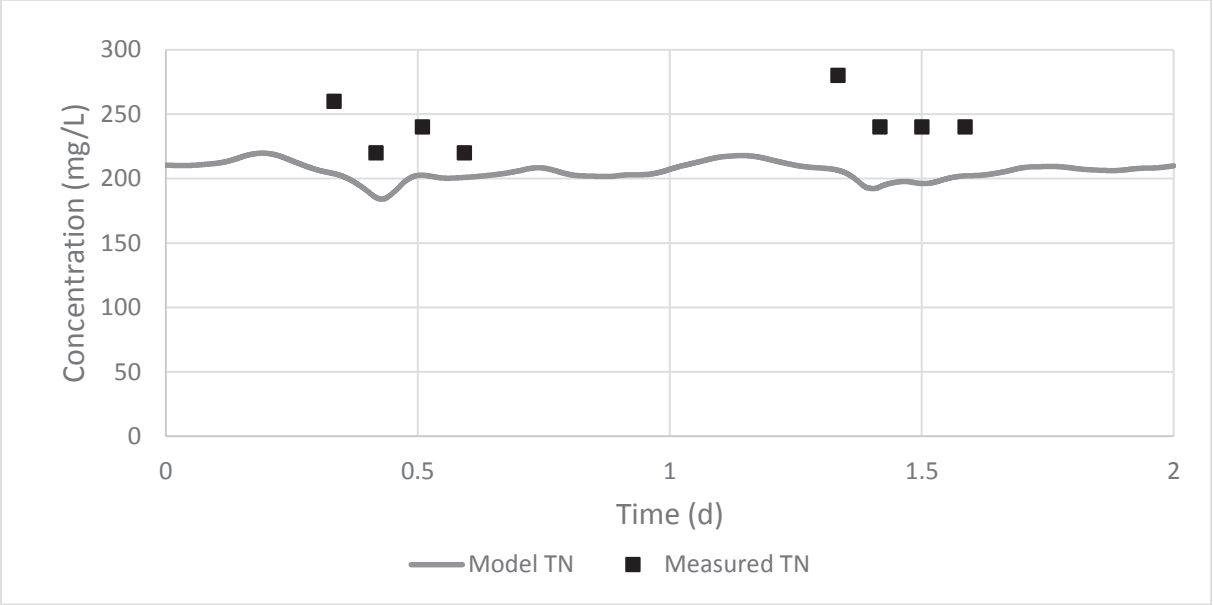

Figure 38 Measured and model TN concentrations in zone 5 of G2:1 during the characterization. The model was able to catch the fluctuations in measured TN to some extent, but model concentrations were approximately 50 mg N/L lower than the measured values.

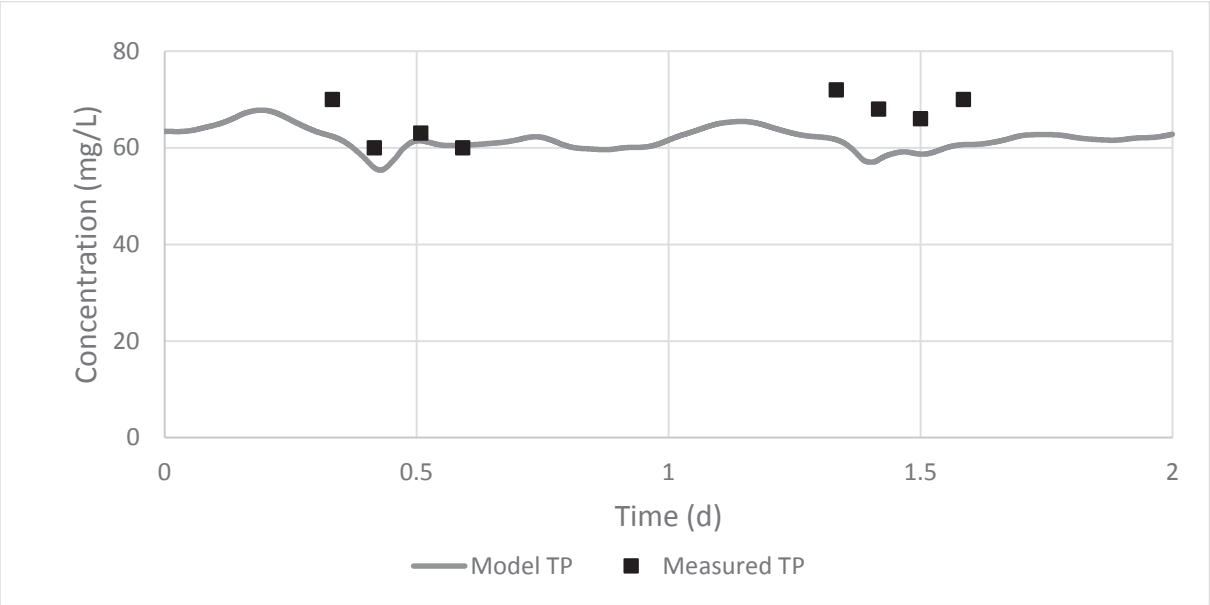

Figure 39 Measured and model TP concentrations in zone 5 of G2:1 during the first characterization. As with TN, the model followed the general variations in measured TP concentrations, but the model values for the second day were on average 10 mg/L lower than the measurements.

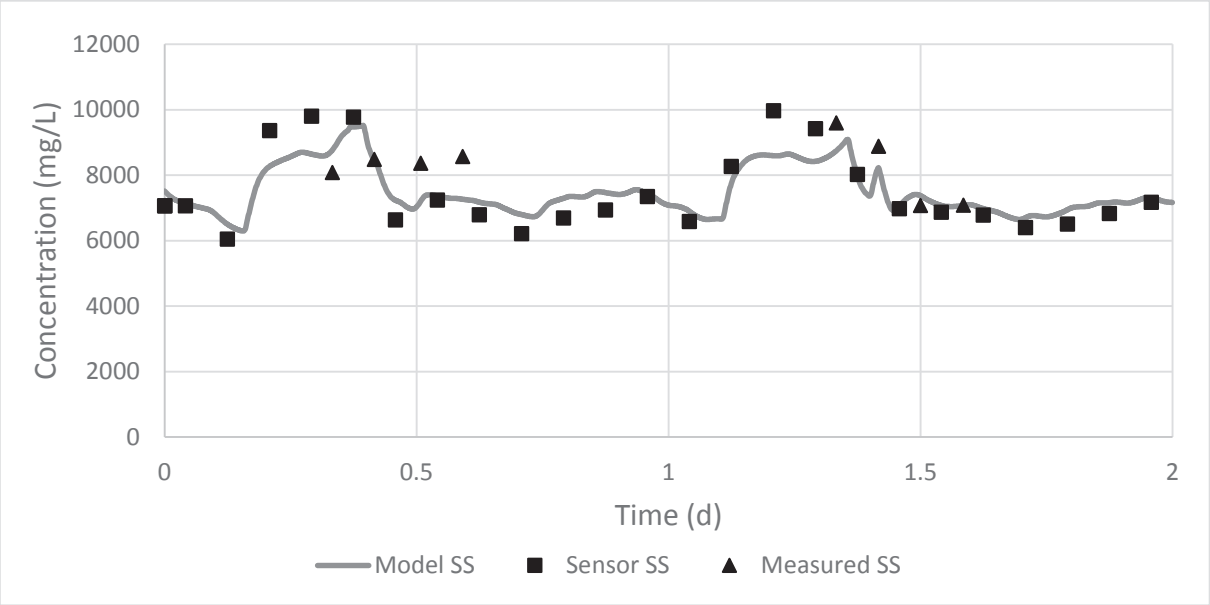

Figure 40 Measured, sensor and model suspended solids concentrations of the waste sludge in G2:1 during the first characterization campaign. The SS concentration in the model generally matched the sensor concentrations very well, but the model did not match the measurements during the first day.

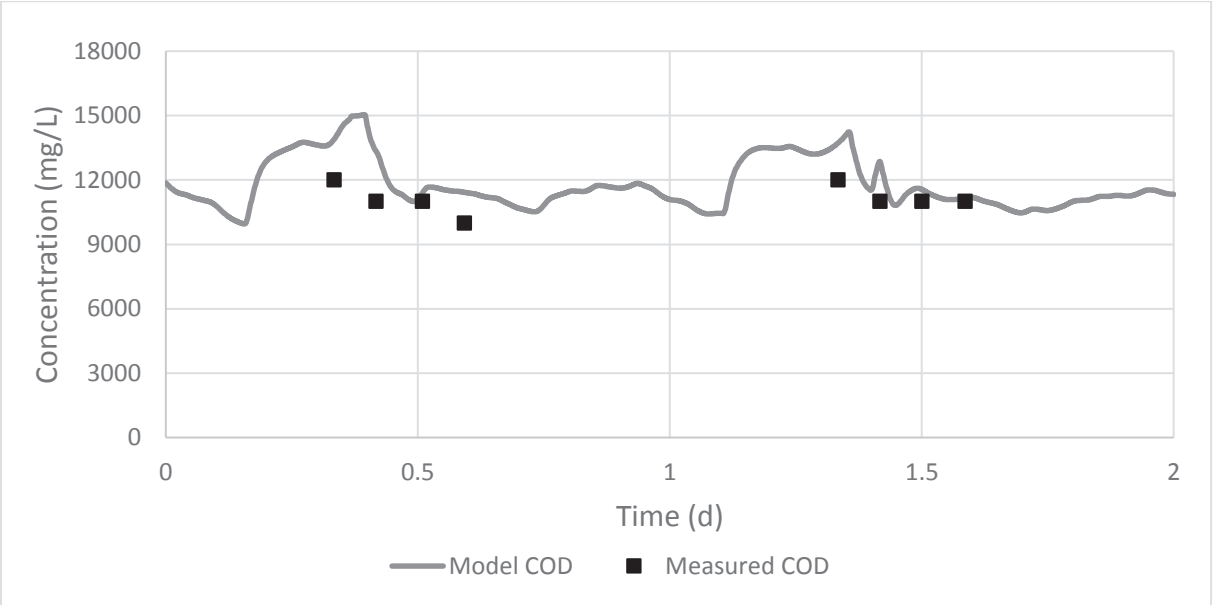

Figure 41 Measured and model COD of the waste sludge in G2:1 during the first characterization campaign. The model COD concentration was in the same range as the measurements, but the model reached higher maximum concentrations than were found in the measurements.

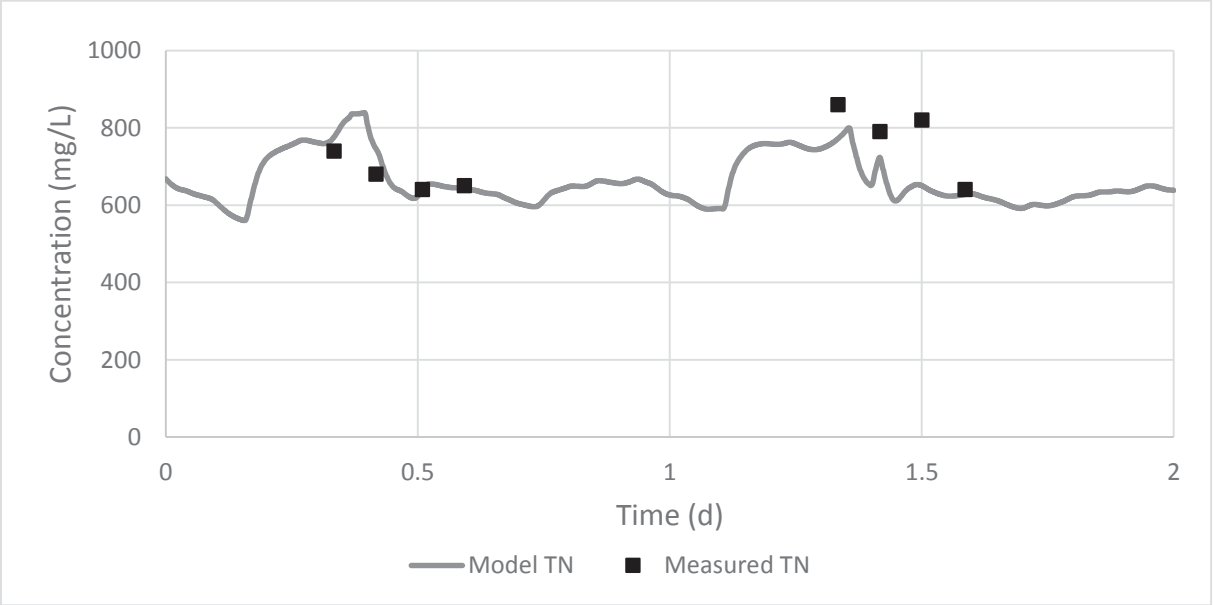

Figure 42 Measured and model TN concentrations in the waste sludge of G2:1 during the first characterization. There was a good match between model and measured TN concentrations during the first day of the campaign, but during the second day the model concentrations were generally lower than the measured concentrations.

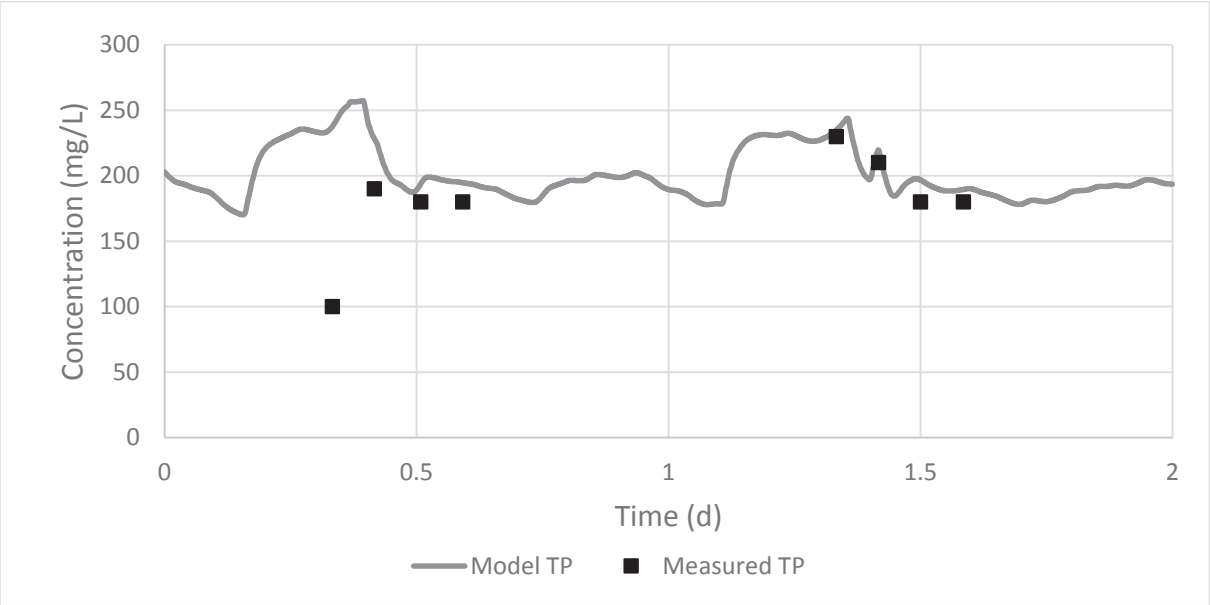

Figure 43 Measured and model TP concentrations in the waste sludge of G2:1 during the first characterization. The model TP concentration matched the measurements, with the exception of the first measurement during day 1.

5.5.5 Effluent calibration

The primary goal to get average values to fit as closely as possible between the model and the real measurements was also the basis of the effluent calibration, but after some minor changes to the inflow fractionation model it was possible to get an even closer fit for several components. Model values COD, COD filtered, TKN, NH_4^+-N and TP all showed similar concentration changes over time as the real measurements, though peaks for nitrogen and phosphorus fractions generally occurred 4-6 hours earlier in the model than in the measurements (see Figure 44-47). A possible explanation could be that while the model treated the activated sludge system as a series of perfectly mixed reactors the real system might behave more like a plug flow reactor. In the perfectly mixed reactors changes in concentration would spread very rapidly whereas there would be a delay in the plug flow reactor. While no tests were performed to investigate whether the real tanks were more similar to plug flow reactors than perfectly mixed reactors a delay of 4-6 hours is similar to the hydraulic retention time in the activated sludge lines, which indicates that the system do resemble a plug flow reactor.

COD filtration tests with both 1.6 µm and 0.1 µm filters were performed on two samples from the effluent, and the analysis showed a 19-23% lower COD concentration in the 0.1 µm filtration test. In order to get comparable results between the COD filtered 1.6 µm measurements and the S_{COD} model values the latter were multiplied by a correction factor of 1.25. For SS, the same factor used for waste sludge, 0.81, was used to transform the X_{TSS} values in the model to comparable SS values.

During the measurement campaign it was suspected that some of the iron sulfate from the pre-precipitation process remained in the wastewater flowing into the activated sludge process and that the iron sulfate therefore had an effect on the phosphorus concentrations in the activated sludge process. A supplementary sample analysis showed a Fe^{2+} concentration of 2.96 mg/L and a Fe^{3+} concentration of 2.37 mg/L in the wastewater entering the activated sludge tanks. Due to the small number of samples for iron analysis taken in the characterization calibration

was used to determine that a fixed X_{MeOH} value of 2 mg/L in the model influent gave a good fit for both TP and phosphate in the effluent.

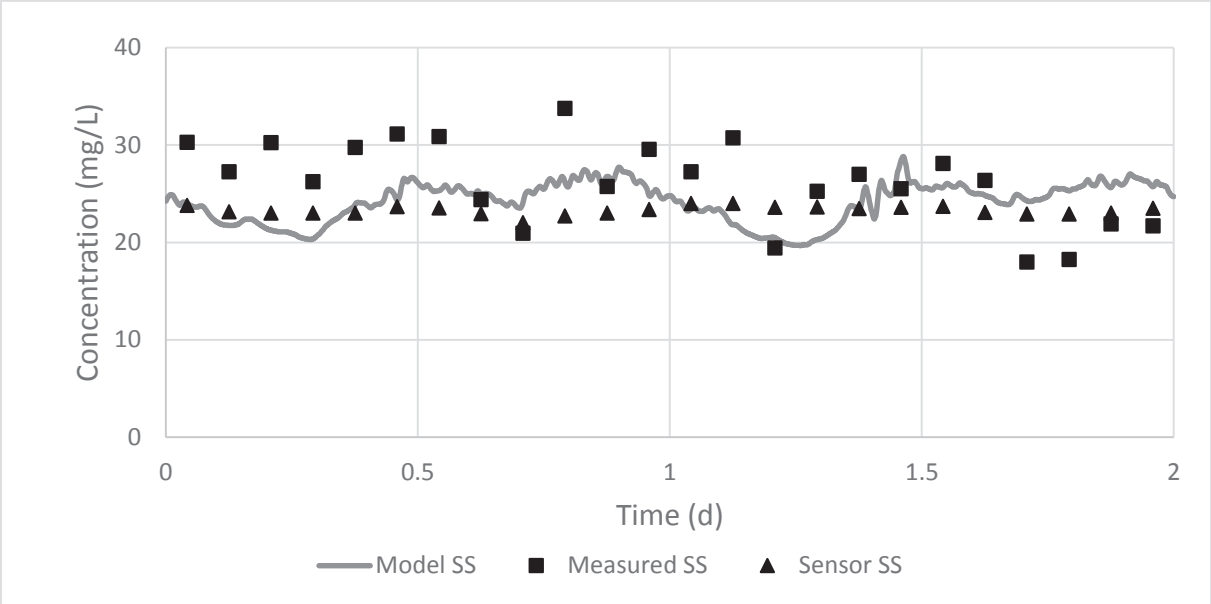

Figure 44 Model, sensor and measured effluent concentrations of suspended solids for G2:1 during the first characterization. The sensor SS concentration was very stable during the two days whereas the measurements showed some variation. The model SS concentration varied slightly throughout the two days, but the variation was smaller than it was for the measured SS concentration.

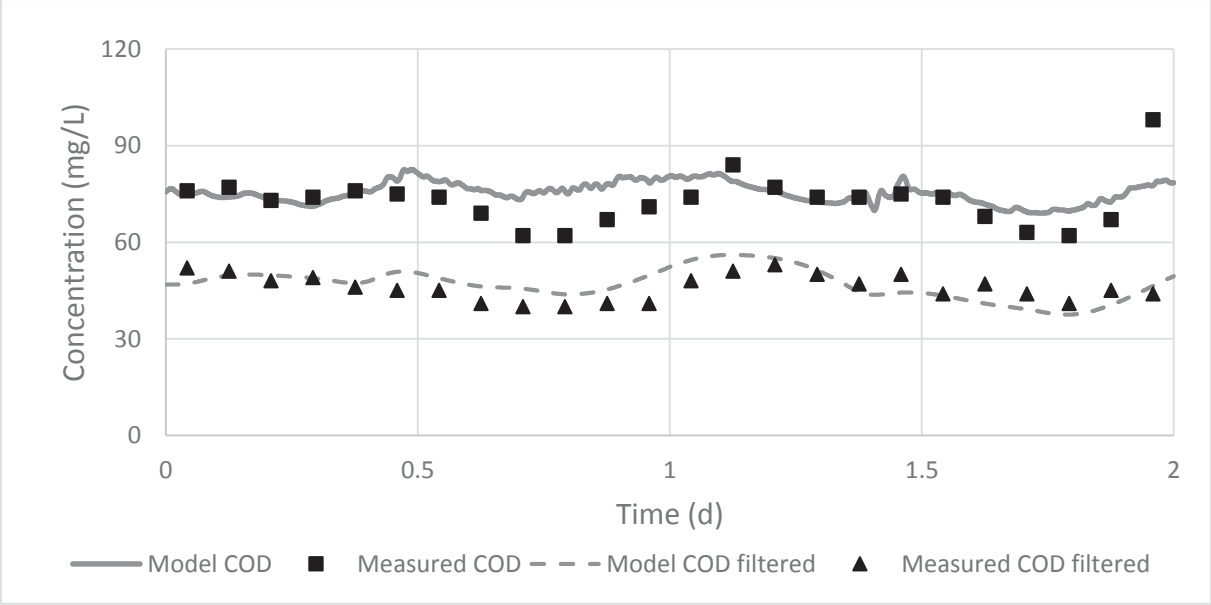

Figure 45 Model and measured effluent concentrations of COD and COD filtered for G2:1 during the first characterization. The model values for both COD and COD filtered were in the same range and for the most part followed the measurements.

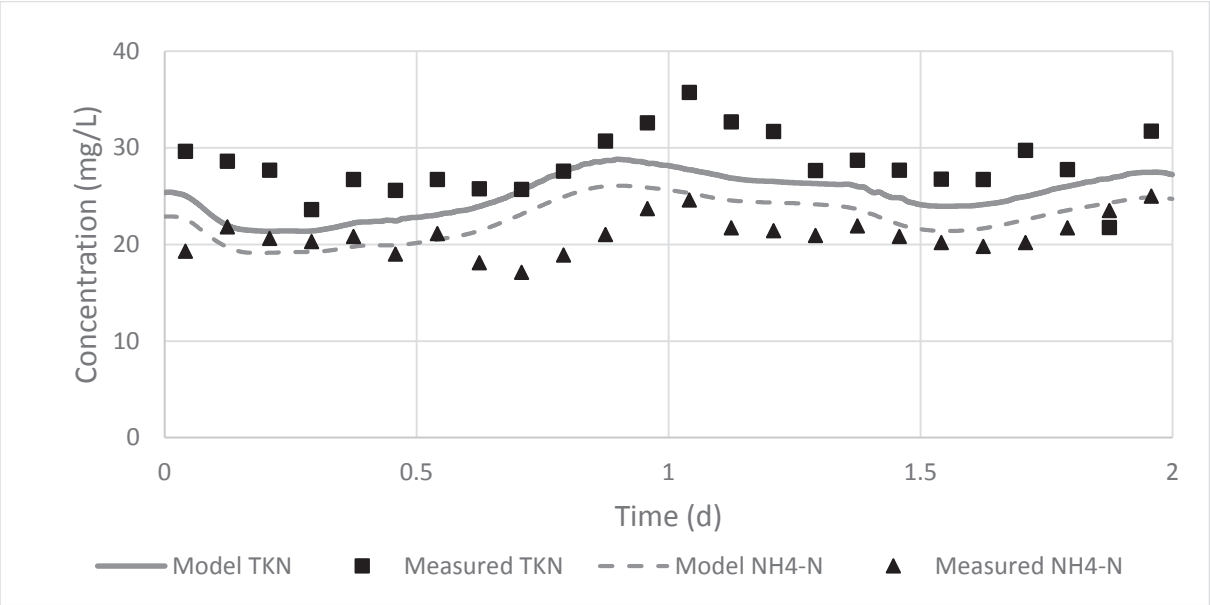

Figure 46 Model and measured effluent concentrations of TKN and ammonium in G2:1 during the first characterization. The difference between TKN and ammonium was significantly smaller in the model compared to the difference between the measured TKN and ammonium concentrations.

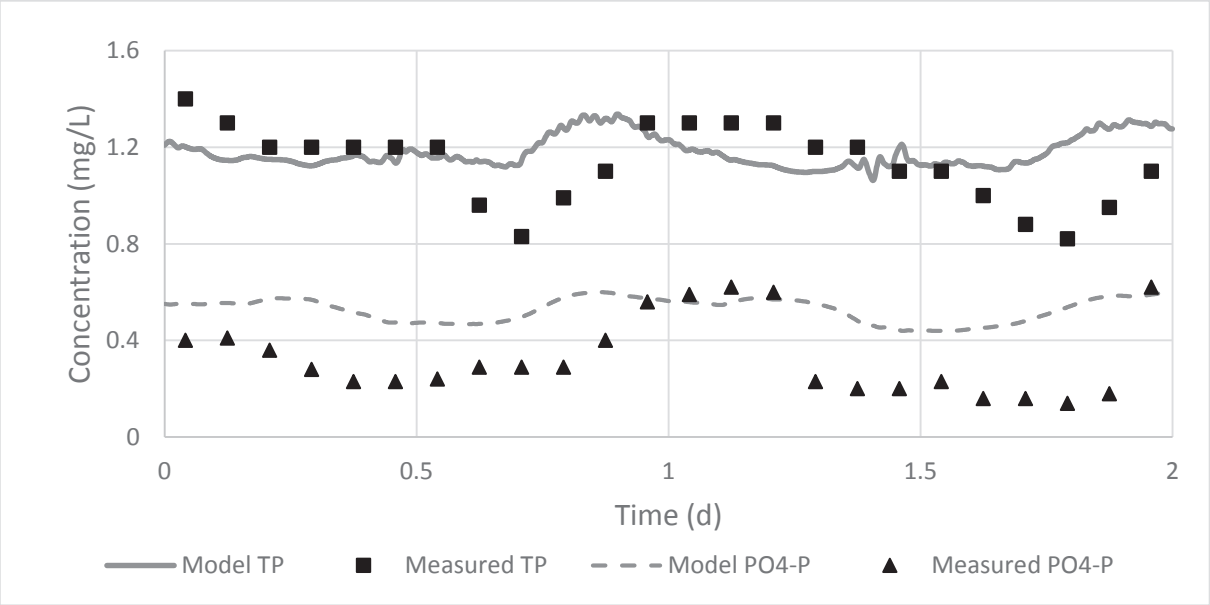

Figure 47 Model and measured effluent concentrations for TP and phosphate in G2:1 during the first characterization. The difference between TP and phosphate concentrations was similar in the model and in the measurements, but the model overestimated the phosphate concentrations and peaks occurred several hours earlier in the model compared to the measurements.

A problem which was not completely overcome in the calibration process was how to increase the organic nitrogen fraction of the TKN in the effluent. It was assumed that some autotrophs present in the incoming wastewater could be active in the activated sludge process, but since they are flushed out and outcompeted by heterotrophs in systems with short SRTs the effect

should have been limited. An autotroph concentration of 0.25 mg/L was added in the influent fractionation model, which gave a slightly increased organic nitrogen fraction in the model effluent, but the concentration was fixed at approximately 2 mg/L whereas the actual value of organic nitrogen, derived from measurements of NH_4^+-N, TN and NO_X^--N was in a range of 5-10 mg/L.

It was noticed during the calibration process that different dissolved oxygen set-point configurations for the three aerated zones only had very small effects on the effluent quality even when comparing very large differences in set-points which would in turn result in large differences in airflow, such as 0.2 – 0.2 – 0.2 mg/L for zones 3-5 respectively compared to 2.0 – 2.0 – 2.0 mg/L. Experiences from the full-scale process showed that the difference in effluent quality given by the model was unreasonably small.

Efforts were made to increase the oxygen dependency of the process by increasing the half saturation coefficient for oxygen K_O, a kinetic parameter that is by default set to 0.2 mg/L in the ASM model. This had an effect on the effluent quality in terms of COD, and support can be found for increasing the parameter in a high-loaded activated sludge process (Wang *et al.,* 2007). However, the parameter would need to be changed to over 1 mg/L in order to generate the differences in treatment quality observed between lines G1:1 and G1:2 during the April sampling campaign (see section 5.7), and Wang *et al.* (2007) only suggests an increase to 0.3 mg/L. Furthermore, altering K_O would primarily change the reduction efficiency of soluble COD, whereas the sample campaign show only a small difference in filtered $COD_{0.1\mu m}$. The difference can instead be found in the slowly biodegradable particular COD, X_S, which does not have time to fully degrade under the operating conditions of a low dissolved oxygen set-point configuration such as the one in use in G1:2 in April 2015.

A problem with the Takács settling model is that it does not differentiate between types of particles, and it was therefore not possible to assign X_S and X_H different settling properties. The model X_H/X_S ratio in the effluent was therefore the same as the ratio in zone 5, and since the relative effect of high versus low aeration on X_H in the model is much smaller than the relative effect on X_S the choice of aeration strategy has very small effects on the effluent concentrations in the model. It is possible that biomass will mainly settle through hindered, more rapid, zone settling whereas particles belonging to the slowly biodegradable COD fraction mainly settle through the slower individual settling process. The actual ratio of X_S and X_H in the effluent could then be very different from the modelled ratio, which would explain why different aeration strategies have a large influence on effluent concentrations. There was unfortunately not enough time to fully investigate these implications within the scope of the project, but it is suggested as a basis for further studies (see section 7).

5.5.6 Recalibration of model to fit G1:1

The MIKE WEST model was calibrated using data from line G2:1, but since full-scale tests of different aeration strategies were going to be performed on block G1 the model was recalibrated using available flow data from line G1:1. Since the flow sensor on G1 in was assumed to give accurate flow measurements and since both line G1:1 and line G1:2 were in operation the flow rate was split by introducing a 0.5 conversion factor (see Figure 48), but no further calibration was deemed necessary.

The input files for the return sludge flow and the waste sludge flow (see Figure 49) were updated with measurement data from G1:1 from the same time period as the first characterization campaign. Both the return and the waste sludge flows were approximately twice as high in G1:1

as in G2:1 during February 11-12th, which indicate that the sludge concentration in the basins were significantly lower in G1:1 at the time.

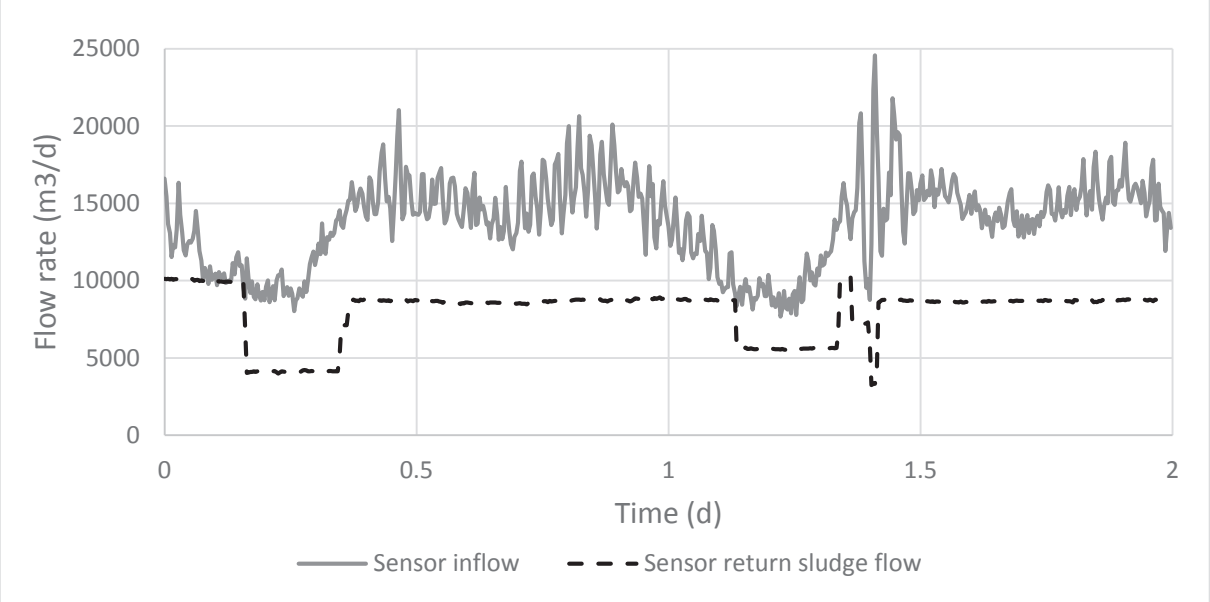

Figure 48 Inflow and return sludge flow rates of G1:1 during the first characterization. The sensor inflow rate was used as the model inflow rate without using any correction factors, which meant that the inflow rate was considered to be 15-20% higher in G1:1 compared to G2:1 during the first characterization.

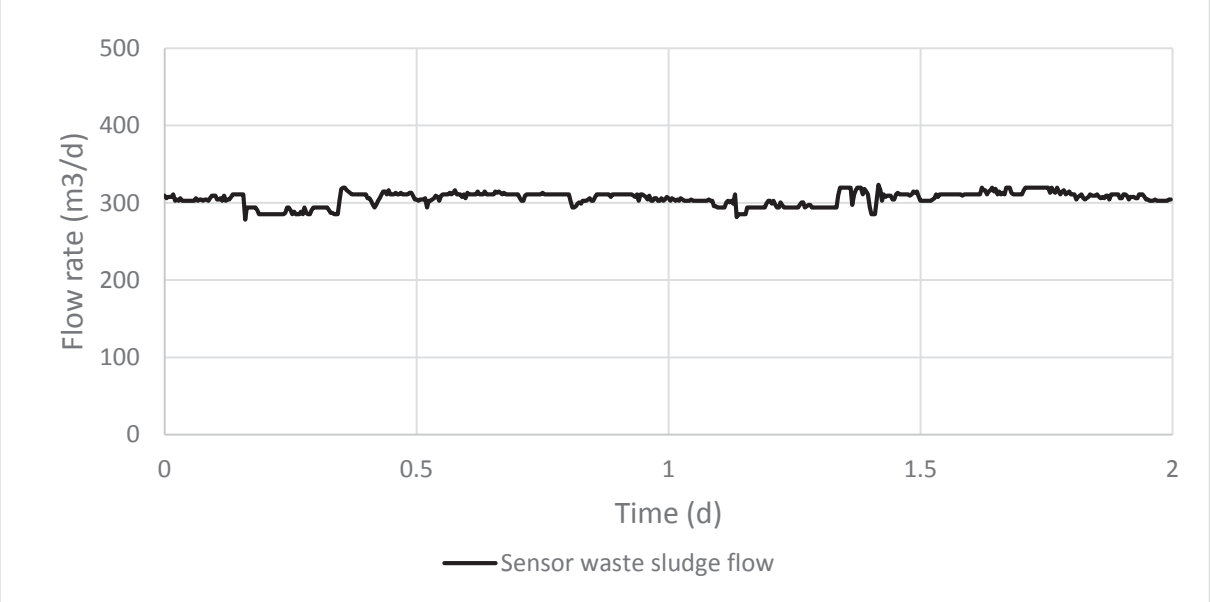

Figure 49 Waste sludge flow for G1:1 during the first characterization. The waste sludge flow rate was fixed at 300 m^3/d and only showed very small changes during the two days.

No effluent or waste sludge data of the concentrations of the different studied compounds were available for line G1:1 and the recalibration therefore focused on calibrating the aeration system. The dissolved oxygen set-points of the aerated zones were set to the same values as in line G2:1: 0.3 – 0.8 – 2.0 mg/L, but the number of diffusers were lower in G1:1 while the

diffuser area was larger. The A and B parameters of all three aerated zones were changed considerably as to increase the fit of the airflows (see Table 9).

Table 9 Model parameters A and B for the aerators in zones 3-5 in G1:1 during the first characterization and recalibration of the model.

	A	B
Zone 3	4.5	-0.5
Zone 4	5.05	2.24
Zone 5	5.5	4.3

While it had been possible to achieve good results when calibrating the airflows of zones 3-5 in G2:1 the recalibration of G1:1 was not completely successful. The modelled airflow of zone 3 (see Figure 50) did not achieve the right magnitude of maximum and minimum flows, and the airflow was instead modelled to achieve an average airflow that was close to the measured average airflow. The calibration of airflows for zone 4 (see Figure 52) and zone 5 (see Figure 54) achieved closer matches between modelled and measured values, and the model concentrations of dissolved oxygen in all three zones were very similar to the real measurements (see Figures 51, 53 and 55).

The maintenance cycle that affected the calibration of the aeration system on G2:1 also occurred on line G1:1, but the effects on the calibration were not significant.

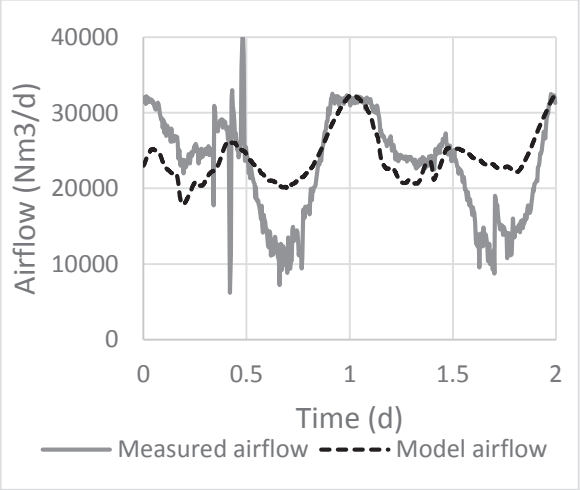

Figure 50 Measured and model airflow in G1:1 zone 3 during the first characterization. Minimums and maximums occurred at similar times for the measurements and the model, but the difference was significantly larger in the measurements than in the model.

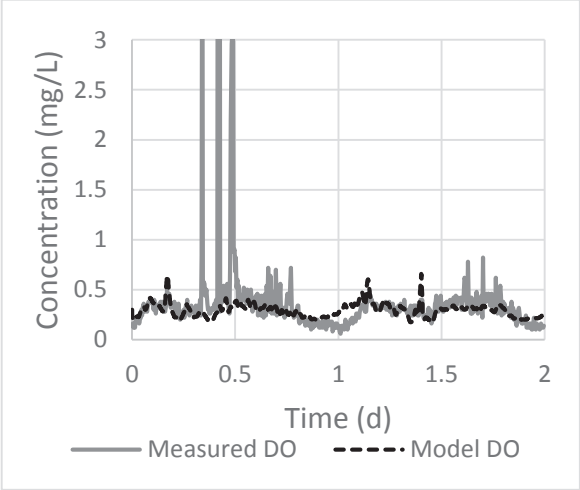

Figure 51 Measured and model dissolved oxygen concentrations in G1:1 zone 3 during the first characterization. The model was able to catch the larger fluctuations in the measurements.

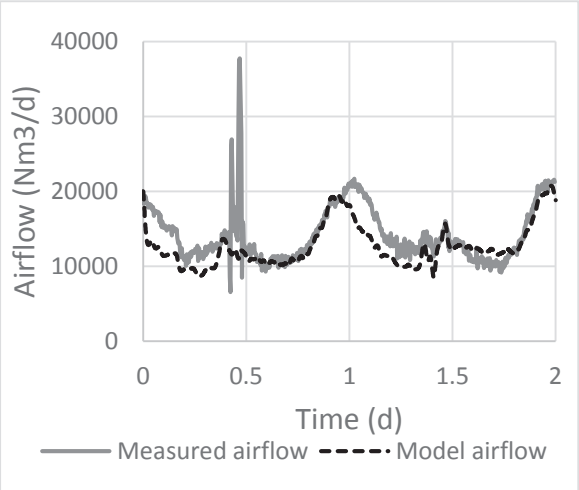

Figure 52 Measured and model airflow in G1:1 zone 4 during the first characterization. In zone 4 the measurement and model airflow were closely matched, though peaks occur 3-4 hours earlier in the model than they did in the measurements.

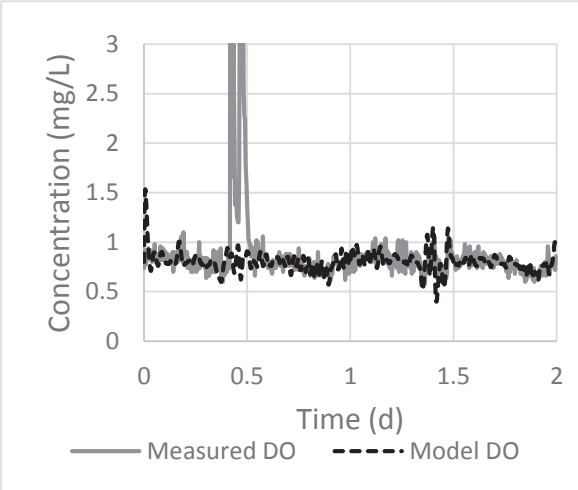

Figure 53 Measured and model dissolved oxygen concentrations in G1:1 zone 4 during the first characterization. Apart from during the routine maintenance in the middle of the first day the model and measured oxygen concentrations followed each other closely.

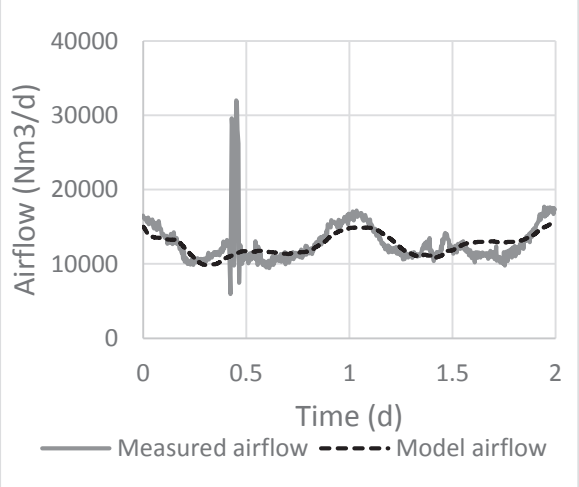

Figure 54 Measured and model airflow in G1:1 zone 5 during the first characterization. Zone 5 had a good match between measured and model airflow.

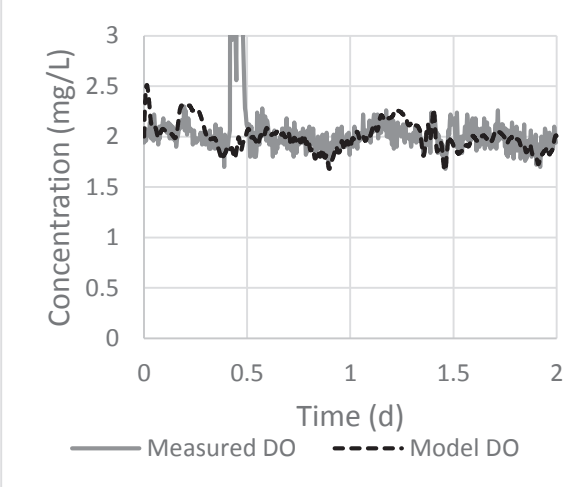

Figure 55 Measured and model dissolved oxygen concentrations in G1:1 zone 5 during the first characterization. The model oxygen concentrations followed the measurements, but the model did not have the short time concentration fluctuations present in the measurements.

The aeration system and other characteristics of G1:2 were assumed to be similar enough to G1:1 meaning that no initial calibration would be necessary for line G1:2. The validation showed that this assumption was not accurate (see section 5.9.3).

5.6 Initial model simulations

The purpose of the initial simulation was to use the calibrated but not validated model to find an aeration strategy that looked promising, and could be tested in full-scale. Results from the full-scale tests were then to be used to validate the model.

The effects of different aeration strategies on a large number of different model variables were studied, including the concentrations of S_A, S_F, X_I, X_S, X_{TSS}, SS, COD and TN in the effluent as well as the X_S and X_{TSS} in zone 5, the alpha factors of zones 3-5, the aerobic SRT, the total airflow and the COD/N ratio in the effluent. It was expected that effluent concentrations would generally be significantly higher in model runs with low DO set-points compared to in model runs with high DO set-points. However, the changes in effluent and waste concentrations in different set-point configurations were very small, and conclusions could therefore not be made based on the resulting effluent concentrations, aerobic SRT or COD/N ratios of different aeration strategies. Furthermore, the X_{TSS} rate in the activated sludge basins were primarily tied to the waste sludge flow and settling parameters, and the variable was therefore not considered to be a good indicator of the results of different aeration strategies.

In contrast, the concentration of X_S was the only COD fraction which changed significantly in the aerated basins depending on the DO set-points. It was assumed that in reality particles which in the model belongs to X_S passes through sedimentation basins to a greater extent than particles belonging to other particulate COD fractions. The sedimentation sub-model was not able to show this difference since the sub-model had the same sedimentation properties for all particle fractions. While comparisons between X_S in zone 5 in different scenarios would not directly translate to differences in COD concentrations in the effluent XS could then be used to indicate if changing the aeration strategy would increase or decrease the effluent water quality.

Comparisons between X_S in zone five, the total airflow and the alpha factors, the latter being used mainly as indicators of which DO set-point ranges that might be appropriate for each aerated zone, was considered to give the most promising results.

Study of the alpha factors showed that changes to the dissolved oxygen set-point in zone 5 had more of an impact on its alpha factor than corresponding changes in other zones had on their respective alpha factors. This indicated that reducing the DO set-point in the last aerated zone, while increasing the set-points of the first two zones, had the potential to generate a more energy efficient treatment process. The effect was more prominent in G2 than in G1, since the number of diffusers in each zone differed much more in G2.

After noticing the effects on the alpha factors the goal was set to find the DO set-point configuration that allowed for the largest decrease in total airflow while maintaining the same effluent treatment efficiency. The efficiency was assumed to be indicated by the X_S concentration in zone 5, and the target therefore became to keep the concentration at or below the concentration in the reference configuration 0.3 – 0.8 – 2.0 mg/L. The results of the scenario analysis was that an aeration strategy using a set-point configuration of 0.6 – 0.6 – 1.0 mg/L would best fulfill the two criteria, by decreasing the total airflow by 5.9 % versus the reference while at the same time slightly increasing the treatment efficiency. In Table 10 the model results of the four aeration strategies tested in full-scale are presented. The old aeration strategy at Sjölunda WWTP, 2.0 mg/L in every aerated zone, was found to have a 24% higher total airflow while X_S was 4% lower.

Table 10 Model simulation effects of different aeration strategies on the total airflow and X_S in zone 5 of G2:1.

DO set-point configuration			Xs zone 5	Diff Xs	Total airflow	Diff airflow
Zone 3	Zone 4	Zone 5	mg/L		Nm^3/d	
0.3	0.8	1.7	125.47	0.11%	34000	-1.87%
0.3	0.8	2.0	125.33		34647	
0.6	0.6	1.0	124.69	-0.51%	32603	-5.90%
2.0	2.0	2.0	120.41	-3.93%	42808	23.55%

The simulation was repeated in the recalibrated G1:1 model, which also gave the result that the most energy efficient aeration strategy, without decreasing treatment efficiency, would be the set-point configuration 0.6 – 0.6 – 1.0 mg/L in zones 3-5. The benefits of using the optimized aeration strategy was found to be smaller than if the same strategy had been implemented in zone G2:1, but there would still be a 4.3% reduction of the total airflow versus the reference set-point configuration (see Table 11). A second optimization to find a strategy with increased treatment efficiency but maintained energy consumption compared to the reference configuration showed that a set-point configuration of 0.8 – 0.9 – 1.0 mg/L best matched these conditions.

Table 11 Model simulation effects of different aeration strategies on the total airflow and X_S in zone 5 of G1:1.

DO set-point configuration			Xs zone 5	Diff Xs	Total airflow	Diff airflow
Zone 3	Zone 4	Zone 5	mg/L		Nm^3/d	
0.3	0.8	1.7	170.31	0.18%	48336	-1.99%
0.3	0.8	2.0	170.00		49319	
0.6	0.6	1.0	169.63	-0.22%	47198	-4.30%
0.8	0.9	1.0	167.22	-1.64%	48902	-0.85%
2.0	2.0	2.0	162.58	-4.36%	57191	15.96%

5.7 24-hour flow-proportional sampling campaign

The 24-hour flow-proportional sampling campaign was performed during the period of April 14th to May 4th 2015. The DO set-point configuration for line G1:1 had been set to 2.0 – 2.0 – 2.0 mg/L for zones 3-5 respectively several weeks prior to the start of the campaign, while line G1:2 used a configuration of 0.3 – 0.8 – 1.7 mg DO/L. On May 1st the aeration strategy for line G1:2 was changed to 0.6 – 0.6 – 1.0 mg DO/L in accordance with the results from the initial simulation and in preparation for the second characterization campaign. Since it could be expected that it would take several days for a process change to come fully into effect the results from the sampling of G1:2 on May 3rd and 4th were not seen as representative of the new aeration strategy, and the comparisons between lines G1:1 and G1:2 made in this section only relate to the first six measurements of the 24-hour flow-proportional sampling campaign.

The SS load was found to be 1700-2000 kg/d during the majority of the 24-hour flow-proportional sampling campaign, with the exception of April 14th, where the load was 2300

kg/d, and on May 4th, where a rainfall event increased the flow rate by 50% over the median flow rate of 10000 m^3/d and the load to 3400 kg/d. The higher load explains why the SS removal efficiency was lower than the average efficiency on both those occasions.

A clear difference in SS removal efficiency could be observed between lines G1:1 and G1:2. The average SS concentration in the effluent was 29 mg/L in G1:1 and 36 mg/L in G1:2 (see Figure 56), which meant that 85% of the suspended solids were removed in G1:1, whereas the less aerated process in G1:2 managed to remove 81% of the SS (see Figure 57).

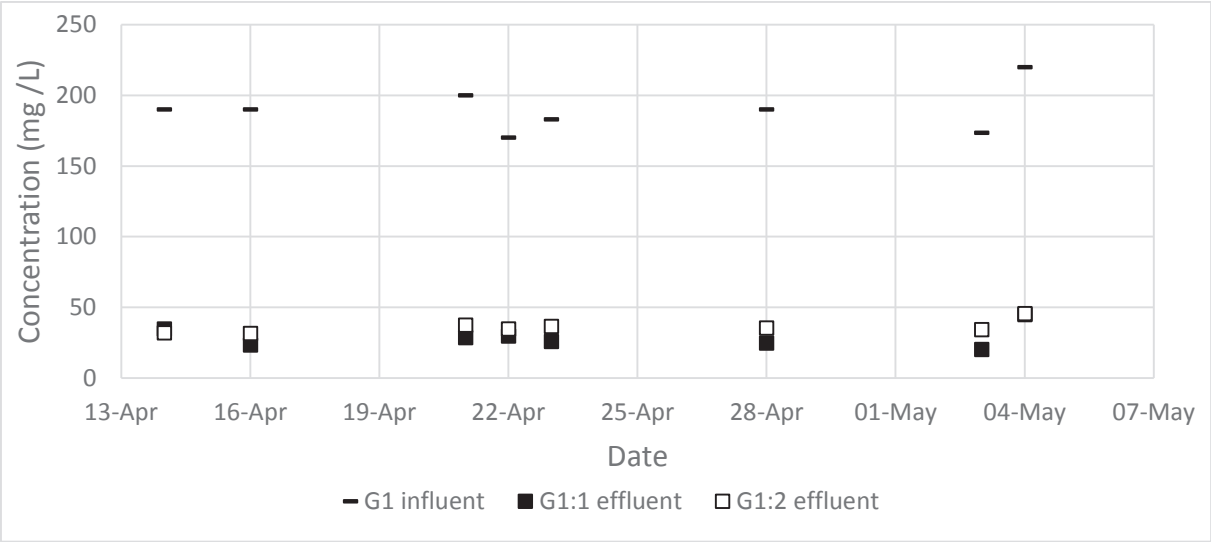

Figure 56 Influent SS concentration and effluent SS concentrations in G1:1 and G1:2 during the 24-hour flow-proportional sampling campaign. The influent SS concentration was relatively stable around 190 mg/L during the measurement campaign. For most samples G1:2 showed slightly higher effluent SS concentration than line G1:1.

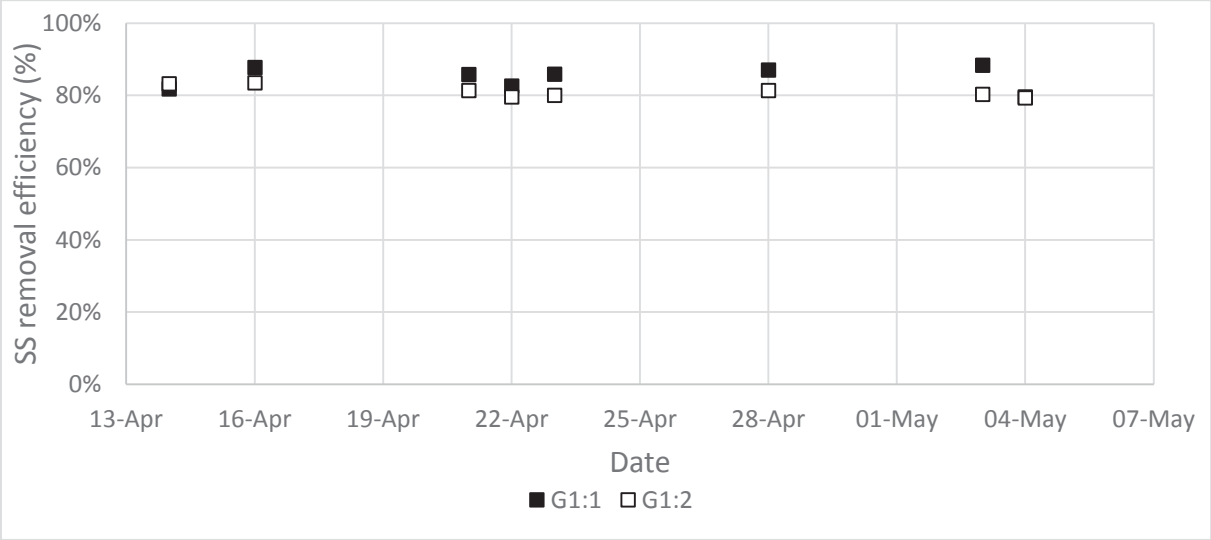

Figure 57 SS removal efficiency in activated sludge lines G1:1 and G1:2 during the 24-hour flow-proportional sampling campaign. The difference between the two lines' ability to remove SS is more visible in this figure than in figure 56. For most samples G1:1 was able to remove approximately 5% more SS than the less aerated line G1:2.

A similar difference could be observed in the COD concentrations and removal rates between the two lines. The average effluent COD concentrations were 69 mg/L in G1:1 and 86 mg/L in G1:2 (see Figure 58) and the treatment efficiencies 79% for G1:1 and 74% for G1:2 (see Figure 59).

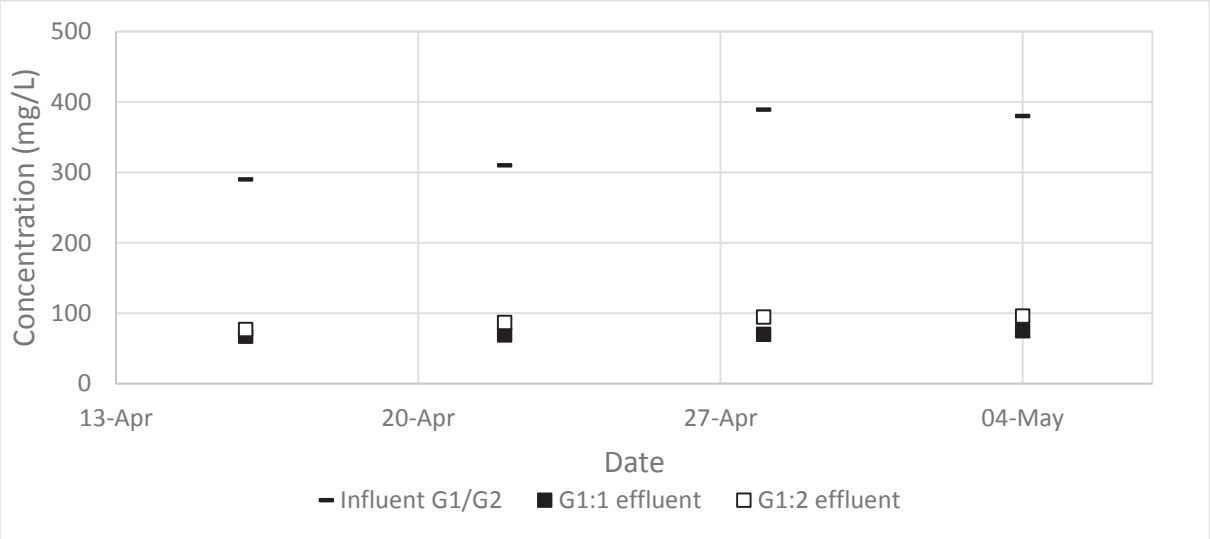

Figure 58 COD concentration in the influent and in the effluents of G1:1 and G1:2 during the 24-hour flow-proportional sampling campaign. Four samples in each line was taken as part of the measurement campaign, and they showed that the COD rate in the influent rose slightly during the period. The COD rate was higher in the effluent from G1:2 than in the effluent from G1:1 at all sampling times.

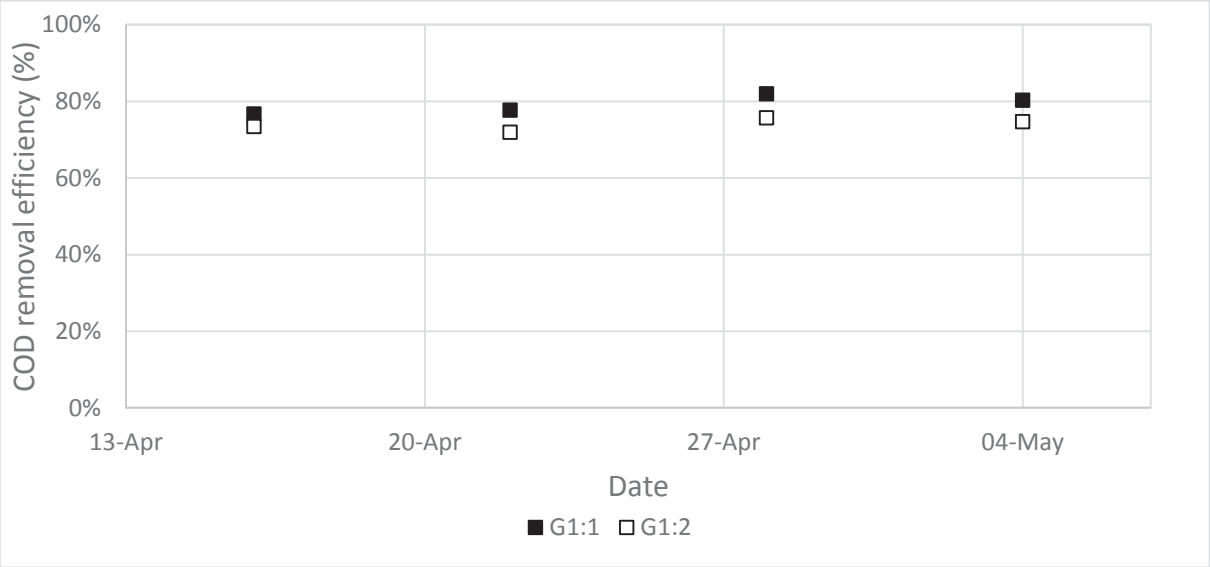

Figure 59 COD removal efficiency for lines G1:1 and G1:2 during the 24-hour flow-proportional sampling campaign. The COD removal rate wass approximately 5% higher for G1:1 than for G1:2 for three of the four sample times.

The concentration differences were smaller in the filtered COD samples. At 1.6 µm filtration an average difference of 8 mg COD/L was observed between G1:1 and G1:2 (see Figure 60), but the difference was only 4 mg COD/L at 0.1 µm filtration (see Figure 61). These results

strengthened the view that the soluble COD that remains in the effluent almost completely belongs to a fraction that is inert in the process, unless so low dissolved oxygen set-points are used that the process becomes unable to properly consume readily biodegradable COD. While no VFA tests were performed as part of the 24-hour flow-proportional sampling campaign VFA analyses performed during both the first and second characterization campaigns showed almost no traces of S_A in the effluent of either line G1:2 or line G2:1, both of which used low DO set-point configurations at the time of their respective characterizations.

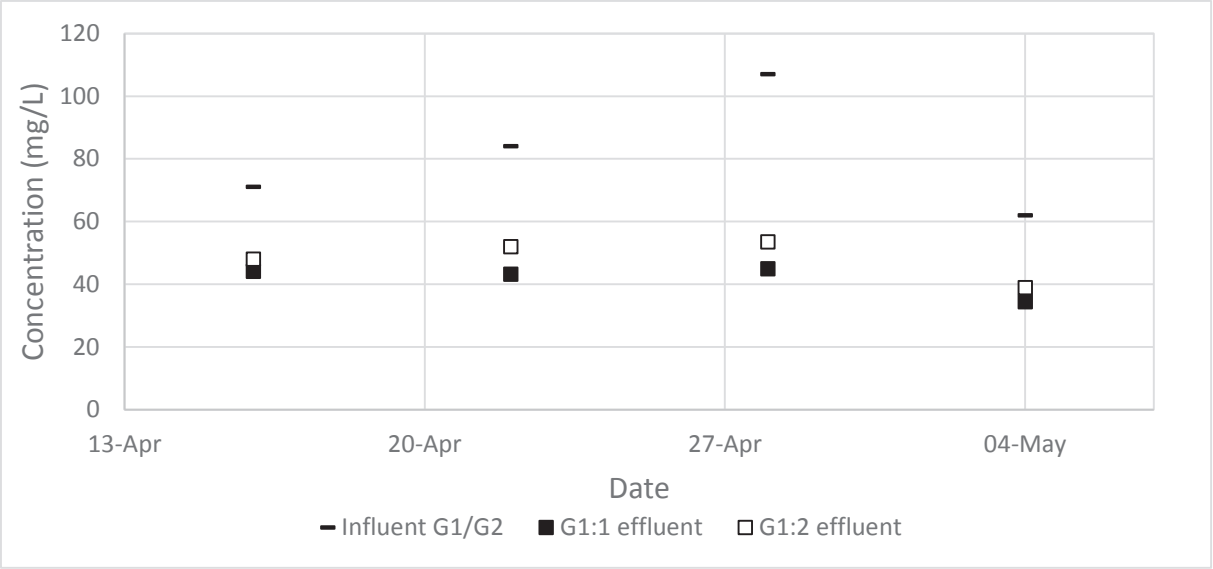

Figure 60 COD filtered 1.6µm concentrations in the influent and effluents of G1:1 and G1:2 during the 24-hour flow-proportional sampling campaign. There were large variations in the influent COD filtered concentration for the four sample times, with a peak occuring on April 28th. The effluent COD concentration was higher in G1:2 than in G1:1 at all sample times.

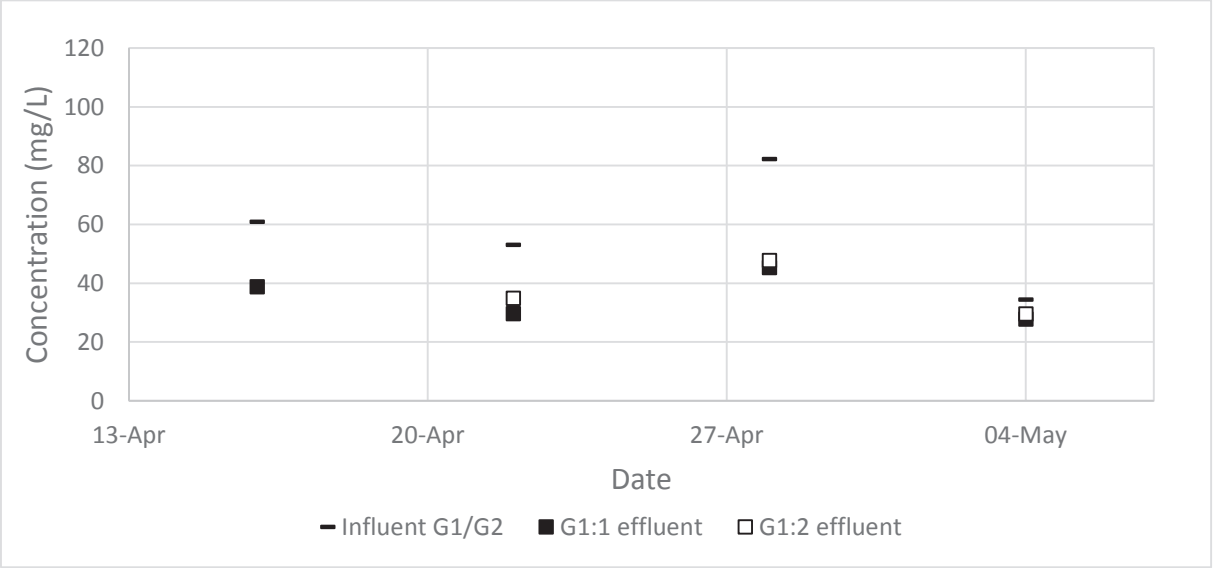

Figure 61 COD filtered 0.1µm concentrations in the influent and effluents of G1:1 and G1:2 during the 24-hour flow-proportional sampling campaign. As for COD filtered 1.6 µm there was a peak concentration at April 28th. For most of the sample times the differences in effluent concentrations for G1:1 and G1:2 were small.

The differences in nitrogen fraction concentrations between G1:1 and G1:2 were too small to be statistically significant, and differences in the COD/N ratio therefore depended on the COD reduction efficiency under the different aeration strategies. A COD/N ratio of 2 is desired in the effluent, but it was found that even with a DO set-point configuration of 2.0 mg/L in all three aerated zones the COD/N ratio would be higher, on average 2.3. With the configuration 0.3 – 0.8 – 1.7 mg/L used in G1:2 the ratio increased to 2.8 however (see Figure 62).

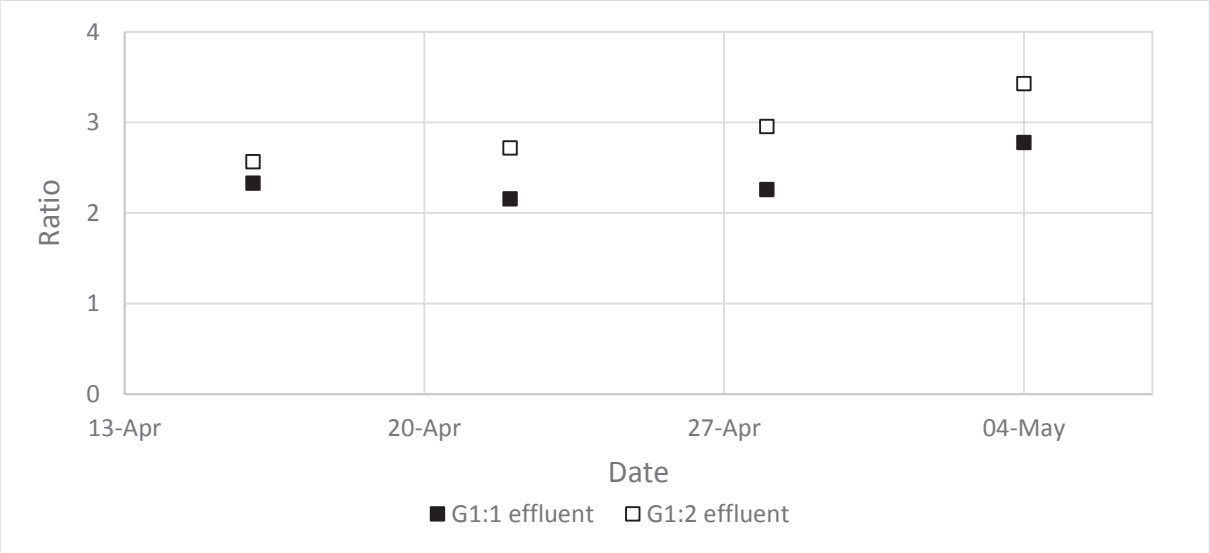

Figure 62 COD/TN ratio in G1:1 and G1:2 during the 24-hour flow-proportional sampling campaign. The difference in COD/TN ratios was significant between G1:1, which kept the ratio at or under 2.5, and G1:2, which had a ratio between 2.5 and 3.5.

After the DO set-points of line G1:2 were changed measurements of the total airflow was taken from the last 11 days before and during the first 5 days after the change. The comparison showed that the total airflow of the process was 5% lower after the change than before May 1st (see Table 12). Meanwhile, the total airflow in the line G1:1, whose aeration strategy had not been changed, was very similar before and after May 1st, which indicated that the changed flow in G1:2 was caused by the process changes and not natural variations in load.

The total airflow in the 2.0 – 2.0 – 2.0 mg/L configuration was found to be 22% higher than in the 0.3 – 0.8 – 1.7 mg/L setup and 28% higher than in the modified 0.6 – 0.6 – 1.0 mg/L configuration. This was larger than the expected differences of 18 % and 21 % that were given by the model, though the comparison between real values do not take into account variances that are caused by the diffuser distribution differences between G1:1 and G1:2.

Table 12 Differences in total airflow before and after the aeration strategy of G1:2 was changed on May 1st 2015.

	G1:1	**G1:2**
	Nm^3/d	Nm^3/d
Before change	50538	41250
After change	50360	39229
Difference	-0.4%	-4.9%

5.8 Second characterization campaign

The second characterization took place on May 11th 2015 on line G1:1, which had a DO set-point configuration of 2.0 – 2.0 – 2.0 mg/L, and line G1:2, which had a DO set-point configuration of 0.6 – 0.6 – 1.0 mg/L. The inflow rate was 25% lower than the yearly average (see Table 13), and 11% lower than the flow rate during the first characterization campaign. The temperature in both the air and the water, especially the former, had increased since the February measurements.

Table 13 Flow rates and temperatures during the second characterization campaign compared to yearly average at Sjölunda WWTP.

	May 11	**Yearly average**
Inflow per line (L/s)	107	141
Air temperature (°C)	14	11.7
Water temperature (°C)	16	16.8

The average concentrations in the influent were very similar to the measurements in February for several of the different compounds. Two exceptions were the SS and COD filtered concentrations, which were 10% higher on May 11th than in February. The fraction of acetate/propionate was almost twice as large (57 mg COD/L compared to 33 mg COD/L) in the second characterization compared to the first. Due to the similarities in concentration the load for COD, TN and TP was around 5-15% lower than in February. Concentrations and loads for all analyzed compounds are presented in Table 14.

Table 14 Influent concentrations and load for the second characterization compared to yearly average (May 2014 to May 2015) at Sjölunda WWTP. The average propionate concentration was below the accuracy threshold of 20 mg COD/L for the analysis method used to determine the concentration. Iron(II/III) was only measured at three occasions during the second characterization and the average value given in the table was not considered to be representative for the entire characterization campaign.

	Concentration (mg/L)		**Load (kg/d)**		
	May 11	Yearly average	May 11	Yearly average	Difference (%)
SS	154	138	1430	1680	-15%
COD	350	300	3280	3650	-10%
COD filtered 1.6 µm	170	95	1610	1150	39%
TN	48	42	450	510	-12%
NH_4^+-N	29.9	25.3	278	308	-10%
NO_2^--N	0.29	1.31	2.7	16.0	-83%
NO_3^--N	0.68	0.51	6.3	6.2	2%
TP	4.7	4.0	44	49	-10%
TP filtered 1.6 µm		0.79		9.6	
PO_4^{3-}-P	1.3		12		
Acetate (mg COD/L)	38.8		360		
Propionate (mg COD/L)	*19.3*		179		
Iron(II/III) (mg Fe/L)	*7.2*		67		

The treatment efficiency of G1:1 was generally higher than expected, and higher than it had been during the 24-hour flow-proportional sampling campaign, which could be explained by the lower than normal load and flow rate. Meanwhile, the treatment efficiency of G1:2 was comparable to the removal rates found in G2:1 in the first characterization. When factoring in the lower load, this indicated that the treatment efficiency might have been slightly lower with the aeration strategy of 0.6 – 0.6 – 1.0 mg DO/L compared to the previous strategy of 0.3 – 0.8 – 2.0 mg DO/L.

The SS concentration in the effluent was approximately 10 mg/L in G1:1 and 27 mg/L in G1:2, which put the SS removal rate at 93% for G1:1 and 83% for G1:2 (see Table 15). The result also showed that the f_{ns} experiment undertaken during the characterization campaign could not be accurate, especially not for G1:1, since they predicted average SS concentrations of at least 29 mg/L in G1:1 and 31 mg/L in G1:2.

COD reduction efficiency were more effective in both G1:1 and in G1:2 than it had been during the 24-hour flow-proportional sampling campaign, with a reduction rate of 87% in G1:1 compared to 79% during the sample campaign and 79% in G1:2 compared to the 74% achieved by the old aeration strategy used in the 24-hour flow-proportional sampling campaign.

The DO set-point configurations were seen to have had only a minor effect on the nitrogen concentrations, something that had also been noticed during the flow-proportional sampling campaign. Due to the very high effectiveness of the COD treatment, the COD/N ratio in G1:1 was 1.5, which was much lower than it had been during the flow-proportional sampling campaign, whereas the ratio for G1:2 was 2.2.

*Table 15 Effluent concentrations and treatment efficiency of the second characterization campaign compared to the average yearly average at Sjölunda WWTP. * The yearly average for nitrate is negative because there typically is some nitrification, in which nitrate is formed, in the aerated basins.*

	Concentrations (mg/L)			Treatment efficiency		
	G1:1	G1:2	Yearly average	G1:1	G1:2	Yearly average
SS	10.3	26.9	17.1	93%	83%	88%
COD	46	74	59	87%	79%	80%
COD filtered 1.6 µm	34	44	40	80%	74%	58%
TN	31	33	29	35%	31%	31%
NH_4^+-N	24.0	24.5	22.5	20%	18%	11%
NO_2^--N	0.011	0.016	0.195	96%	94%	85%
NO_3^--N	0.35	0.36	1.85	48%	47%	-263*%
TP	0.4	0.8	0.9	93%	83%	78%
TP filtered 1.6 µm			0.36			55%
PO_4^{3-}-P	0.06	0.08		95%	94%	

There were large differences in the mass balances for both G1:1 and G1:2. TP and SS both showed influent loads that were 24% lower for G1:1 and 33% lower for G1:2 than the combined effluent and waste loads. However, TN was found to be in balance for the system calculations

of both lines. When considering discrepancies in the mass balances an important aspect to note is that the second characterization only included 24 hours of measurements, and furthermore that only measurements of the inflow and effluent showed the concentration differences throughout the day. The SS and TP measurements for the activated sludge in zone 5 and for the waste sludge were grab samples, taken at four different times that were all around the middle of the day, and there might have been concentration variations during the morning or evening hours that were not picked up by the samples and that would have reduced the imbalance. Additionally, in reality it takes time for particles to move through the activated sludge process, whereas the mass balance equations used in the calculations assume instantaneous mixing, and this lack of a delay could also have distorted the mass balances.

Both SS and TP concentrations were observed to be rising in the last hours of the second characterization (see Figure 63 and appendix Figure 86-89), and it is also possible that there were peak concentrations in the hours before the characterization campaign which might have caused the imbalance.

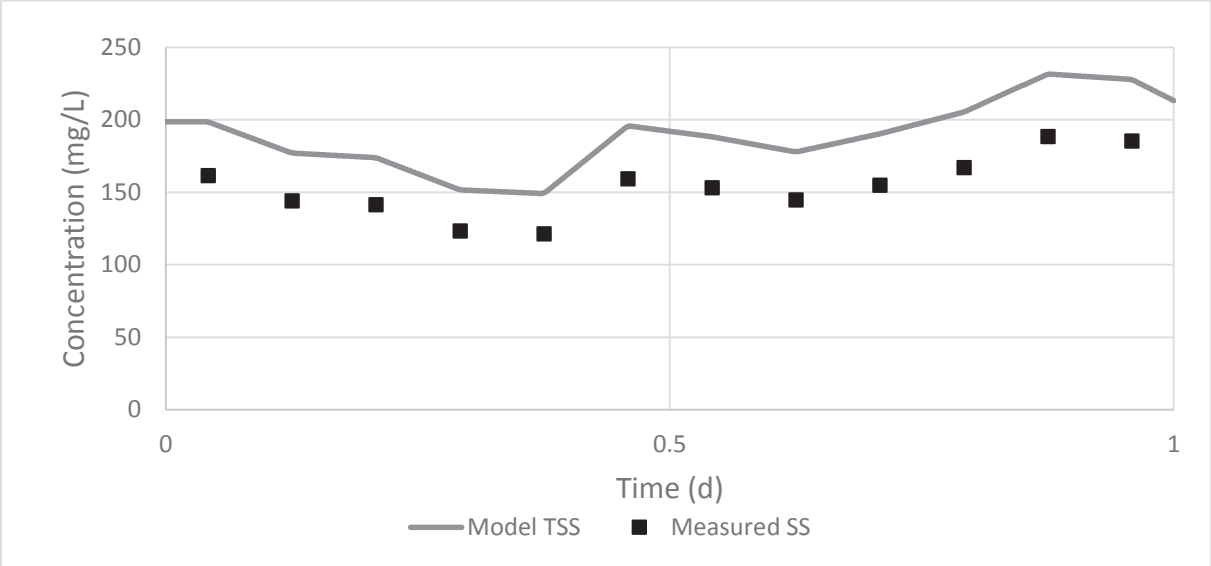

Figure 63 Concentrations of measured SS and model TSS in the influent during the second characterization. The model TSS values were set to be 23% higher than the measured values.

Mass balances over the secondary clarifier were also severely distorted. G1:1 showed an influent load that was 12-17% higher than the effluent load for all three mass balances of SS, TP and TN whereas the effluent loads of SS, TP and TN in G1:2 were all 22-32% lower than the influent loads. This could indicate that the return sludge flow sensors showed lower measurements than the actual flow, that there were variations in the SS and TP concentrations in the sludge that were not picked up in the limited characterization campaign or possibly a combination of the two explanations.

While it has to be taken into account that the mass balances did not add up, and that further investigations on whether sensors had reported the wrong values or if other factors had caused these issues would be necessary, SRT calculations showed very different results for the two lines, results that were also different from the SRT in the first characterization. In the first characterization the SRT was calculated to be approximately 1.9 days. During the second characterization the combination of low inflow rates and comparatively high waste sludge flow rates caused the average SRT to drop to 1.4 days in G1:1 and 1.0 days in G1:2. It cannot be

ruled out that the difference in SRT between G2:1 in February and G1:2 in May hampered the treatment efficiency of G1:2, and it is therefore difficult to say anything conclusive about how the treatment efficiency had been affected by the change in aeration strategies.

The total airflow of G1:1 was 48024 Nm^3/d, or 17.4% higher than the total airflow of 40896 Nm^3/d for G1:2.

5.9 Model validation and recalibration

5.9.1 Comments on differences in sludge flow between G1:1 and G1:2

The second characterization campaign showed low inflow rates which worked to enhance differences between the sludge flow systems of the two G1 lines.

When the inflow rate for G1 climbs over 300 L/s (approximately 26000 m^3/d) the pumping system is designed to start running two extra pumps, bringing the total number of pumps per line up to four. The system reverts to two pumps at flow rates below 200 L/s (17000 m^3/d). During the second characterization the return sludge pumping system for G1:1 and G1:2 appeared to have behaved differently however, despite getting the inflow data from the same sensor. Where the number of pumps increased to four in G1:1 around 10.00 (see Figure 64), the increase does not seem to have happened until around 12.00 in G1:2, and then only for a few minutes before the system reverted to only using two pumps (see Figure 65).

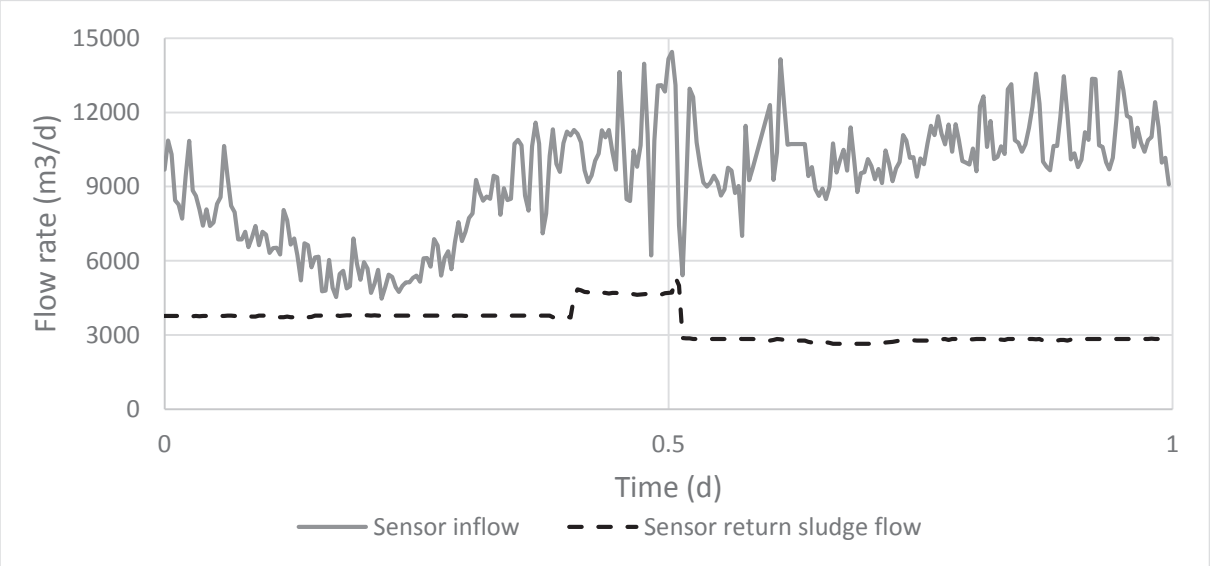

Figure 64 Inflow for each G1 line and the return sludge flow rate for G1:1 during the second characterization campaign. The inflow rate followed the standard daily flow rate pattern for the first half of the day, with low flow in the early morning followed by high flow rates in the middle of the day, but during the second half of the day the flow rate remained high, around 10000 m^3/d. The return sludge flow rate for G1:1 increased slightly around 10.00 but almost halved at 12.00 to approximately 3000 m^3/d.

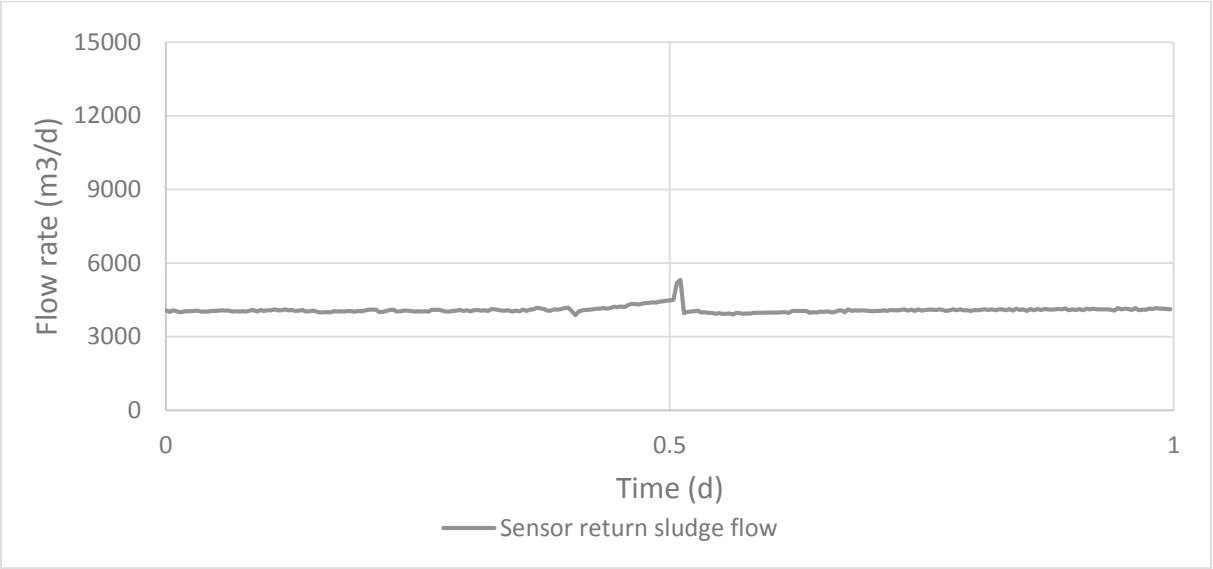

Figure 65 Return sludge flow rate for G1:2 during the second characterization campaign. The return sludge flow rate was very stable at 4000 m^3/d during the entire measurement campaign.

Previous examinations of return sludge flow data from G1:1 had revealed significant differences in pumping capacity between the different sets of return sludge pumps in the line. Since G1:1 alternate between pumps to ensure that all pumps are used at different times even during periods of low inflow rates this led to significant differences in return sludge flows between G1:1 and G1:2 that contributed to making it more difficult to compare the two lines.

Differences in flow could also be observed for the waste sludge flow, where the flow rate varied between 240 and 250 m^3/d for G1:1, and 260 to 270 m^3/d in G1:2 (see Figure 66 and Figure 67).

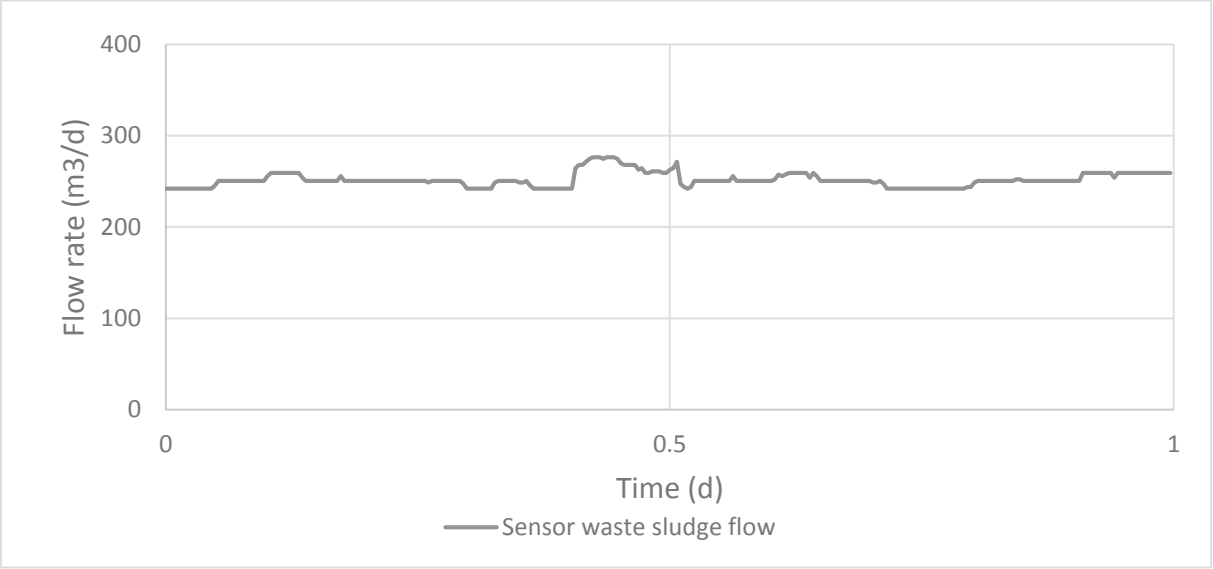

Figure 66 Waste sludge flow rate of G1:1 during the second characterization. The waste sludge flow rate was fixed at 250 m^3/d, with slightly higher flow rates being registered around 10.00-11.00.

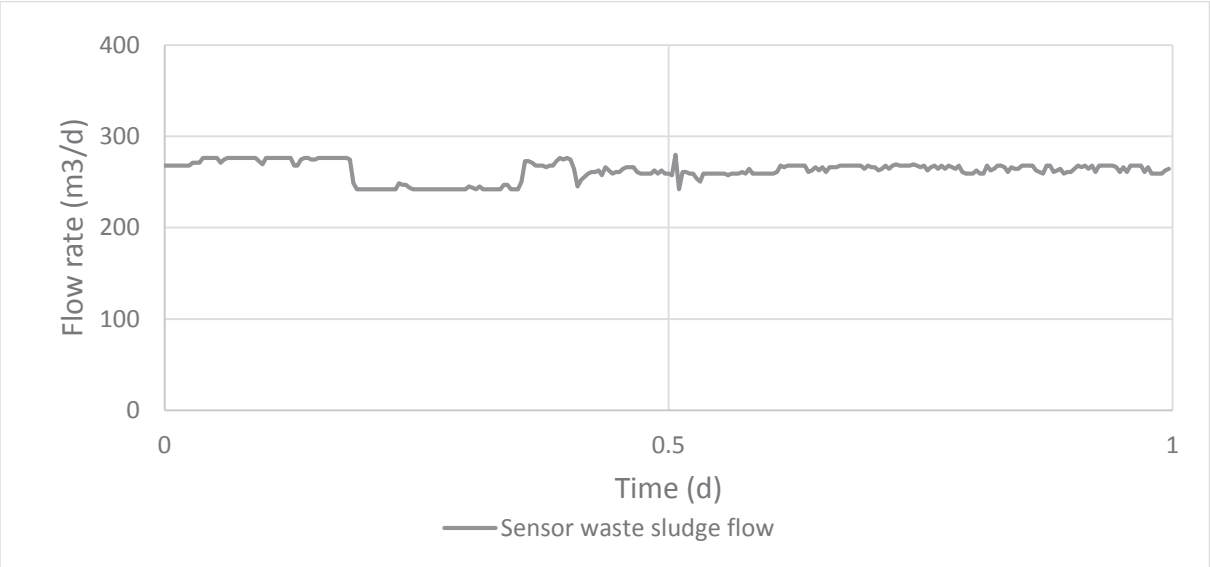

Figure 67 Waste sludge flow rate of G1:2 during the second characterization. As with G1:1 the waste sludge flow rate was fixed, but for G1:2 the fixation point was slightly higher, 260 m^3/d. Minor deviations from this point occurred during the first half of the day.

5.9.2 Validation of G1:1

Sedimentation properties were changed in the model to account for experimental results found after the calibration of the model. SVI was set to 98 mL/g, v_0 to 170 m/d, v_0' to 110 m/d and r_p to 0.00286 m^3/g. While experiments on the fraction of non-settleable solids indicated that it would be 0.011 this was shown to be impossible given the measured SS concentrations in the effluent, and the validation was instead run using an f_{ns} of 0.004, which would give a minimum SS concentration of under 10 mg/L in the effluent.

COD filtered 0.1 µm tests were performed on both the influent and effluent wastewater. The tests showed that the correction factor 0.80 for S_{COD} from COD filtered 1.6 µm input data that was found in the initial calibration was still valid for the second characterization, whereas the correction factor in the effluent had to be reduced from 1.25 to 1.05. This was consistent with the assumption that COD filtered 1.6 µm included a part of slowly biodegradable organic matter X_S which was not picked up in COD filtered 0.1 µm tests. Since X_S was considerably lower in the effluent of a highly aerated activated sludge process than in a more conservatively aerated process, while the soluble inert organic matter S_I would be approximately the same in the effluent of both processes, the ratio between biodegradable and inert organic matter that passed through 1.6 µm filters would be lower. The TSS/SS ratio of 1.23 in the influent and effluent from the initial calibration was kept as no new experiments to determine this ratio were made during the second characterization.

After running the model with these changes, and with the influent, flow and temperature data from the second characterization, the model was found to have significant problems with its calibration.

The model airflow of zone 3 was found to align very well with the measured airflow for the first 14 hours of the dynamic simulation, but after that point the model hit the maximum airflow rate, while measurements showed that the airflow dropped before rising up to the maximum airflow after 21 hours (see Figure 68). While neither the model nor the real aeration system was

able to maintain a dissolved oxygen concentration of 2 mg/L in zone 3 for the entire day this difference made the dissolved oxygen concentration drop to approximately 1 mg/L in the model after 17 hours, whereas it did not start to drop in the measurements until approximately 20:00 (see Figure 69). Furthermore, the model DO concentrations had higher oscillations, and some recalibration of the PI regulator could therefore be necessary.

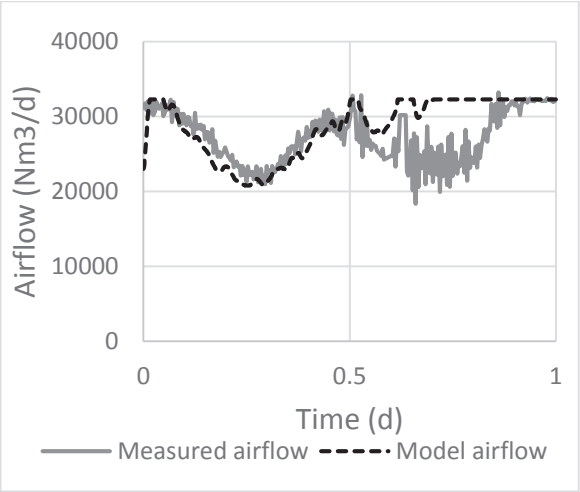

Figure 68 Model and measured airflow of G1:1 zone 3 during the second characterization.

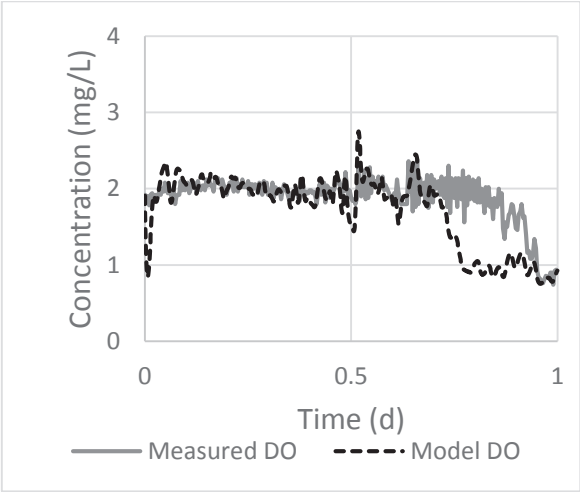

Figure 69 Model and measured dissolved oxygen concentration in G1:1 zone 3 during the second characterization.

Zone 4 had better alignment between the model and measured oxygen concentrations than zone 3 (see Figure 71), and the model airflow was furthermore able to follow the shape of the measured airflow during the entire day (see Figure 70). However, the model airflow was on average 2-3000 Nm^3/d lower than the measured airflow, so calibration would be necessary to increase the model airflow rate without increasing the dissolved oxygen concentration.

The airflow of zone 5 had the most significant calibration problems (see Figure 72), with the model airflow hitting the minimum flow after less than 2 hours, and staying at this flow rate for the remainder of the simulation, thus not being able to properly maintain a DO concentration of 2 mg/L (see Figure 73). The PI-controller of zone 5 was using a longer integral time, than the controllers on the aerators in the other zones, so decreasing T_I could solve parts of the problem, but it would also be necessary to make significant changes to the A and B parameters of the aerator.

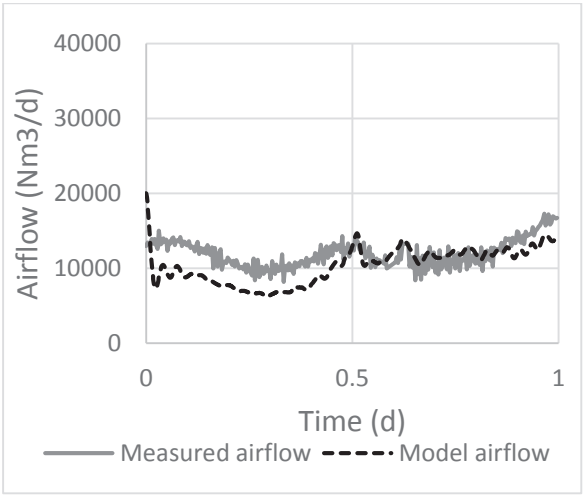

Figure 70 Model and measured airflow of G1:1 zone 4 during the second characterization.

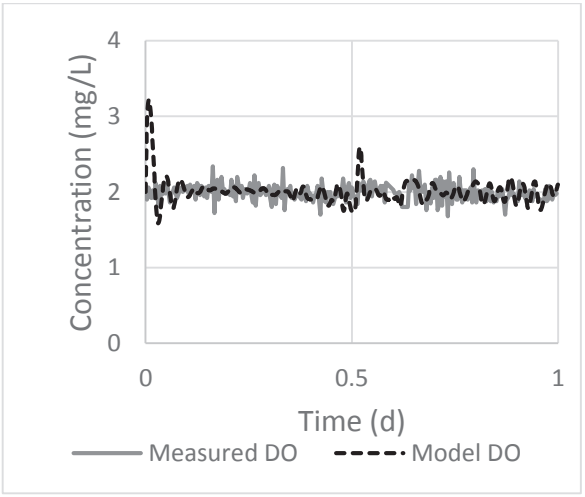

Figure 71 Model and measured dissolved oxygen concentration in G1:1 zone 3 during the second characterization.

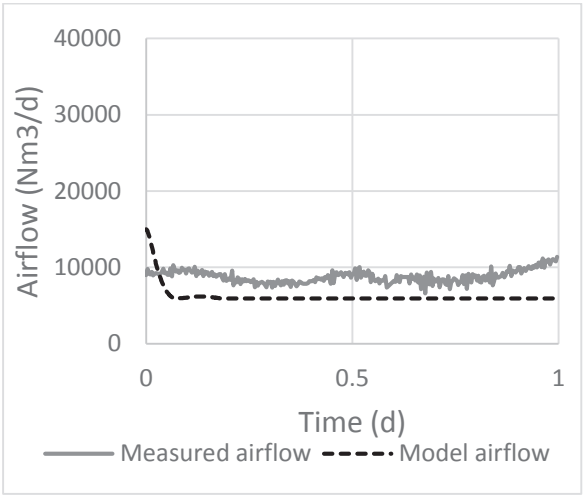

Figure 72 Model and measured airflow of G1:1 zone 5 during the second characterization.

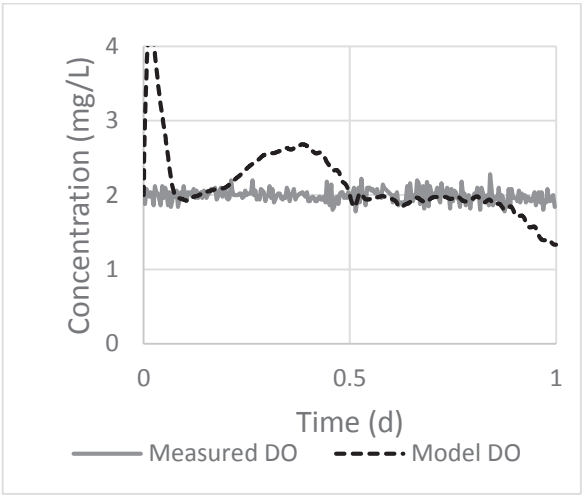

Figure 73 Model and measured dissolved oxygen concentration in G1:1 zone 5 during the second characterization.

Problems with the calibration was even more evident when studying the concentrations of SS, COD, TN and TP in zone 5 and the waste sludge. Model concentrations were all significantly below the measured concentrations. In zone 5 (see Figure 74 and appendix Figure 90-92) SS and COD concentrations were approximately 25% lower in the model than in the measurements, with the difference being even larger for TN and TP at 40% and 33% lower concentrations in the model. The waste sludge (see Figure 75 and appendix Figure 93-95) showed similar differences. SS was 32%, COD 19%, TN 31% and TP 28% lower in the model than in the measurements.

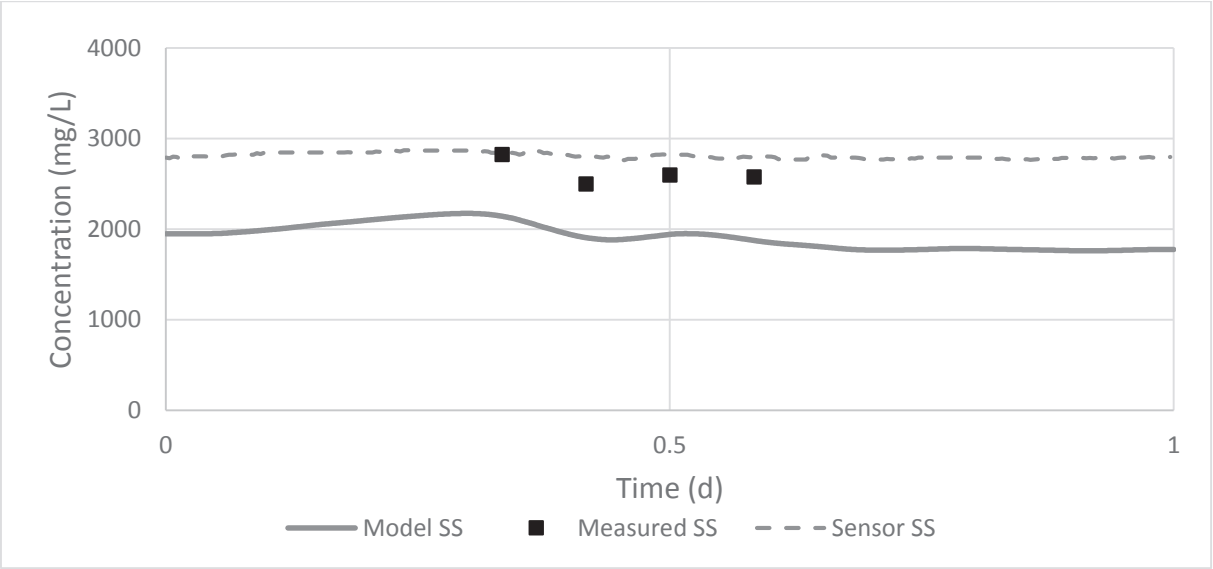

Figure 74 Model, sensor and measured suspended solids concentrations in G1:1 zone 5 during the second characterization. The model SS concentration wass on average 6-700 mg/L lower than both the sensor values and the measurements.

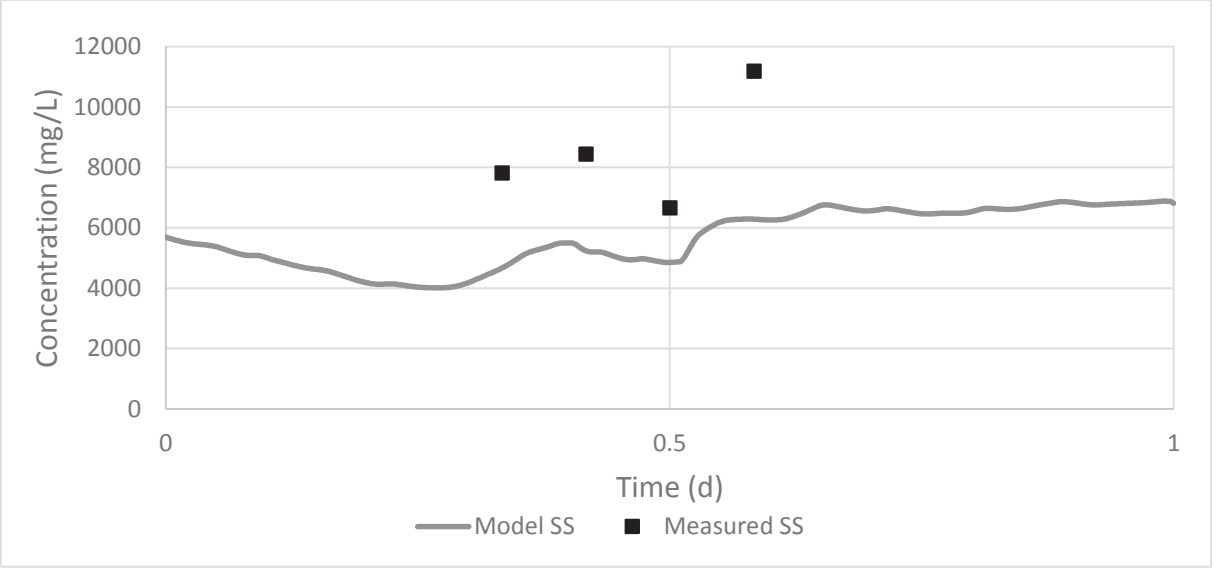

Figure 75 Model and measured suspended solids concentrations in the waste sludge from G1:1 during the second characterization. As in zone 5 the model SS was significantly lower than the measured SS, with differences of on average 3000 mg/L.

Results from the validation of the effluent looked better than the sludge for TN and COD, but worse for SS and TP (see Figure 76 and appendix Figure 96-98). TN was reasonably well calibrated, but the problem with the fraction of organic nitrogen being too small compared to the NH_4^+-N fraction that were seen in the initial calibration could still be witnessed in the validation. COD filtrated was approximately 5 mg/L lower in the model than in the measurements, whereas COD was 10-15 mg/L higher, which could partially be explained by issues with the settling model (see Section 5.5.5) in that the X_H/X_S ratio was much higher in the model than the ratio between biomass and slowly biodegradable organic matter is likely to have been in the real effluent, and COD would then be overestimated in systems that would be able to break down much more X_S due to increased aeration. The problems with the settling model

was particularly apparent for SS and TP concentrations, that were more than twice as large in the model as in the measurements from the second characterization. It is possible that the change of v_0 from 600, that had been used in the initial calibration, to 170 m/d, which had been found after reinvestigating earlier settling results, had been too drastic.

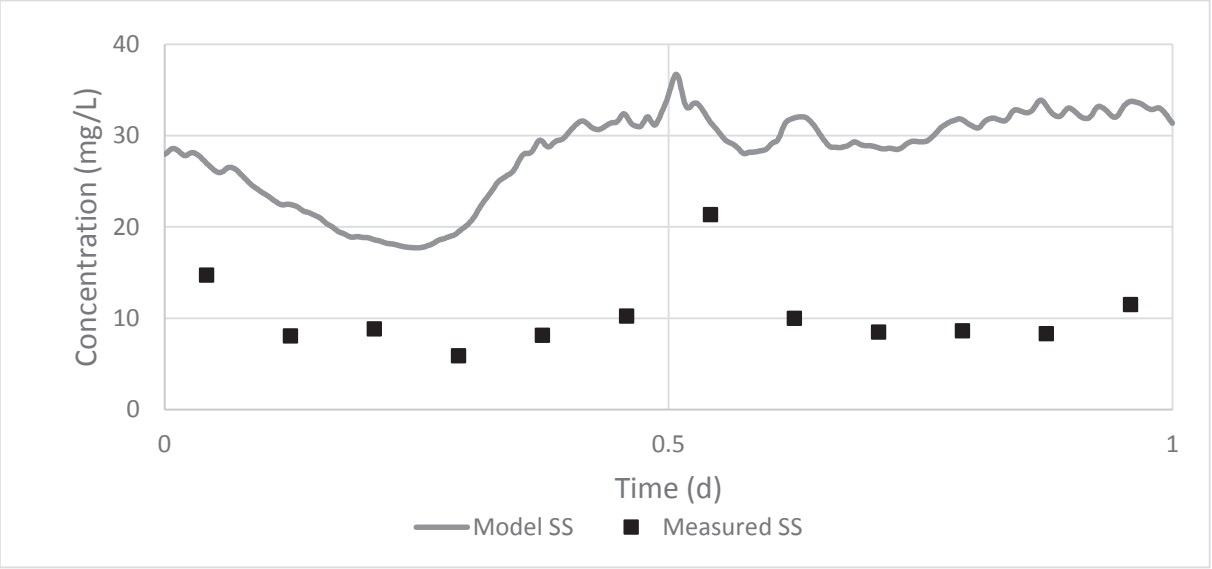

Figure 76 Model and measured suspended solids from the effluent of G1:1 during the second characterization.

5.9.3 Validation of G1:2

As with the validation of G1:1 some of the fractions and properties used in the initial calibration of G2:1 had to be changed due to new experimental data. SVI had been measured to be slightly lower in G1:2 than in G1:1, 93 mL/g, while the same values for v_0, v_0' and r_p could be used. f_{ns} had been experimentally determined to be 0.016, but just as for G1:1 the value was too high to be possible given the measured ratio of SS in the effluent and SS in the influent, and it was instead kept at 0.0075, the fraction used in the first characterization.

COD filtered 0.1 µm and 1.6 µm tests showed that a correction factor of 0.80 for S_{COD}/COD filtered 1.6 µm was still valid for both the influent and effluent fractionation models.

The number of diffusers and maximum- and minimum air flows of the aerators in zones 3-5 were changed to match the real configuration in line G1:2, but no further calibration of the aerators in G1:2 had been made prior to the validation, and the A and B model parameters were therefore set to the values that had been found to give good calibration during the aeration model recalibration of G1:1 (see Section 5.5.6).

The validation of the model showed that similar problems to the aeration model that could be observed in G1:1 could also be found in G1:2, but that the difference in aeration strategies meant the discrepancies between model and measurements occurred in other zones. Zone 3 had a model airflow that was closely matched to the measured airflow for the first 12 hours, but a significant gap between model and measured flow then appeared (see Figure 77). The DO rate had higher oscillations in the model than in the measurements (see Figure 78), which meant that there is a need to look at both A and B in the aerator model and the parameters of the PI regulator.

Since there are DO sensors in each aerated zone an alternative option would be to simplify the model by directly inputting DO concentrations, instead of simulating the concentrations through an aeration sub-model. This would reduce the complexity of the model and could increase the accuracy of the model during the calibration or validation phase. However, this solution could at the same time make scenario analyses even more inaccurate, since it would likely require using fixed DO concentrations in the aerated zones during the analyses. Furthermore, it would not be possible to estimate the airflow without using an aeration sub-model, and as an effect the model would not be able to simulate the effect of different scenarios on the power consumption of the activated sludge process.

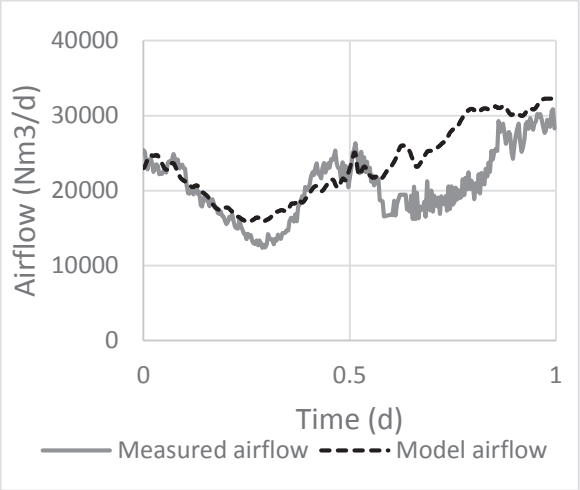

Figure 77 Model and measured airflow of G1:2 zone 3 during the second characterization.

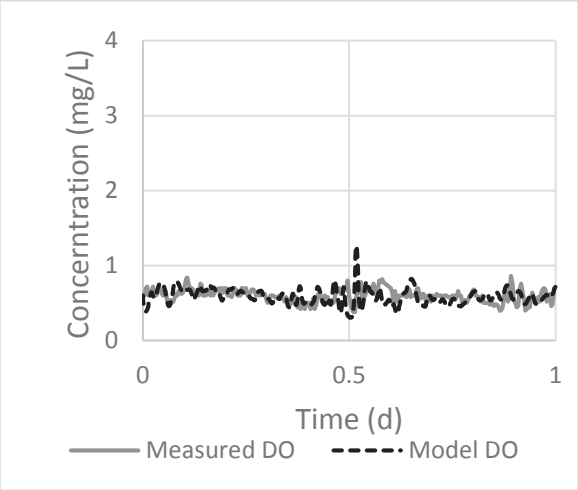

Figure 78 Model and measured dissolved oxygen concentration in G1:2 zone 3 during the second characterization.

Both zones 4 and 5 (see Figure 79 and Figure 80) had model airflows which quickly approached the minimum airflow, which gave poor match to the measurement airflows, and, as a consequence led to an inability for the model to maintain the set-point concentrations for DO, causing large differences in DO concentrations versus the measurements (see Figure 81 and Figure 82). It is interesting to note that the model airflows and DO in zone 4 give good results for the last 8 hours of the characterization.

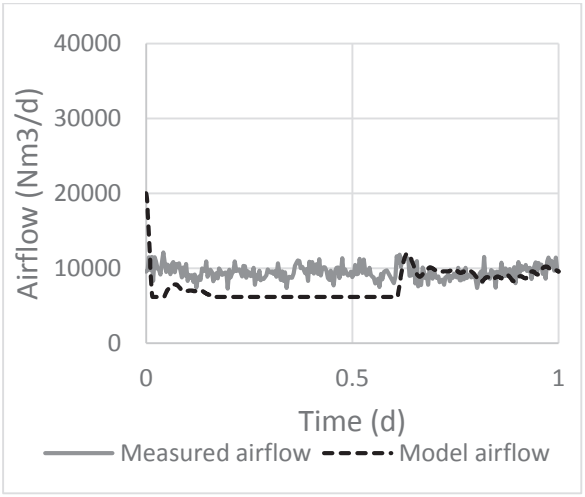

Figure 79 Model and measured airflow of G1:2 zone 4 during the second characterization.

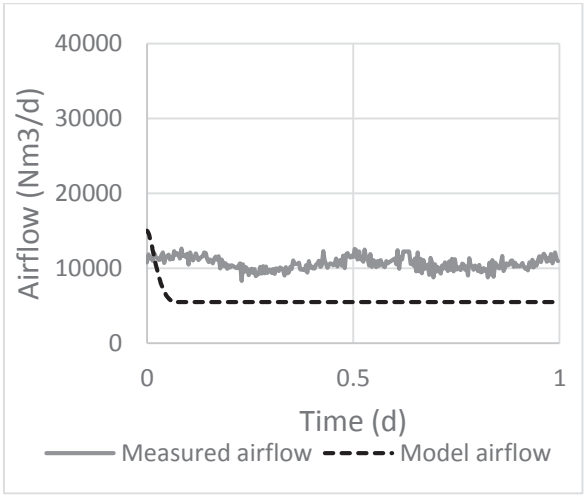

Figure 80 Model and measured airflow of G1:2 zone 5 during the second characterization.

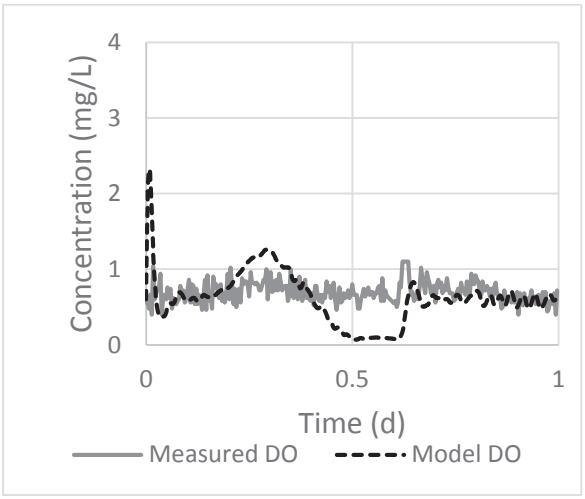

Figure 81 Model and measured dissolved oxygen concentration in G1:2 zone 4 during the second characterization.

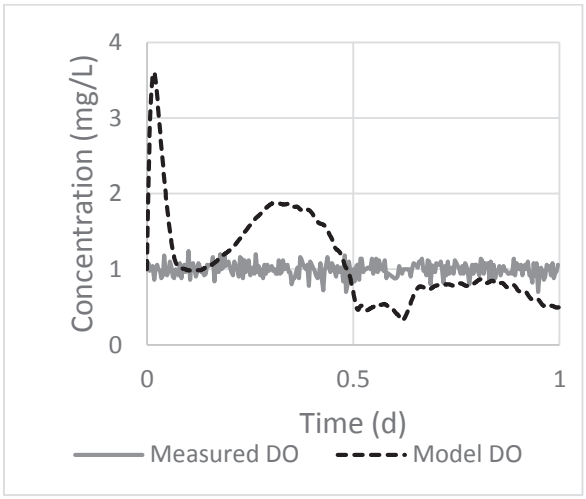

Figure 82 Model and measured dissolved oxygen concentration in G1:2 zone 5 during the second characterization.

The model showed a good fit for SS and TP compared to measurements, and reasonably small differences for COD and TN, with the former being approximately 10% lower and the latter 10% higher in the model compared to measurements in zone 5 (see Figure 83 and appendix Figure 99-101). The waste sludge flow showed error ranges between the model and measurements that were very similar to those seen in G1:1 however. SS was 33%, COD 18% and both TN and TP 28% lower in the model than in the measurements (see Figure 84 and appendix Figure 102-104).

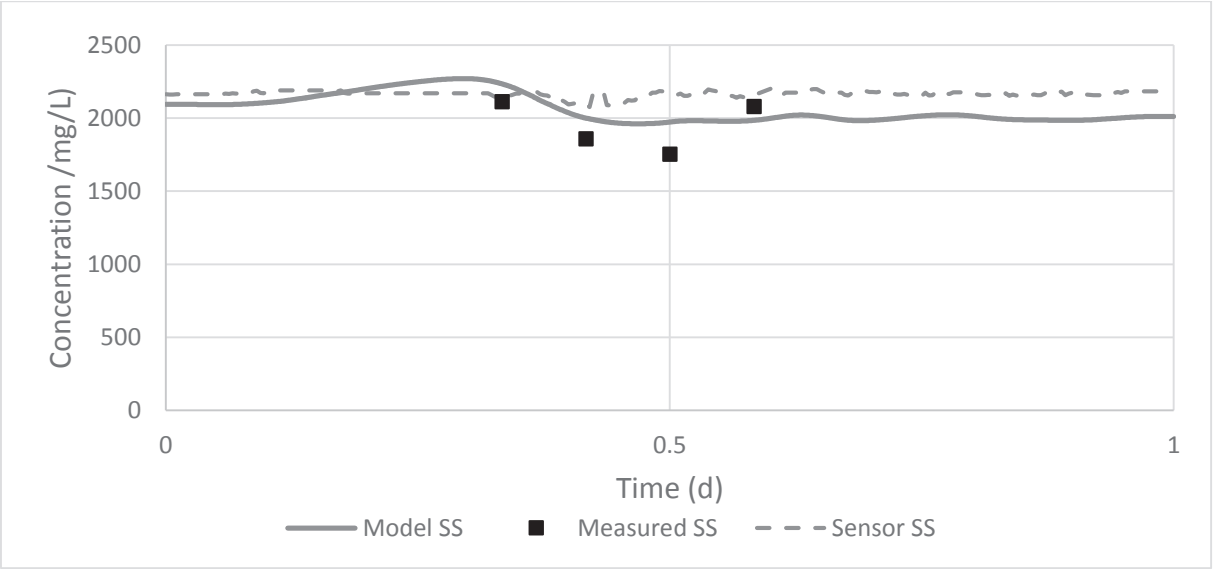

Figure 83 Model, sensor and measured suspended solids concentrations in G1:2 zone 5 during the second characterization. The model SS concentration was similar in magnitude to the measurements and sensor SS concentrations.

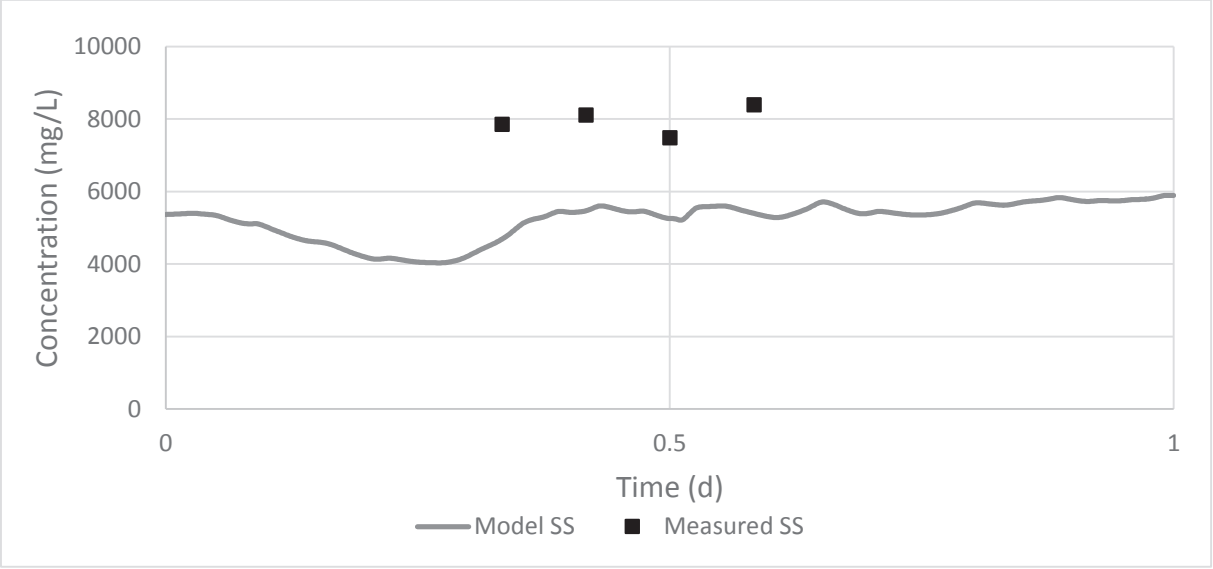

Figure 84 Model and measured suspended solids concentrations in the sludge waste of G1:2 during the second characterization. The model SS concentrations were close to 3000 mg/L lower than the measurement concentrations in the sludge waste.

Validation of the effluent showed that the model better predicted the effluent quality for the conditions in G1:2 than in G1:1. Both TN and TP had good matches between the model and the measurements, but just as in the validation of G1:1 the model underappreciated the organic nitrogen concentration. Suspended solids concentrations had only small differences between the model and measurements in the first 12 hours, but for the last hours of the day, when measurements showed that the concentration dropped to around 25 mg/L, the model maintained an SS concentration of approximately 35 mg/L. COD had the largest differences between model and measured concentrations in the effluent, with total COD in the model being 10 mg/L lower than the measurements whereas COD filtered was almost 20 mg/L, or 45%, lower in the model than in the characterization data (see Figure 85 and appendix Figure 105-Figure 107).

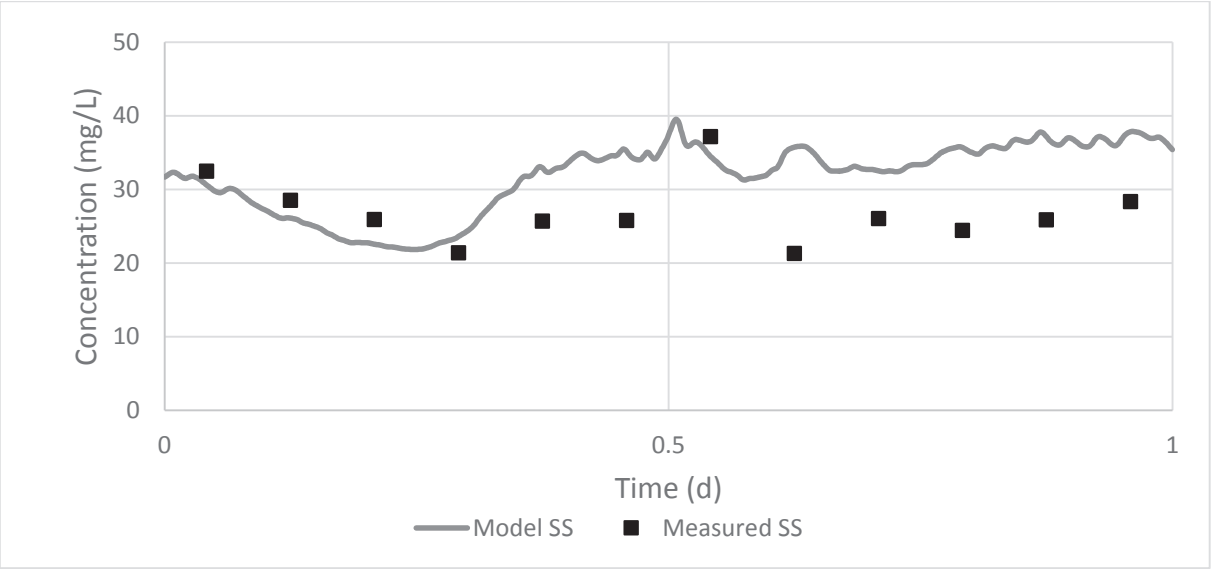

Figure 85 Model and measured suspended solids concentrations in the G1:2 effluent during the second characterization. The model SS concentration was similar to concentration found in the measurements during the first hours of the day, but was on average 10 mg/L higher than the measurements during the last 15 hours.

5.9.4 Recalibration of the model

The validation of the model based on the different aeration strategies employed in lines G1:1 and G1:2 showed significant problems with the model performance, especially concerning sludge concentrations, effluent concentrations for G1:1 and the aeration sub-models in both lines. The small impact different aeration strategies had on the model contributed to these problems, since full-scale tests showed that different strategies caused considerable differences, especially in the effluent concentrations.

Further investigation showed that the mass balances in the measurement data did not add up, and that the differences were even larger than the imbalances that had been found during the first characterization. The SRTs of the two lines were furthermore found to be very different, and also differed significantly from the SRT that occurred during the initial calibration of the model, which would have made it difficult to compare the different aeration strategies. Nobel (2015) showed that a reduction in SRT also reduces the removal efficiency of the activated sludge process, and that at SRTs under 1.5 days the effects start to become noticeable. Potential beneficial effects from a new aeration strategy could therefore be negated by the negative effects of a reduced SRT.

Given the problems that were found during the validation of the model and the very limited time that remained in the project at the conclusion of the second characterization campaign it was not considered to be possible to undertake the extensive investigations of G1 and perform a recalibration of the model that had previously been performed on line G2:1 when similar, though less severe, problems were found after the first characterization and model set-up, and which were required to be able to recalibrate the model.

The aeration model was shown to be relatively well calibrated for some zones, but requires some adjustments for other zones where the model would hit the maximum or minimum

airflow, which would in turn give different dissolved oxygen concentrations from the measurements in the model.

5.10 Final simulations and evaluation of scenarios

The inability to fully trust the model, and especially effluent results led to a need to depend on results from measurement campaigns for evaluating the aeration strategies. This also limited the number of DO set-point configurations that were comparable without resorting to speculation to the four configurations that had been tested in full-scale during the measurement campaigns: 0.3 – 0.8 – 1.7, 0.3 – 0.8 – 2.0, 0.6 – 0.6 – 1.0 and 2.0 – 2.0 – 2.0 mg/L.

Even for these four DO set-point configurations there were circumstances that make comparisons more difficult. The SRT was 1.9 days for line G2:1 during the first characterization campaign, whereas it varied between 1.0 and 1.2 days for line G1:1 and between 1.0 and 1.3 days for line G1:2 during the 24-hour flow-proportional sampling and the second characterization campaigns. Nobel (2015) showed that in an SRT range of 1-2 days the removal efficiency of SS and COD is reduced if SRT decreases. Temperature differences also need to be considered. In the first characterization the water temperature was 14°C, while it was 16°C during the second characterization. The activated sludge processes generally work better at higher water temperatures. The treatment quality in the G1 lines in May was therefore likely improved due to the higher temperature, but reduced due to a lower SRT compared to the treatment quality in G2:1 in February.

Furthermore, G2:1 had an aeration system that was different from the G1 lines in that it had more but smaller diffusers, and that the diffusers were unevenly distributed, with significantly more diffusers in zone 3 than in zone 5, whereas the G1 lines had approximately the same number of diffusers in each of the three aerated zones. This would mostly influence the airflow required to maintain a specific DO concentration in each zone and in effect the energy consumption.

5.10.1 Treatment quality

Full-scale tests from the 24-hour flow-proportional sampling campaign showed that the COD removal rate in the activated sludge process was 71% in the 0.3 – 0.8 – 1.7 configuration and 79% in the 2.0 – 2.0 – 2.0 mg DO/L configuration. A difference of the same magnitude could be seen in the second characterization, where G1:2, using the set-points 0.6 – 0.6 – 1.0 mg DO/L, had a COD removal efficiency of 79%. Meanwhile, G1:1 with the set-points 2.0 – 2.0 – 2.0 mg/L achieved a removal rate of 87%. The results can be compared to the COD removal efficiency of the first characterization, where the use of a 0.3 – 0.8 – 2.0 mg DO/L configuration removed 80% of the COD, a value that is similar to the removal efficiency of that achieved by 0.6 – 0.6 – 1.0 mg DO/L.

The strategy has only been fully tested in low flow conditions, and it is possible that the treatment quality would be lower than the quality of the 0.3 – 0.8 – 1.7 strategy under higher COD load or flow rates. Meanwhile, the SS load was very similar during both characterization campaigns, and where a removal rate of 81% was achieved using 0.3 – 0.8 – 2.0 mg DO/L in the aerated zones of G2:1 in the first characterization the removal rate in G1:2 during the second characterization using 0.6 – 0.6 – 1.0 mg DO/L was 83%, which supports the WEST model's estimation that two processes would perform equally well with regards to treatment quality.

5.10.2 Energy consumption

Total airflow was used as the measurement when evaluating the energy consumption. While the measurements give an indication if an aeration strategy is more or less energy consuming than another strategy it overvalues the actual energy savings since it does not take such factors as energy losses and fixed energy demand from the air blower into account. The difference in airflow, which the model was able to predict fairly well, should therefore not be seen as the potential energy savings of optimizing the aeration strategy.

The calibrated model predicted that the decrease in total airflow would be 2.3% if the aeration strategy was changed from 0.3 – 0.8 – 1.7 to 0.6 – 0.6 – 1.0 mg/L. Measurements from before and after the change indicate that the actual reduction of airflow was approximately 4.5 – 5%.

A similar comparison between model predictions and real measurements could be made for the second characterization between line G1:1 with a 2.0 – 2.0 – 2.0 mg DO/L aeration strategy and line G1:2 with a 0.6 – 0.6 – 1.0 mg/L strategy. G1:1 was expected to have 21.2% higher total airflow than G1:2 based on model predictions, whereas full-scale tests showed a difference of 17.4%.

If the target would be to decrease energy consumption as much as possible without reducing the treatment efficiency both model data and full-scale tests indicate that the aeration strategy 0.6 – 0.6 – 1.0 mg/L would give the best results.

5.10.3 COD/N ratio

The full-scale tests of different aeration strategies gave a strong indication that the choice of aeration strategy had a significant effect on the COD/N ratio due to the large differences in COD in the effluent between a high DO and a low DO strategy. The 24-hour flow-proportional sampling campaign showed a COD/N ratio of 2.8 in the line using the 0.3 – 0.8 – 1.7 configuration, while the 2.0 – 2.0 – 2.0 configuration had a ratio of 2.3. In the validation the difference in ratios were of even greater magnitude: 2.2 for the 0.6 – 0.6 – 1.0 mg DO/L set-point configuration versus a COD/N ratio of 1.5 in the 2.0 – 2.0 – 2.0 configuration.

However, both historical data from the period when Sjölunda WWTP used setpoints of 2.0 mg/L in each aerated zone, and the results from the 24-hour flow-proportional sampling campaign indicate that it is not possible to reach a COD/N ratio of 2.0 even with the aeration strategy 2.0 – 2.0 – 2.0 mg/L unless the influent flow rate is low. A combination of operational changes, including an overall increase in DO concentrations in the aerated zones, would be necessary to meet the target COD/N ratio.

5.10.4 Biogas production

The biomethane potential tests performed on activated sludge from one activated sludge process that had aerated zone set-points of 0.3 – 0.8 – 1.7 mg/L and activated sludge from a process with the set-point configuration 2.0 – 2.0 – 2.0 mg/L showed that the potential was the same for both aeration strategies.

It is possible that there are differences in the sludge production from each activated sludge line that could cause a difference in the biogas production, but lack of data regarding the ratio of the sludge that would be degradable in an anaerobic digester made it difficult to estimate such a difference.

5.10.5 Final comments on the evaluation

Treatment efficiency is the most important aspect of the activated sludge process, and from that perspective a process with high dissolved oxygen concentrations is preferential to one that is optimized for low energy consumption. Even at oxygen concentrations of 2 mg/L the activated sludge process does not appear to be able to reach a COD/N ratio of 2 however, which means that increased oxygen rates likely cannot be the only operational change if the activated sludge process is going to become ready for a subsequent Manammox step.

The set-point configuration 0.6 – 0.6 – 1.0 mg DO/L was shown to give similar treatment efficiency results as 0.3 – 0.8 – 2.0 mg DO/L in the full-scale tests, but different loads and possible variations due to temperature and other conditions makes it difficult to trust that these results are fully representable of what effect changing the aeration strategy would have. If the aeration strategy of using 0.6 – 0.6 – 1.0 mg DO/L in the three aerated zones could be seen as comparable to the strategy 0.3 – 0.8 – 1.7/2.0 mg DO/L in terms of treatment quality and COD/N ratio then it creates a good foundation for future optimization of the activated sludge process. The DO set-points for the zones could then be fine-tuned upwards to create a treatment process that achieves better removal efficiencies but without significantly increased energy demands.

Limitations to the existing aeration system, such as difficulties to maintain the necessary pressure and capacity issues could present a problem when implementing a new aeration strategy. Strategies that have high DO set-points in the first aerated zone (zone 3) or low DO set-points in zones 4 and 5 risk experiencing problems to maintain the desired DO concentrations during periods of high and low flow rates. This could limit both the energy- and the treatment efficiencies of the aeration strategy.

5.11 Evaluation of modelling as an approach to optimize aeration

Models have a significant advantage over full-scale or even pilot-scale experiments in that a very large number of different scenarios can be tested with relatively small investments of time and resources. The attempt to set up a model of the activated sludge process at Sjölunda WWTP showed that creating a useful model can be very difficult however. While the model appeared to work well after the initial calibration the problems with accurately portraying changes to the treatment quality which appeared when trying to find optimal DO set-point configurations in the scenario analyses indicated that the model might have needed significant recalibration. This was confirmed during the validation, where the model failed to accurately estimate both airflows and most substance concentrations from the second characterization.

The ASM models were designed for activated sludge processes with long SRTs. ASM models might be able to accurately portray the most important biological reactions in activated sludge processes with long SRTs, but other reactions that have a negligible effect at long SRTs but are important at short SRTs are therefore not included in the models. Since X_S was the only COD fraction that was noticeably affected by changes to aeration in the model it can be suspected that the link between aeration and treatment quality is not strong enough in the ASM models, at least not under high-loaded conditions.

Furthermore, while there are sedimentation models that are more accurate than the Takács model no model that is able to assign different sedimentation velocities for different particle sizes while simultaneously taking other effects of the aeration rate into account is available

today. It might therefore not be possible to create a model that can predict the effect of aeration on effluent concentrations.

The model appeared to be better at estimating airflow rates and oxygen concentrations in the aerated basins, though it would be necessary to recalibrate the aeration sub-model. It is unclear how accurate the sub-model can become, but this could potentially mean that a model could be used to estimate the energy consumption of different aeration strategies. Estimation of the airflow with different DO set-point configurations without being able to connect the changes in airflow to changes in water quality is of questionable usefulness for the optimization of the aeration system at Sjölunda WWTP however, since the main goal is to maintain or increase the treatment efficiency.

When these factors are considered it becomes clear that using models without significant full-scale test data to back up results is not currently a viable approach to optimize the aeration strategy of the Sjölunda WWTP activated sludge process. More research into sedimentation models and kinetic models which work for high-loaded activated sludge would be necessary before this changes.

6 Conclusions

Full-scale tests of WEST model scenarios at Sjölunda wastewater treatment plant showed that it was possible to get reasonably good estimations of the total airflow, and by extension the energy requirements of different aeration strategies, using a calibrated WEST model of the treatment plant. The model was not able to give good estimates on the treatment efficiency or COD/N ratio of different aeration strategies however. Additionally, there is currently too little research on how activated sludge models function under high-loaded conditions, and such studies would be necessary before it would be possible to rely on modelling as an approach for optimizing aeration strategies in a HLAS setting. Since using a model was not a suitable method it was necessary to rely on full-scale tests to form conclusions about the most optimal aeration strategy for the activated sludge process at Sjölunda WWTP.

From an energy consumption perspective it is most beneficial to keep the dissolved oxygen set-points of the three aerated zones as similar as possible, and the dissolved oxygen set-point of zone 5 low. Full-scale tests and the WEST model indicate that it is possible to reduce the total airflow by 2-5% with a set-point configuration of 0.6 – 0.6 – 1.0 mg/L compared to the configurations 0.3 – 0.8 – 1.7/2.0 mg/L while maintaining the same, or a slightly higher treatment efficiency. While the potential gain is greater in an aeration system with a G2:1 design than in systems with evenly distributed diffusers like in the G1 lines there was a clear gain with both aeration system designs.

The biomethane potential was found to be very similar in activated sludge from two processes which ran on very low and very high DO set-point configurations, and the biomethane potential is not significantly affected by the oxygen rate in the basins.

The recommended aeration strategy for the activated sludge process at Sjölunda wastewater treatment plant is to start at dissolved oxygen concentrations of 0.6 – 0.6 – 1.0 mg/L and to gradually increase the rate until a desirable treatment efficiency is found. It is necessary to combine changes to the aeration strategy with other options, such as SRT control strategies, if the process is to be able to reach a COD/N ratio of 2.0.

7 Future studies

A number of avenues for future studies were found during the project. The most significant issue with modelling different aeration scenarios was the very minor effect the changes in strategies had on effluent quality. If it is going to be possible to properly use a model it would therefore be necessary to investigate the settling properties of sludge subjected to different aeration strategies more thoroughly. It would furthermore be necessary to develop a settling model that is able to handle particle fractions differently, and not assume that all particles will behave in the same way.

The understanding of settling- and sludge properties would benefit from a microbial characterization and a microscopic analysis of the sludge that would show which types of bacteria that are present in the sludge and how their numbers are affected by different aeration strategies. This could in turn give a better understanding of the circumstances in which low aeration lead to growth of bacteria that cause foaming issues or that reduce the settling properties of the sludge. Other tests that could increase the understanding and accuracy of the model would be tests to determine the sludge blanket level in the secondary settlers and experiments to determine how well mixed the activated sludge zones are.

If effects of aeration is to be properly compared then it is necessary to test two lines that have the same SRT so that effects that might be caused by the SRT can be ruled out as a factor. In that regard, it's beneficial to have return sludge pumps that give similar flow rates, and waste sludge flows that have the same set-point. Performing full-scale tests of different aeration strategies on SRT-controlled lines would likely give the best results.

8 Reference list

Alleman, J.E. and Prakasam, T.B.S., 1983. Reflections on Seven Decades of Activated Sludge History. *Journal Water Pollution Control Federation*, 55(5), pp.436-443.

Baillod, C.R., Paulson, W.L., McKeown, J.J. and Campbell, H.J.Jr., 1986. Accuracy and precision of plant scale and shop clean water oxygen transfer tests. *Journal Water Pollution Control Federation*, 58(4), pp.290-299.

Ballinger, S.J., Head, I.M., Curtis, T.P. and Godley, A.R., 2002. The effect of C/N ratio on ammonia oxidizing bacteria community structure in a laboratory nitrification-denitrification reactor. *Water Science and Technology*, 46(1-2), pp.543-550.

Boyle, W. C., Craven, A., Danley, W. and Rieth, M., 1989. *Oxygen Transfer Studies at the Madison Metropolitan Sewerage District Facilities*, EPA/600/R-94/096, Washington D.C.: U.S: Environmental Protection Agency.

Carlsson, B. and Hallin, S., 2003. *Control engineering and microbiology in wastewater treatment plants* (in Swedish), VA-Forsk 2003-27, Stockholm: Svenskt Vatten AB.

Catunda P.F.C. and van Haandel, A.C., 1992. Activated sludge settling Part I: Experimental determination of activated sludge settleability. *Water SA*, 18(3), pp.165-172.

Dick, R.I. and Vesilind, P.A., 1969. The Sludge Volume Index: What Is It? *Journal Water Pollution Control Federation*, 41(7), pp.1285-1291.

Daigger, G.T. and Roper Jr., R.E., 1985. The Relationship between SVI and Activated Sludge Settling Chracteristics. *Journal Water Pollution Control Federation*, 57(8), pp.859-866.

DHI, 2014. *WEST models guide.* Hørsholm: DHI.

Ekama, G.A., Dold, P.L. and Marais, G.v.R., 1986. Procedured for determining influent COD fractions and the maximum specific growth rate of heterotrophs in activated sludge systems. *Water Science & Technology*, 18, pp.91-114.

Fang, F., Ni, B., Li, W., Sheng, G. and Yu, H., 2011. A simulation-based integrated approach to optimize the biological nutrient removal process in a full-scale wastewater treatment plant. *Chemical Engineering Journal*, 174, pp.635-643.

Fernandez, F.J., Castro, M.C., Rodrigo, M.A. and Cañiares, P., 2011. Reduction of aeration costs by tuning a multi-set point on/off controller: A case study. *Control Engineering Practice*, 19, pp.1231-1237.

Germain, E., Nelles, F., Drews, A., Pearce, P., Kraume, M., Reid, E., Judd, S.J. and Stephenson, T., 2007. Biomass effects on oxygen transfer in membrane bioreactors. *Water Research*, 41, pp.1038-1044.

Gernaey, K.V. and Jørgensen, S.B., 2004. Benchmarking combined biological phosphorus and nitrogen removal wastewater treatment processes. *Control Engineering Practice*, 12, pp.357-373.

Gori, R., Balducci, A., Caretti, C. and Lubello, C., 2014. Monitoring the oxygen transfer efficiency of full-scale aeration systems: investigation method and experimental results. *Water Science & Technology*, 70(1), pp.8-14.

Gustavsson, D., 2009. *Aeration requirements G1-3, Sjölunda ARV* (in Swedish). Malmö: VA SYD. 2009-SJÖ007.

Gustavsson, D., Persson, F., Aspegren, H., Stålhandske, L. and la Cour Jansen, J., 2012. Anammox i huvudströmmen – vad är problemet? *VATTEN*, 68, pp.195-208.

Gustavsson, D., Aspegren, H., Stålhandske, L. and la Cour Jansen, J., 2013. Mainstream anammox at Sjölunda Wastewater Treatment Plant – pilot operation of sludge liquor treatment and start-up of the full process. *Proceedings of 13th Nordic Wastewater Conference*. Malmö, Sweden, October 8-10, 2013.

Hansen, T.L., Ejbye Schmidt, J., Angelidaki, I., Marca, E., la Cour Jansen, J., Mosbaek, J. & T.H. Christensen, 2004. Method for determination of methane potentials of solid organic waste. *Waste Management*, 24, pp.393-400

Hagman, M. & J. la Cour Jansen, 2007. Oxygen uptake rate measurements for application at wastewater treatment plants. *Vatten*, 63(2), pp.122-128

Henkel, J., Cornel, P. and Wagner, M., 2011. Oxygen transfer in activated sludge – new insights and potentials for cost saving. *Water Science & Technology*, 63(12), pp.3034-3038.

Henze, M., Gujer, W., Mino, T. & M. van Loosdrecht, 2000. *Activated Sludge Models ASM1, ASM2, ASM2d and ASM3*. London: IWA Publishing

Kampschreur, M.J., Temmink, H., Kleerebezem, R., Jetten, M.S.M. and van Loosdrecht, M.C.M., 2009. Nitrous oxide emission during wastewater treatment. *Water Research*, 43, pp.4093-4103.

Kandare, G. and Nevado Reviriego, A., 2011. Adaptive predictive expert control of dissolved oxygen concentration in a wastewater treatment plant. *Water Science & Technology*, 64(5), pp.1130-1136.

Klingstedt, T., 2015. *Modelling the COD Reducing Treatment Processes at Sjölunda WWTP*. MSc. Lund University.

Liu, C., Li, S. and Zhang, F., 2011. The oxygen transfer efficiency and economic cost analysis of aeration system in municipal wastewater treatment plant. *Energy Procedia*, 5, pp.2437-2443.

Lysberg, E. and Neth, M., 2012. *Characterisation of influent water: Determination of COD-fractions* (in Swedish). Göteborg: Gryaab AB. Gryaab Rapport 2012:14.

Martinello, N., 2013. *Integrating experimental analyses and a dynamic model for enhancing the energy efficiency of a high-loaded activated sludge plant*. MSc. University of Padova.

Martins, A.M.P., Pagilla, K., Heijnen, J.J. and van Loosdrecht, M.C.M., 2004. Filamentous bulking sludge – a critical review. *Water Research*, 38, pp.793-817.

Nobel, P.I., 2015. *High-Loaded Activated Sludge: Improvements of an SRT-controlled System through a Model Based Approach*. MSc. Lund University.

Olsson, G., 2012. ICA and me – A subjective review. *Water Research*, 46, pp.1585-1624.

Pal, P., Khairnar, K. and Paunikar, W. N., 2014. Causes and remedies for filamentous foaming in activated sludge treatment plant. *Global NEST Journal*, 16(4), pp.762-772.

Pittoors, E., Guo, Y. and Van Hulle, S.W.H., 2014. Modeling Dissolved Oxygen Concentration for Optimizing Aeration Systems and Reducing Oxygen Consumption in Activated Sludge Processes: A Review. *Chemical Engineering Communications*, 201(8), pp.983-1002.

Polizzi, C., 2013. *Dynamic evaluation of a high loaded activated sludge plant as pretreatment for deammonification in the mainstream*. MSc. University of Padova.

Rieger, L., Gillot, S., Langergraber, G., Ohtsuki, T., Shaw, A., Takács, I. & S. Winkler, 2013. *Guidelines for Using Activated Sludge Models.* London: IWA Publishing

Rosso, D., Iranpour, R. and Stenstrom, M.K., 2005. Fifteen Years of Offgas Transfer Efficiency Measurements on Fine-Pore Aerators: Key Role of Sludge Age and Normalizaed Air Flux. *Water Environmental Research*, 77(3), pp.266-273.

Rosso, D. and Stenstrom, M.K., 2006. Economic Implications of Fine-Pore Diffuser Aging. *Water Environment Research*, 78(8), pp.810-815.

Rydh, J. and Åkesson, A., 2007. *Energy Conservation in Wastewater Treatment Operation – a Case Study at Sjölunda and Klagshamn WWTPs*. MSc. Lund University.

Schierholz, E.L., Gulliver, J.S., Wilhelms, S.C. and Henneman, H.E., 2006. Gas transfer from air diffusers. *Water Research*, 40, pp.1018-1026.

SIS (1981). *Determination of dry matter and ignition residue in water, sludge and sediment*. SS 028113. Stockholm: Swedish Standards Institute.

Sulzer, 2012. *ABS Nopon disc diffuser system KKI 215*. Winterthur: Sulzer Ltd.

Takács, I., Patry, G.G. and Nolasco, D., 1991. A Dynamic Model of the Clarification-Thickening Process. *Water Research*, 25(10), pp.1263-1271.

Thunberg, A., 2006. *Energy optimization of the aeration at Käppala wastewater treatment plant in Stockholm* (in Swedish). MSc. Uppsala University.

VA SYD, 2011. *The Sjölunda Wastewater Treatment Plant*. Malmö: VA SYD.

VA SYD, 2014. *Sjölunda Wastewater Treatment Plant Malmö: Environmental report in accordance with the Environmental Code for year 2013* (in Swedish). Malmö: VA SYD.

Wang, C., Zeng, Y., Lou, J. and Wu, P., 2007. Dynamic simulation of a WWTP operated at low dissolved oxygen condition by integrating activated sludge model and a floc model. *Biochemical Engineering Journal*, 33, pp.217-227.

Vanrolleghem, P.A., 2002. *Principles of Respirometry in Activated Sludge Wastewater Treatment*. Gent: Ghent University.

Warfvinge, P., 2011. *Process Calculations and Reactor Calculations for Environmental Engineering*. Edition 2011/2012. Lund University.

Wentzel, M.C., Mbewe, A. and Ekama, G.A., 1995. Batch test for measurement of readily biodegradable COD and active organism concentrations in municipal waste water. *Water SA*, 21(2), pp.117-124.

Åmand, L., Olsson, G. and Carlsson, B., 2013. Aeration control – a review. *Water Science & Technology*, 67(11), pp.2374-2398.

9 Appendices

Second characterization

Influent compounds

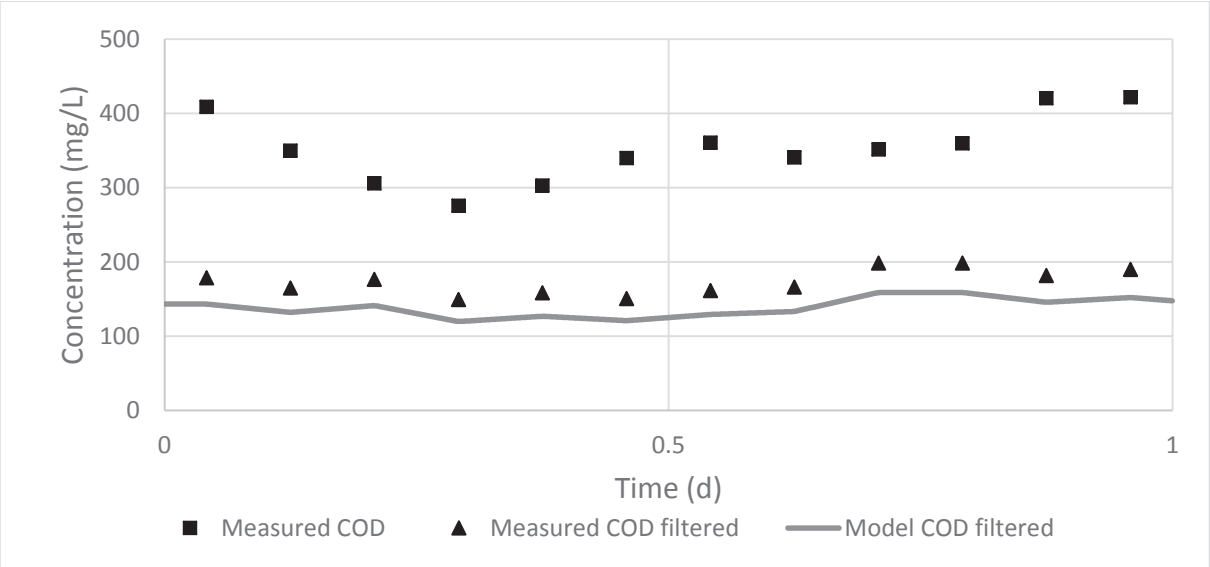

Figure 86 Measured COD, COD filtered and model soluble COD concentrations in the influent to G1 during the second characterization. The model COD filtered concentration was set to be 80% of the measured COD filtered concentration.

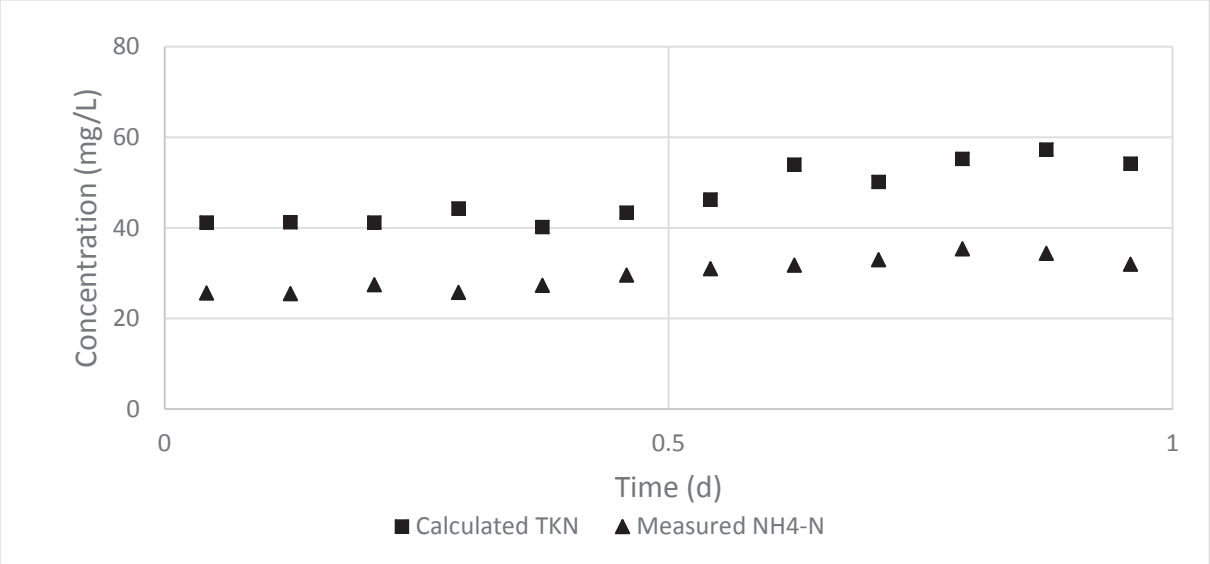

Figure 87 Calculated TKN and ammonium concentrations in the influent to G1 during the second characterization. TKN and ammonium concentrations increased throughout the day. Organic nitrogen, the difference between TKN and ammonium in the figure, was in the range of 15-20 mg/L in the majority of the samples.

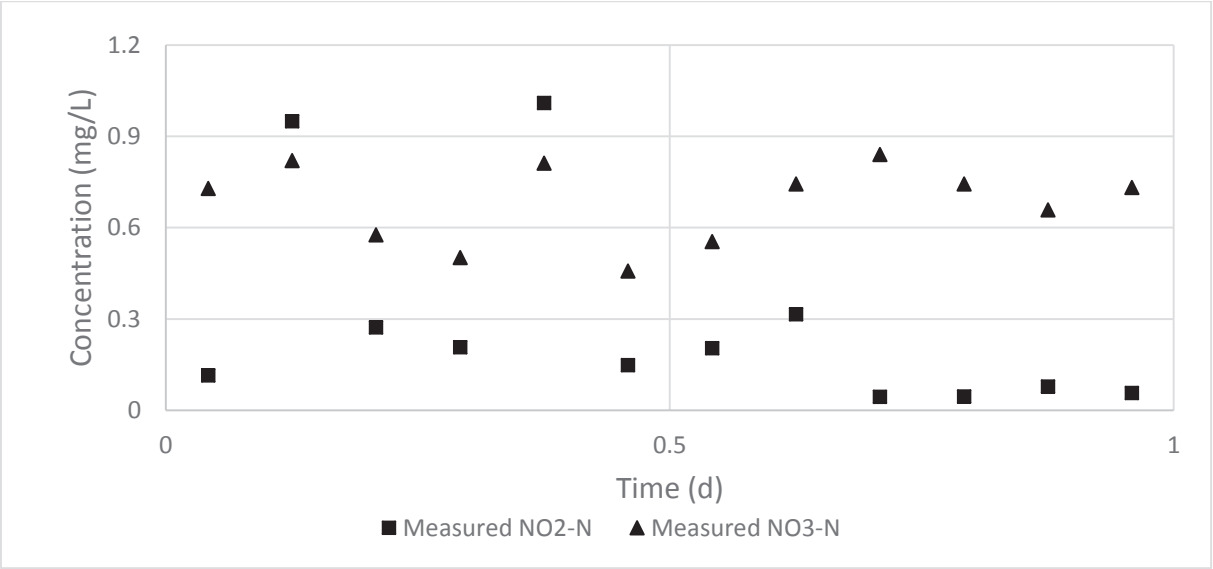

Figure 88 Nitrite and nitrate concentrations in the influent to G1 during the second characterization. Like the first characterization campaign peak concentrations of nitrite could be observed every six hours for the first half of the day, but during the second half the nitrite concentration was very low in each sample.

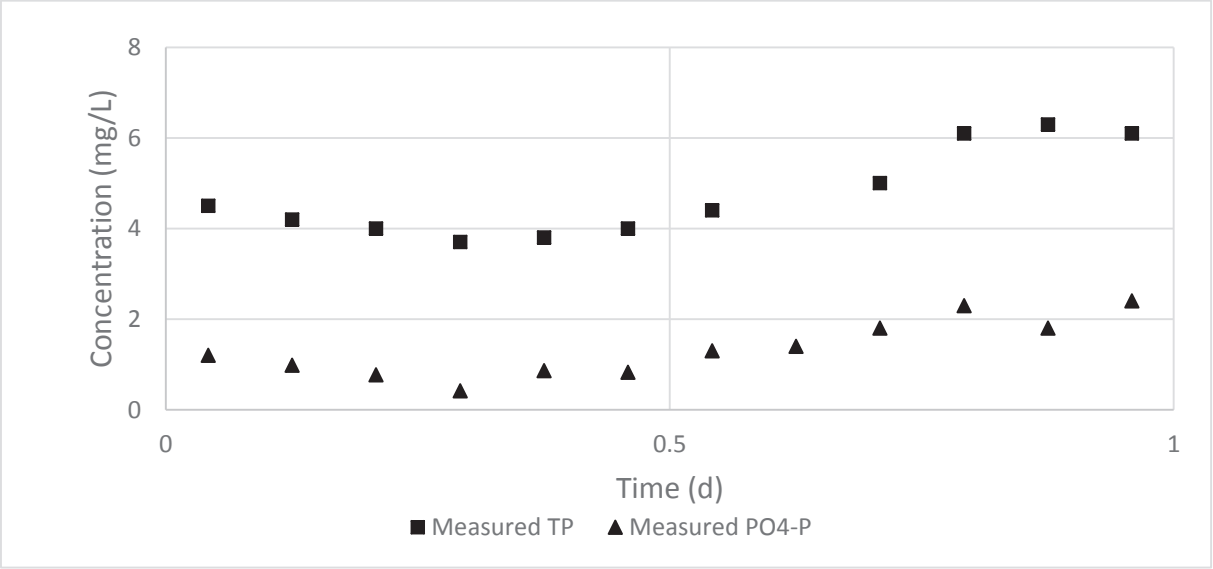

Figure 89 TP and phosphate in the influent to G1 during the second characterization. TP and phosphate concentrations had a minimum at 07.00 and a maximum during the evening. Organic phosphorus, the difference between TP and phosphate, was relatively stable at 3 mg/L during the campaign.

G1:1 zone 5

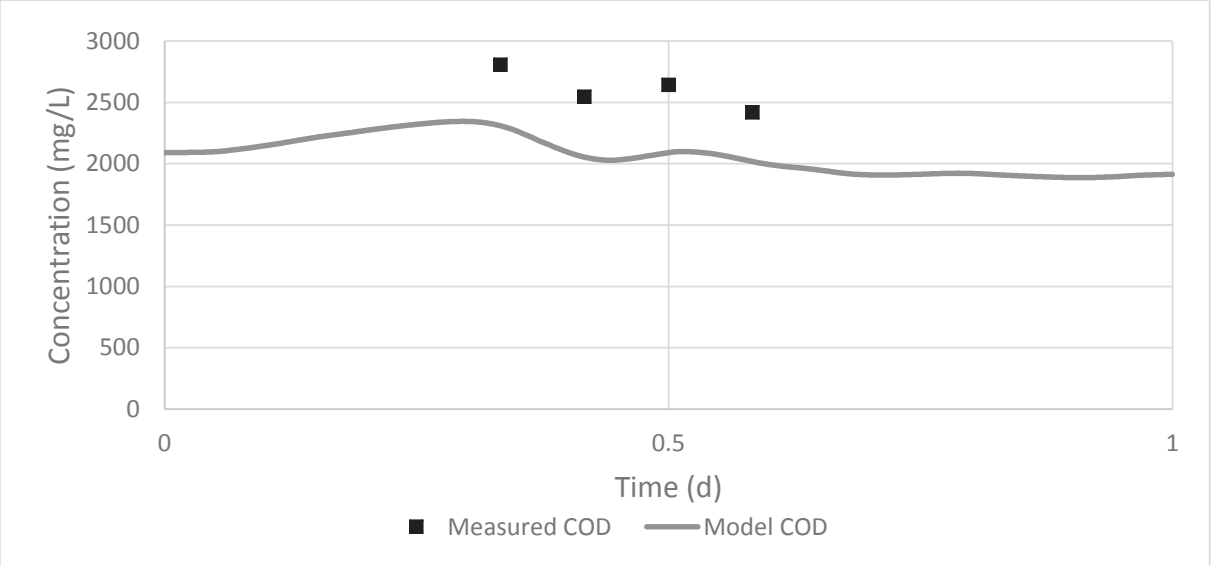

Figure 90 Model and measured COD concentrations in G1:1 zone 5 during the second characterization. Model COD followed the general shape of the measurements, but the model concentration was on average 500 mg/L below the measured concentrations.

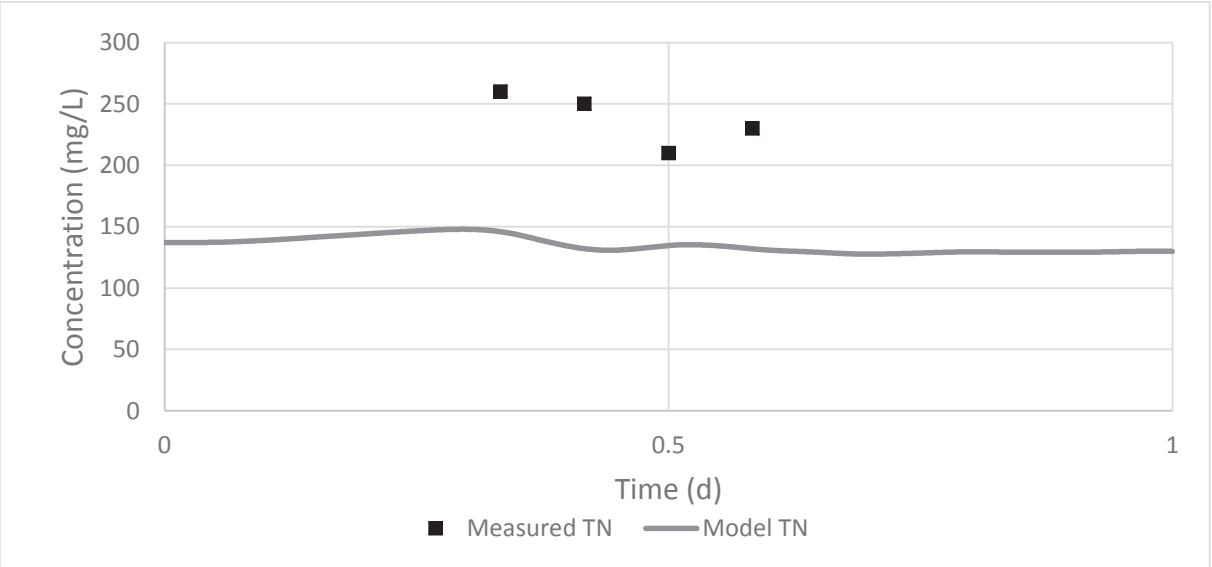

Figure 91 Model and measured TN in G1:1 zone 5 during the second characterization. The model was not able to match the measurements, with model TN concentrations being on average 100 mg/L lower than the measured concentrations.

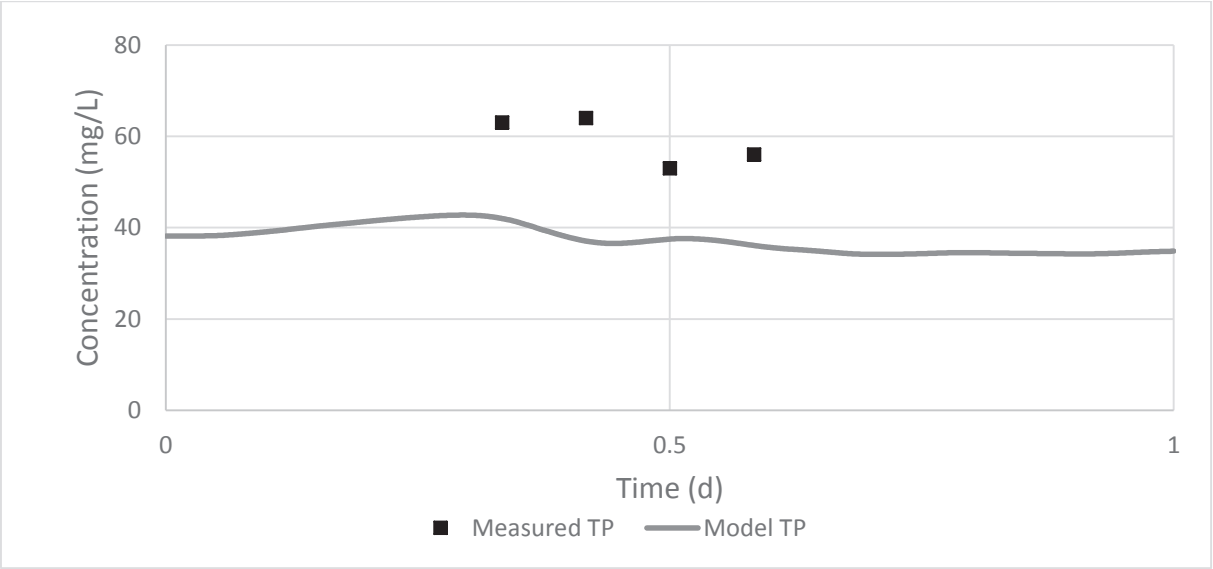

Figure 92 Model and measured TP in G1:1 zone 5 during the second characterization. As with TN the model was not able to reach the same concentration range as the measurements, and the model concentrations were about 20 mg/L lower.

G1:1 waste sludge

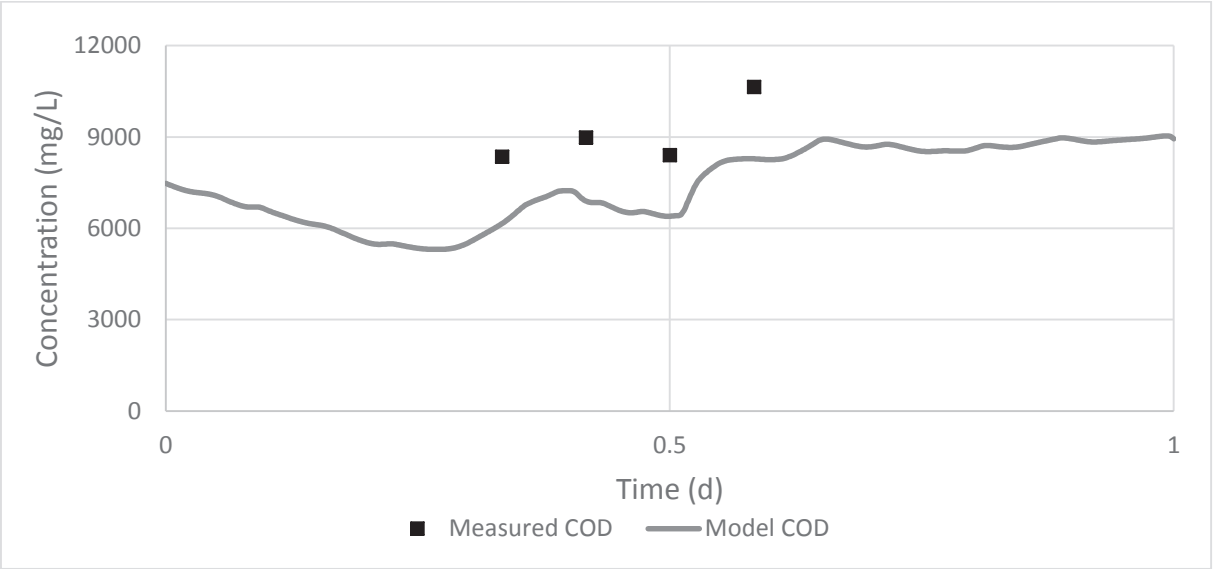

Figure 93 Model and measured COD concentrations in the waste sludge of G1:1 during the second characterization. The model had a similar shape to the measurements, but model waste sludge COD concentrations were on average 2000 mg/L lower than measured concentrations.

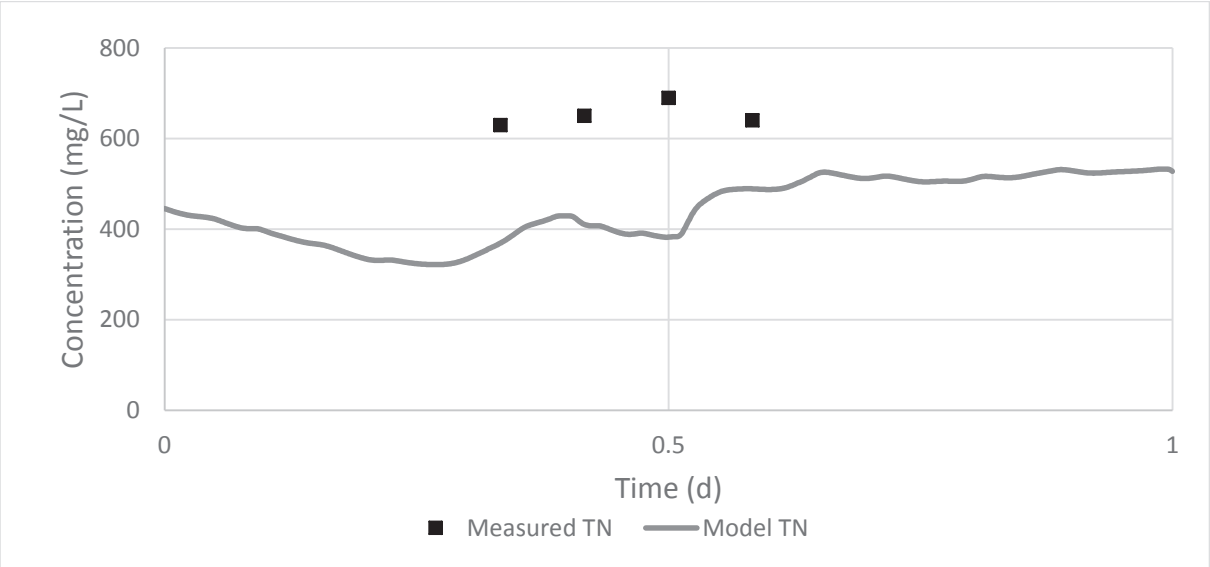

Figure 94 Model and measured TN concentrations in the waste sludge of G1:1 during the second characterization. The model concentrations were significantly lower than the measured concentrations, and the model had a local minimum concentration of TN where measurements instead showed a maximum.

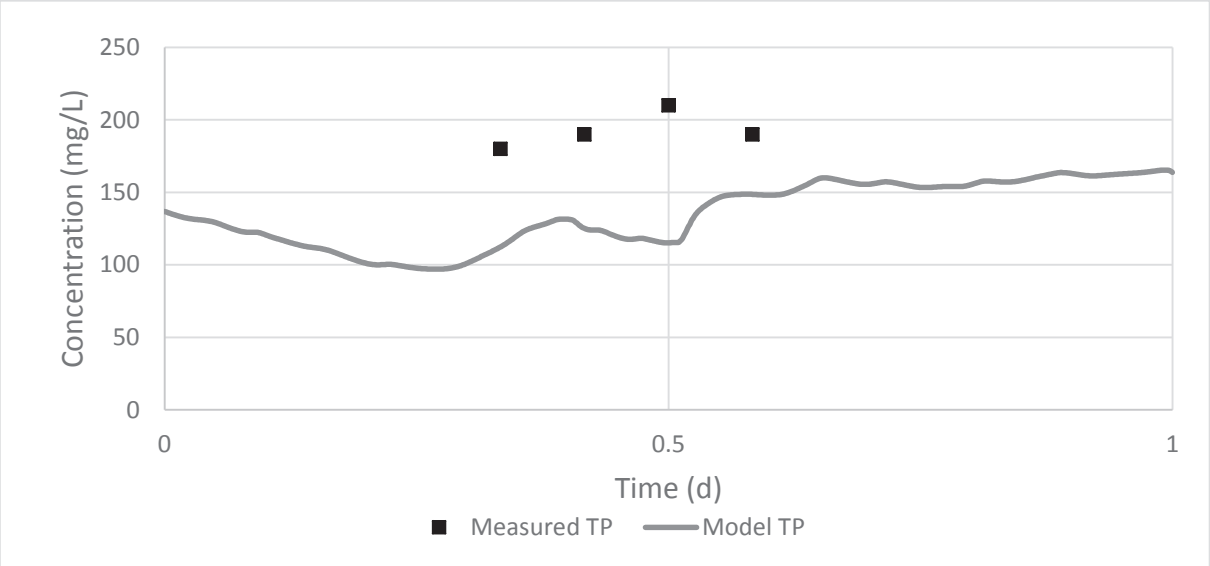

Figure 95 Model and measured TP concentrations in the waste sludge of G1:1 during the second characterization. As with TN, there was a large difference in model and measured concentrations, approximately 50 mg/L, and the peak TN concentration occured later in the model than in the measurements.

G1:1 effluent

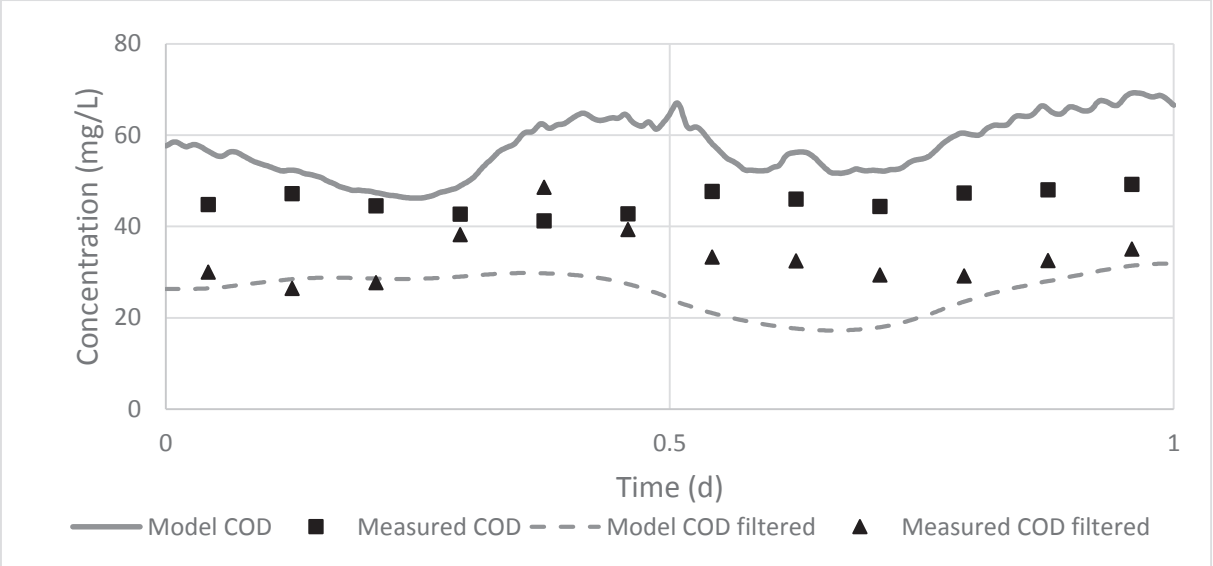

Figure 96 Model and measured COD and COD filtered in the effluent to G1:1 during the second characterization. Measurements showed that COD was relatively stable throughout the day whereas the model had distinct minimums and maximums. This caused periods where the COD concentration was 50% higher in the model than in the measurements. For COD filtered the model matched the measurements during the first and last hours of the day, but unlike the measurements the model did not have a peak in the middle of the day.

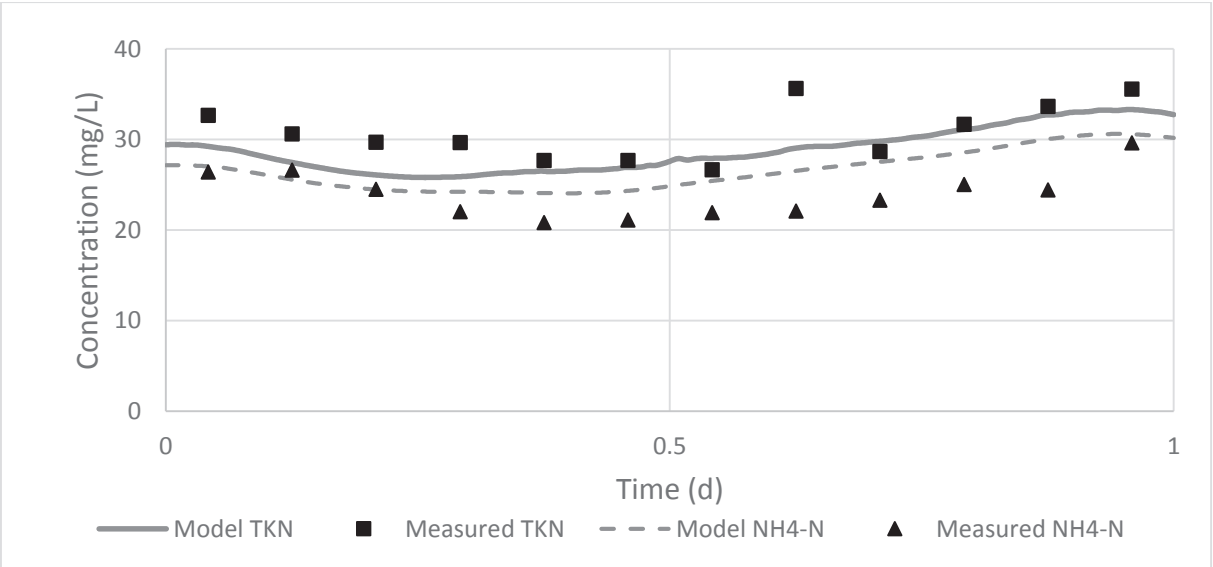

Figure 97 Model and measured TKN and ammonium concentrations in the effluent to G1:1 during the second characterization. Model concentrations were in the same range as the measurements for both TKN and ammonium, and the models also matched the concentration fluctuations relatively well. The difference between TKN and ammonium (organic nitrogen) was not properly displayed in the model however. In measurements this difference was 10-15 mg/L, but in the model organic nitrogen had a concentration of less than 5 mg/L.

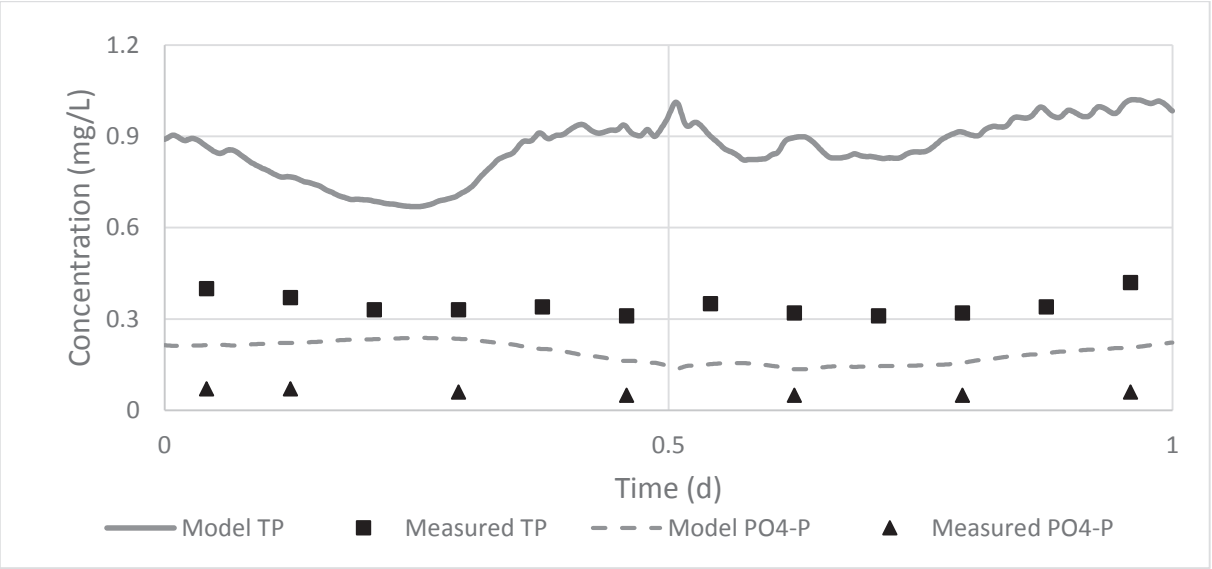

Figure 98 Model and measured TP and phosphate concentrations in the effluent to G1:1 during the second characterization. The model strongly overvalued both the TP and the phosphate concentrations in the effluent.

G1:2 zone 5

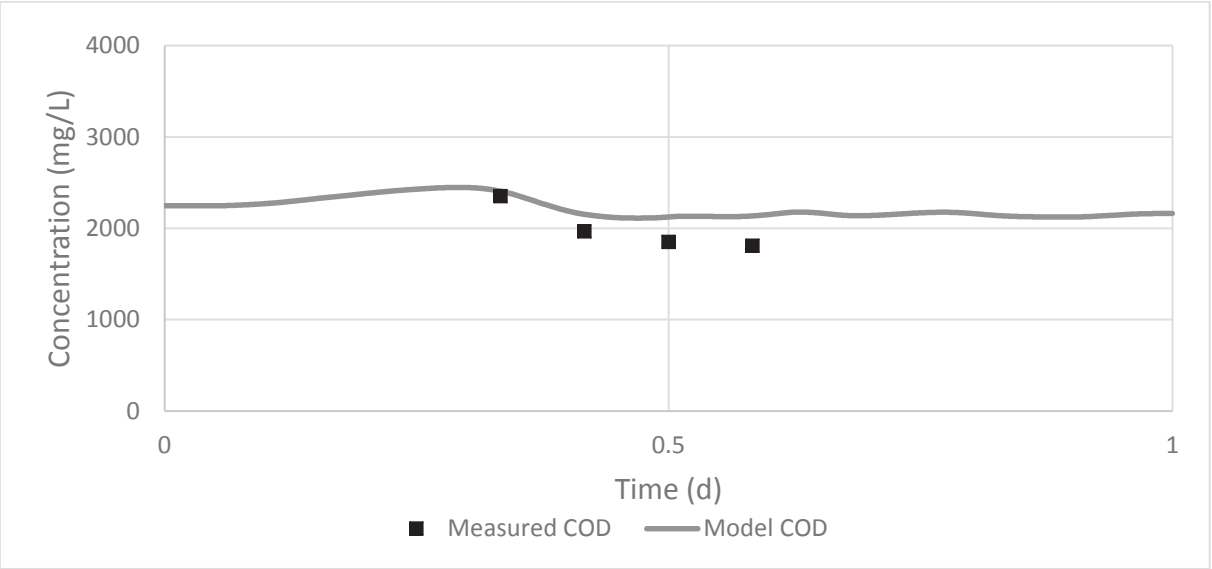

Figure 99 Measured and model COD concentrations in G1:2 zone 5 during the second characterization. There was a relatively good match, both in magnitude and in change over time, between the model COD and measured COD.

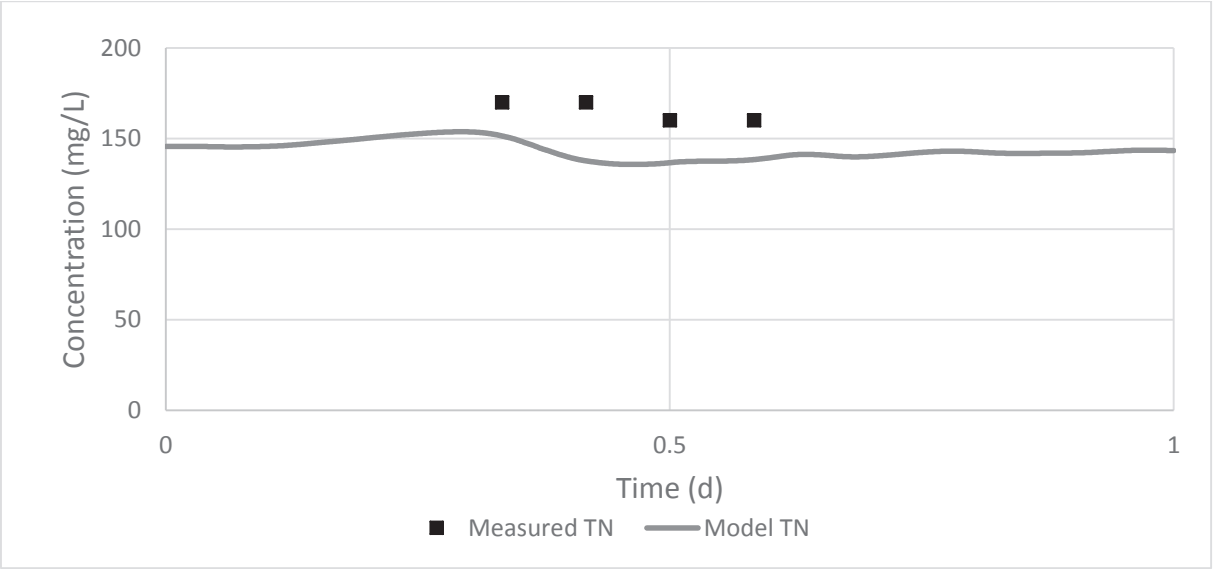

Figure 100 Measured and model TN concentrations in G1:2 zone 5 during the second characterization. Model TN concentrations were approximately 20 mg/L lower than the concentrations found in measurements.

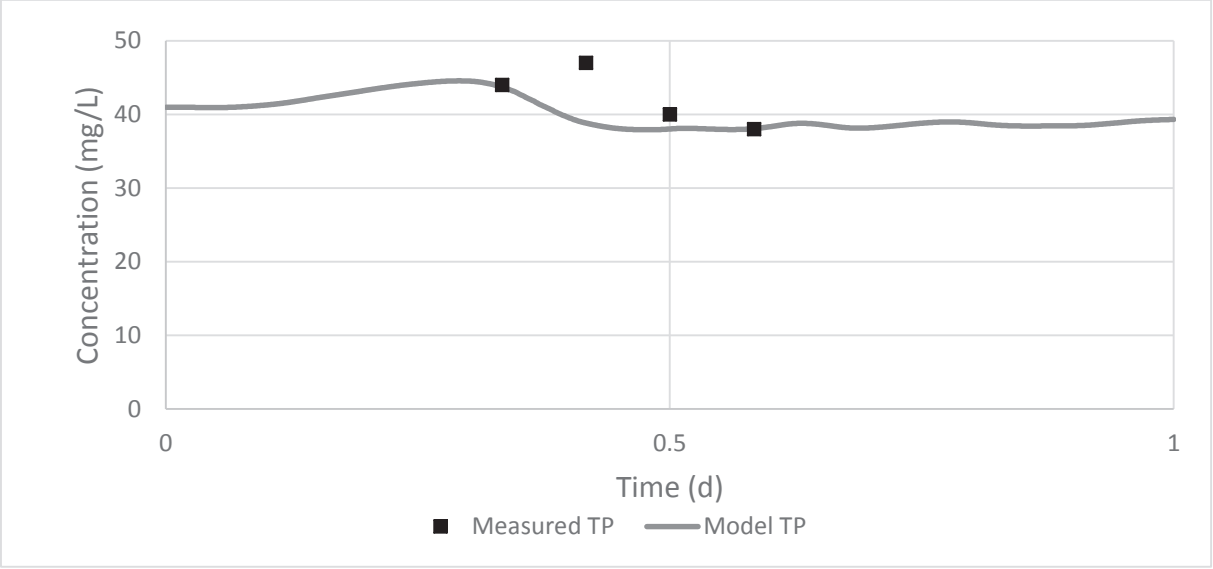

Figure 101 Measured and model TP concentrations in G1:2 zone 5 during the second characterization. Model TP concentrations were in the same range as the measurements, but a peak in TP occurred 2-3 hours earlier in the model than in the samples.

G1:2 waste sludge

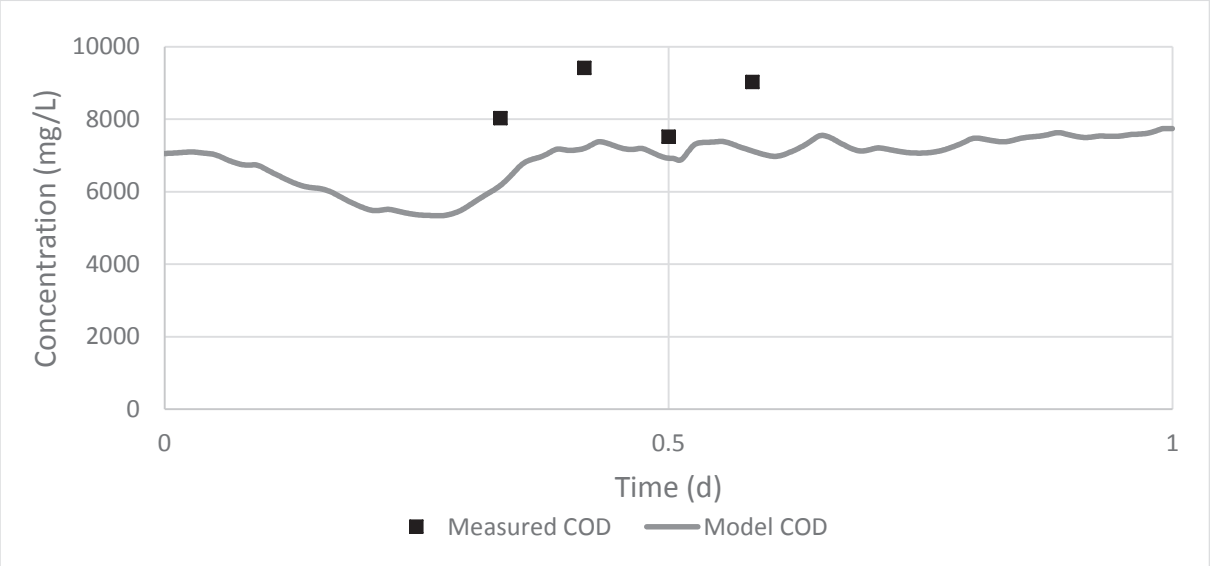

Figure 102 Measured and model COD concentrations in the waste sludge of G1:2 during the second characterization. The model COD concentration was significantly lower than the measured COD concentration for most samples and the model did not mirror the fluctuations in measurement concentrations.

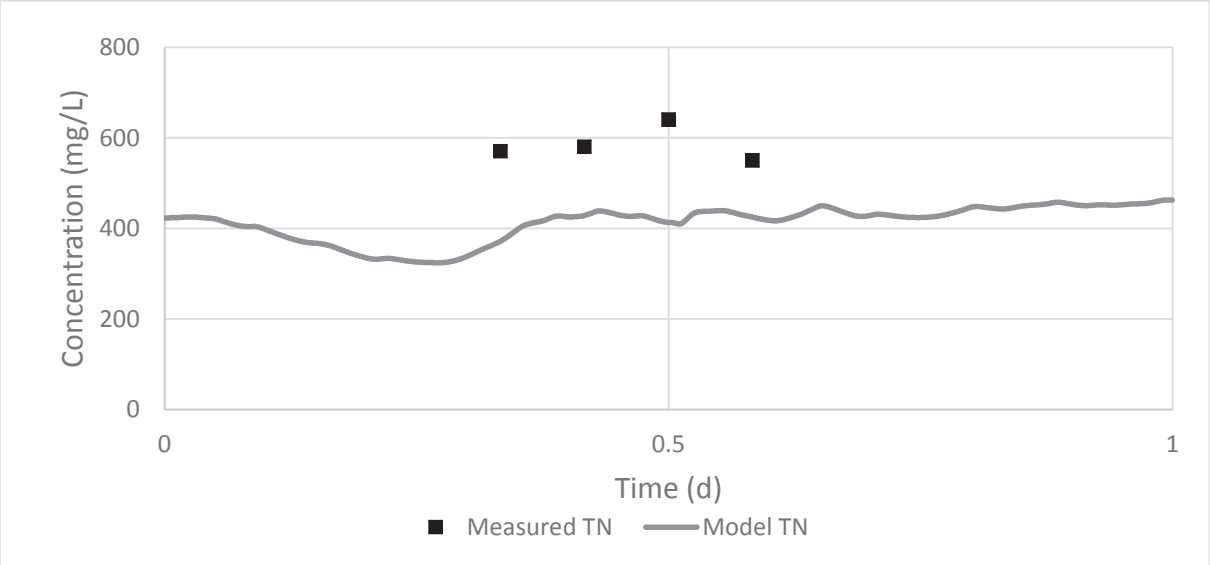

Figure 103 Measured and model TN concentrations in the waste sludge of G1:2 during the second characterization. As was the case for G1:1 the waste sludge TN concentration was approximately 200 mg/L lower in the model than in the measurements.

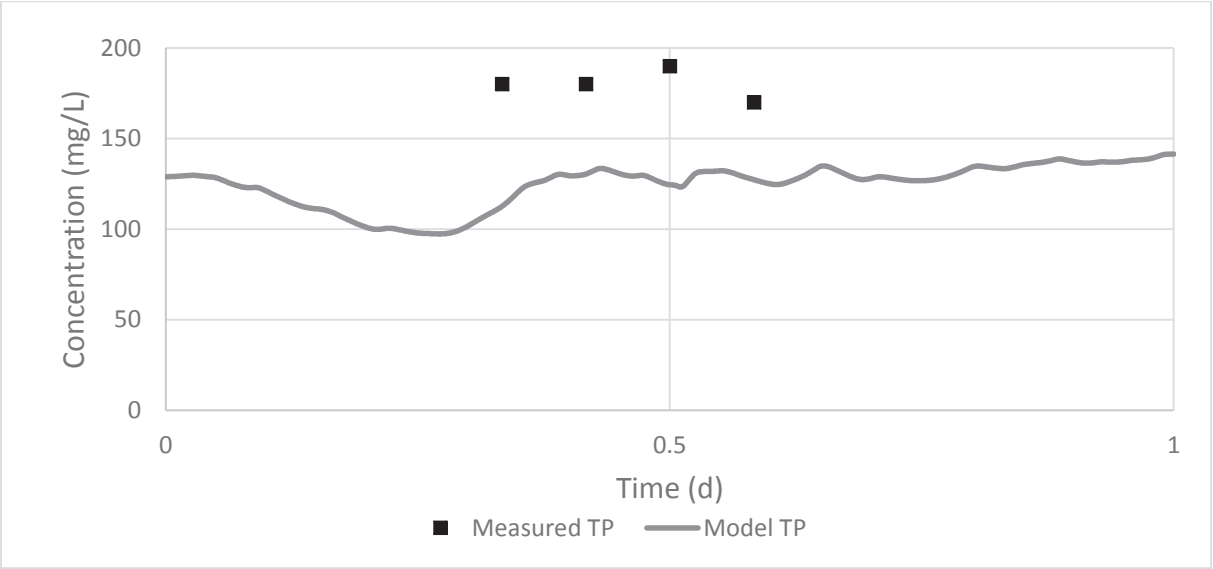

Figure 104 Measured and model TP concentrations in the waste sludge of G1:2 during the second characterization. Model TP concentrations were 50 mg/L lower than the measurement TP concentrations.

G1:2 effluent

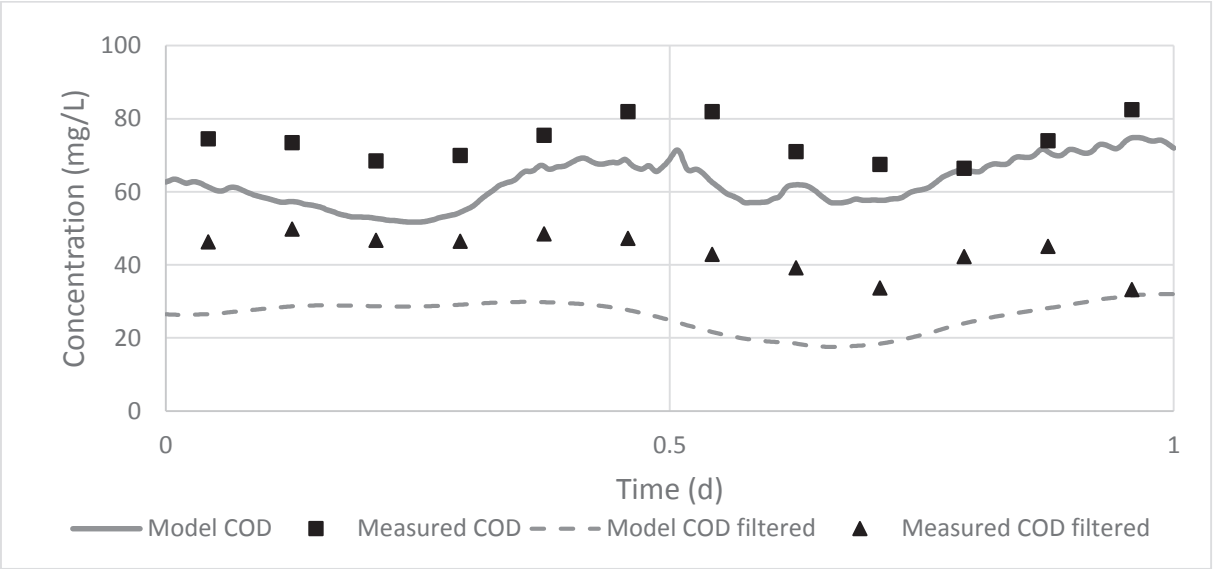

Figure 105 Measured and model COD and COD filtered concentrations in the effluent to G1:2 during the second characterization. Both the model COD and the model COD filtered concentrations had local minimum and maximum peak values at the same time as the measurement concentrations, but the model concentrations were lower than the measurement concentrations. The difference was especially large for COD filtered, where model values were only a slightly over 50% of the measurement concentrations.

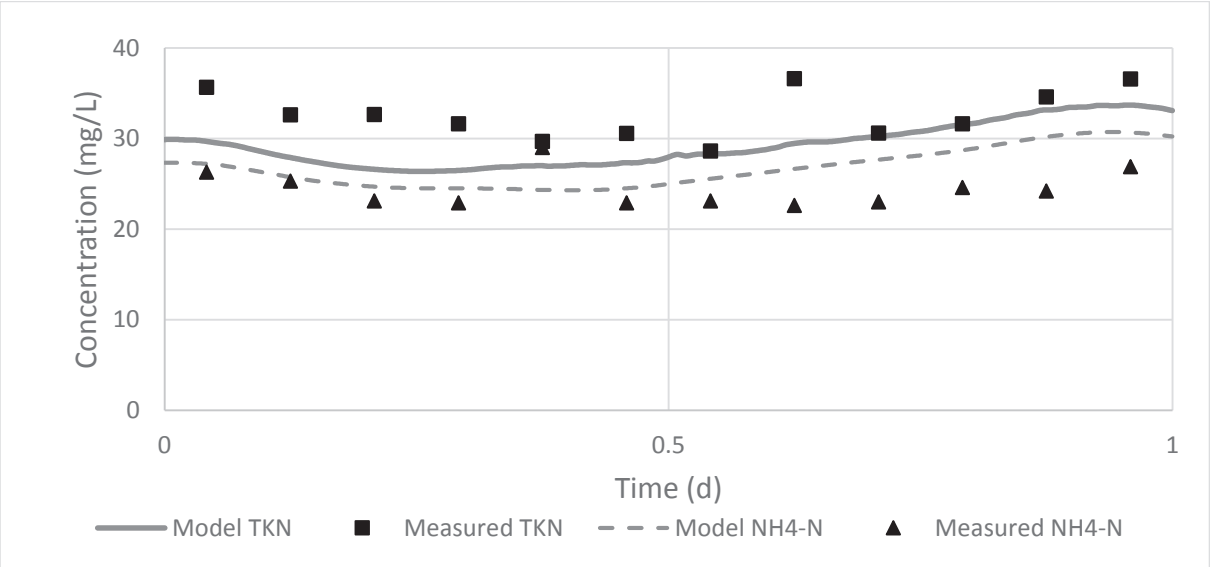

Figure 106 Measured and model TKN and ammonium in the effluent to G1:2 during the second characterization. The model was able to produce concentrations that were in the same range as the measurements for both TKN and ammonium, but just as was the case for the effluent of line G1:1 the difference between TKN and ammonium was much smaller in the model than in the measurements.

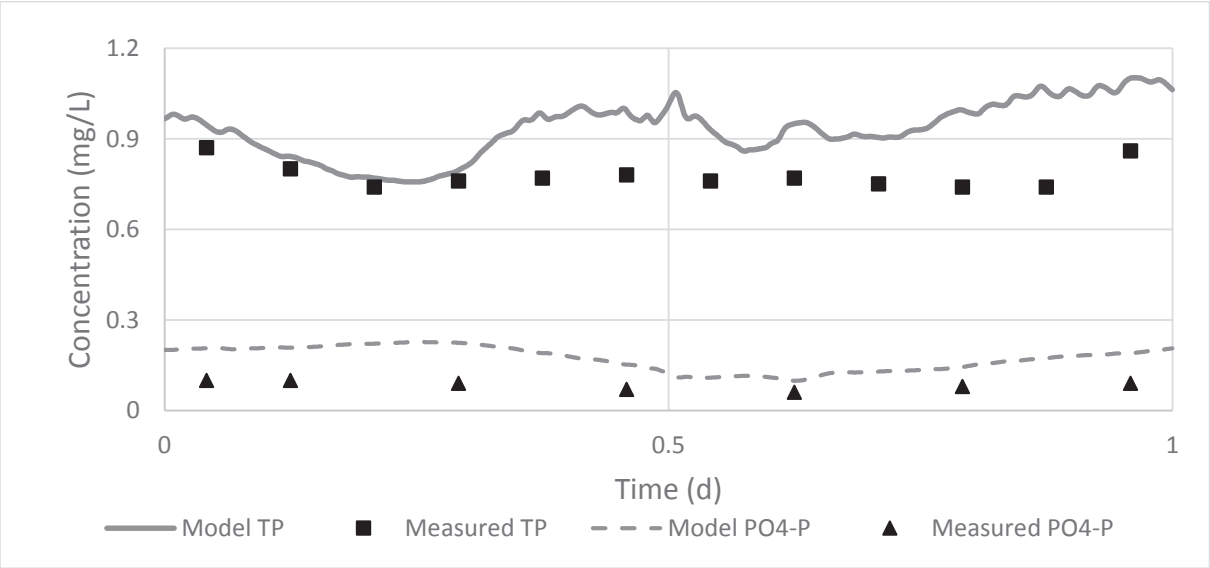

Figure 107 Measured and model TP and phosphate concentrations in the effluent to G1:2 during the second characterization. There was a relatively good match between model and measured concentrations for both TP and phosphate.

Bättre luftning förbättrar avloppsvattenreningen

Sjölunda avloppsreningsverk är ett av de största reningsverken i Sverige och tar hand om avloppsvatten från stora delar av det snabbt växande Malmö. Befolkningsökningen sätter press på verket, där vattenreningen måste förbättras för att reningsverket ska kunna ta hand om ökande volymer avloppsvatten. För att nå detta mål drivs flera förbättringsprojekt på Sjölundaverket, däribland projekt som fokuserar på aktivtslamprocessen, en av de viktigaste och mest energikrävande reningsmetoderna.

Aktivtslamprocessen är med sina hundra år en av de äldsta reningsmetoderna i avloppsvattenrening. Processen är biologisk, vilket innebär att reningen sköts av bakterier som förekommer naturligt i avloppsvattnet istället för genom tillsats av kemikalier. Syftet med processen är att ta bort organiskt material och näringsämnen från vattnet. Bakterierna, som kallas aktivt slam, hålls kvar i processen en viss tid – för Sjölundaverket i 1-2 dagar – innan slammet tas om hand för att omvandlas till biogas och gödsel.

För att aktivt slam ska kunna rena avloppsvatten krävs syre, och detta sprutas in som luftbubblor genom membran i botten på slambassängerna. Denna luftning styrs av automatiska system som mäter syrenivån i bassängerna och justerar luftflödet om syrenivån blir för hög eller för låg.

Aktivtslamprocessen står för 30% av energiförbrukningen på Sjölundaverket och då luftningen står för majoriteten av denna förbrukning går det att spara mycket energi på att begränsa luftningen. Samtidigt är ett reningsverks viktigaste uppgift naturligtvis att rena vatten från föroreningar och det är därför viktigt att syrenivåerna inte sjunker så mycket att det påverkar bakteriernas reningsförmåga. I arbetet med att göra luftningen effektivare blir då utgångspunkten frågan: Kan luftningen ändras så att energiförbrukningen sänks utan att vattenreningen försämras? För att svara på den frågan måste vi veta var i slambassängerna som reningen sker. ”Äter” bakterierna lika mycket i slutet av slambassängerna, eller tas det mesta organiska materialet om hand redan i början av processen? Behövs det i det senare fallet lika mycket luft i den sista slambassängen som i bassänger som ligger i början av reningssteget?

Detta kan undersökas och besvaras genom större mätkampanjer, vilka är resurskrävande men samtidigt ger tydliga resultat. Datormodeller som simulerar processerna kan vara en snabbare metod, men det kan krävas mycket arbete för att skapa fungerande modeller som ger tillförlitliga resultat då aktivtslamprocessen är mycket komplex. På Sjölundaverket användes både mätkampanjer och en datormodell som en del i luftningsprojektet.

Det visade sig vara mätkampanjerna som gav de mest användbara resultaten. Mätningarna visade att det aktiva slammet använde mest syre i början av processen och att det därför kunde gå att förbättra vattenreningen samtidigt som energiförbrukningen sänks genom att öka luftningen i början av processen och minska den i slutet.